Signal Processing for GNSS Reflectometry

Corentin Lubeigt

February 14, 2023

Ph.D. supervision: **Lorenzo Ortega**, **Jordi Vilà-Valls** and **Eric Chaumette**
CNES supervision: **Laurent Lestarquit**

Introduction

Credit: Man Made wallpapers

The example of sea height

How to estimate water level?

The example of sea height

In situ approaches

- Local measurements:
  - flood level markers,
  - GPS buoys.
- Need of a lot of data points to get a global coverage...

parc-cotentin-bessin.fr

ndbc.noaa.gov

The example of sea height

In situ approaches

- Local measurements:
  - flood level markers,
  - GPS buoys.
- Need of a lot of data points to get a global coverage...

parc-cotentin-bessin.fr

ndbc.noaa.gov

Remote sensing approaches

- Remote measurements:
  - radar flood gauge,
  - satellites.
- Local to global coverage.

water.weather.gov

CNES

In situ approaches

- Local measurements:
  - flood level markers,
  - GPS buoys.
- Need of a lot of data points global coverage...

ote sensing approaches

- neasurements:
  - flood gauge,
  - lites.
- global coverage.

parc-cotentin-bessin.fr

ndbc.

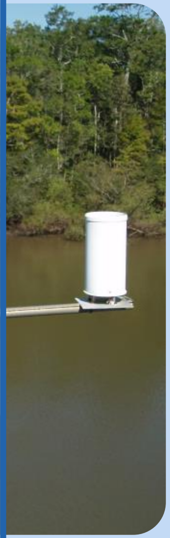

her.gov

CNES

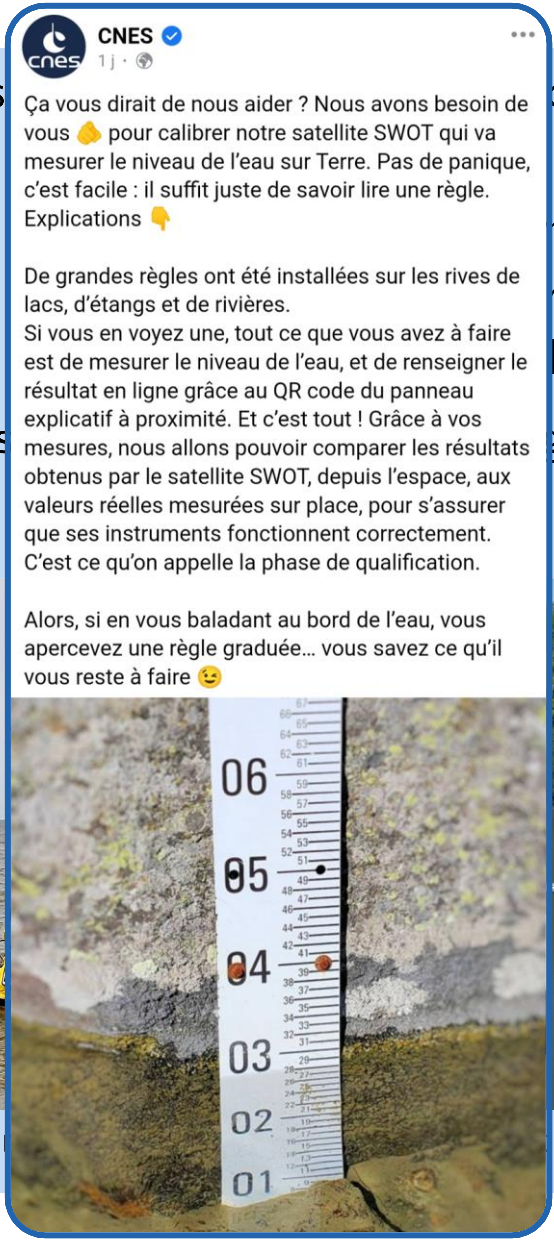

CNES
1 j ·

Ça vous dirait de nous aider ? Nous avons besoin de vous 🫵 pour calibrer notre satellite SWOT qui va mesurer le niveau de l'eau sur Terre. Pas de panique, c'est facile : il suffit juste de savoir lire une règle. Explications 👇

De grandes règles ont été installées sur les rives de lacs, d'étangs et de rivières.
Si vous en voyez une, tout ce que vous avez à faire est de mesurer le niveau de l'eau, et de renseigner le résultat en ligne grâce au QR code du panneau explicatif à proximité. Et c'est tout ! Grâce à vos mesures, nous allons pouvoir comparer les résultats obtenus par le satellite SWOT, depuis l'espace, aux valeurs réelles mesurées sur place, pour s'assurer que ses instruments fonctionnent correctement. C'est ce qu'on appelle la phase de qualification.

Alors, si en vous baladant au bord de l'eau, vous apercevez une règle graduée... vous savez ce qu'il vous reste à faire 😉

Remote sensing

Acquisition of information about an object without making physical contact with it.

Remote sensing

Acquisition of information about an object without making physical contact with it.

- Applications: the object is not accessible (astronomy, atmosphere, oceans, meteorology, ...).

Remote sensing

Acquisition of information about an object without making physical contact with it.

- Applications: the object is not accessible (astronomy, atmosphere, oceans, meteorology, ...).
- Active remote sensing:
  - a signal is emitted to the object and its reflection is detected by the sensor,
  - radar, lidar, sonar, etc.

Remote sensing

Acquisition of information about an object without making physical contact with it.

- Applications: the object is not accessible (astronomy, atmosphere, oceans, meteorology, ...).
- Active remote sensing:
  - a signal is emitted to the object and its reflection is detected by the sensor,
  - radar, lidar, sonar, etc.
- Passive remote sensing:
  - when the reflection of an external source is detected by the sensor,
  - hyperspectral imaging, radiometers.

Remote sensing

Acquisition of information about an object without making physical contact with it.

- Applications: the object is not accessible (astronomy, atmosphere, oceans, meteorology, ...).
- Active remote sensing:
  - a signal is emitted to the object and its reflection is detected by the sensor,
  - radar, lidar, sonar, etc.
- Passive remote sensing:
  - when the reflection of an external source is detected by the sensor,
  - hyperspectral imaging, radiometers.
- Type of signal: Electromagnetic and acoustic waves. Choice of the wavelength:
  - L-band (15 - 30 cm): tree leaves (biomass, snow depth),
  - X-band (2.5 - 3.75 cm): rain drops (precipitations),
  - K-band (1.11 - 1.67 cm): water vapor (clouds).

Remote sensing

Acquisition of information about an object without making physical contact with it.

- Applications: the object is not accessible (astronomy, atmosphere, oceans, meteorology, ...).
- Active remote sensing:
  - a signal is emitted to the object and its reflection is detected by the sensor,
  - radar, lidar, sonar, etc.
- Passive remote sensing:
  - when the reflection of an external source is detected by the sensor,
  - hyperspectral imaging, radiometers.
- Type of signal: Electromagnetic and acoustic waves. Choice of the wavelength:
  - L-band (15 - 30 cm): tree leaves (biomass, snow depth),
  - X-band (2.5 - 3.75 cm): rain drops (precipitations),
  - K-band (1.11 - 1.67 cm): water vapor (clouds).

Global Navigation Satellite System (GNSS)

Positioning system.

GNSS principle

Positioning system.

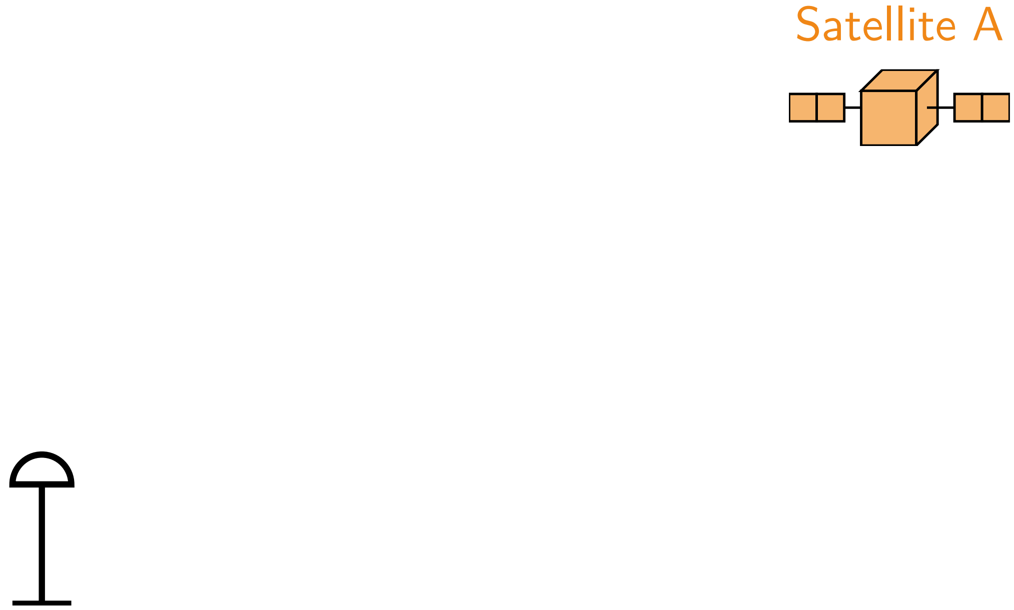

Positioning system.
Satellite constellations: GPS, GALILEO, BeiDou, GLONASS and others.

GNSS principle

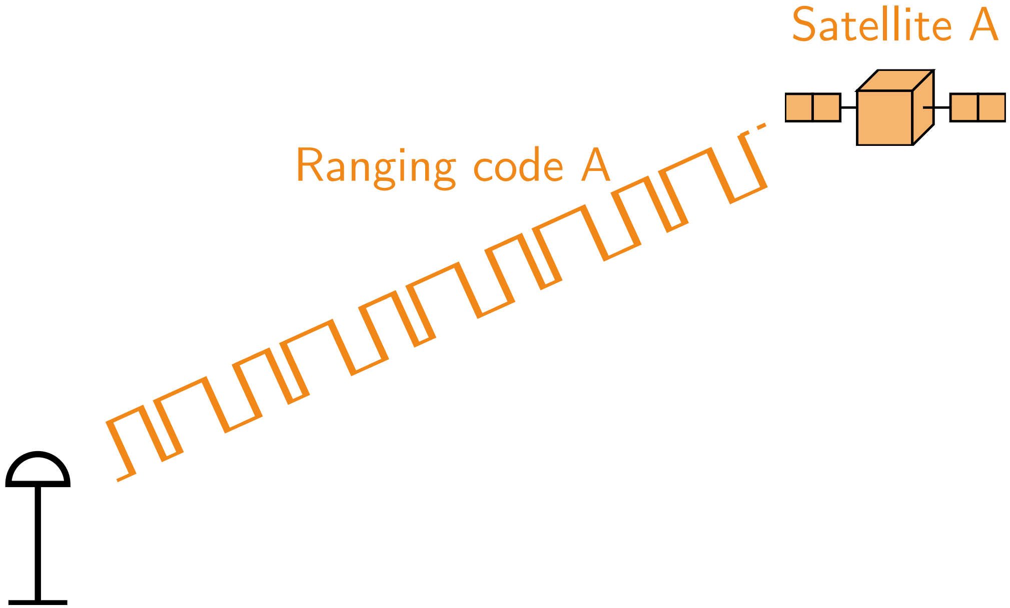

GNSS principle

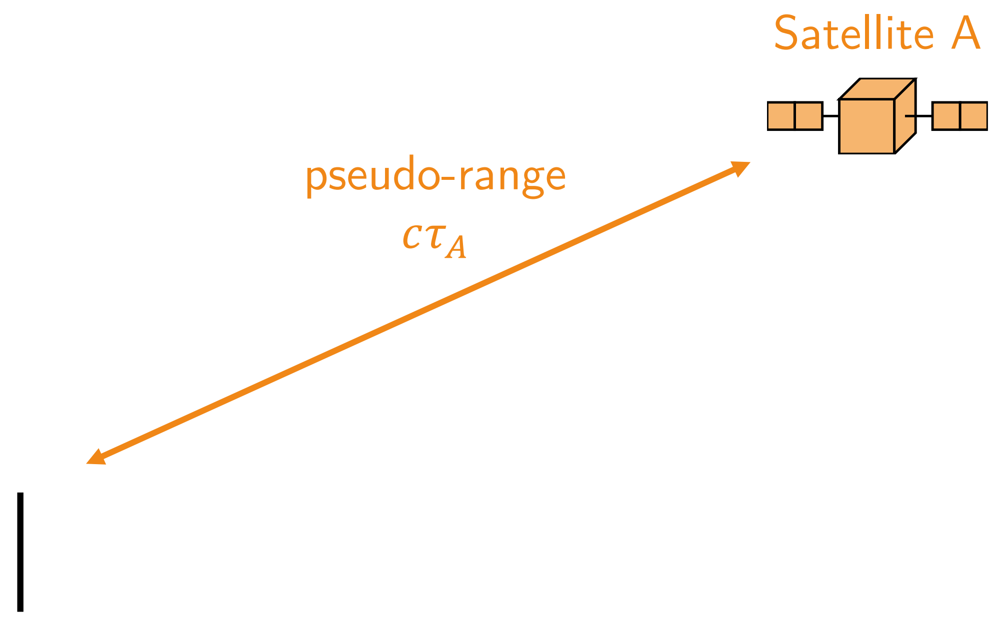

Pseudo-range ≠ geometric distance:
tropospheric delay, ionospheric delay, clock biases and others to be compensated.

GNSS principle

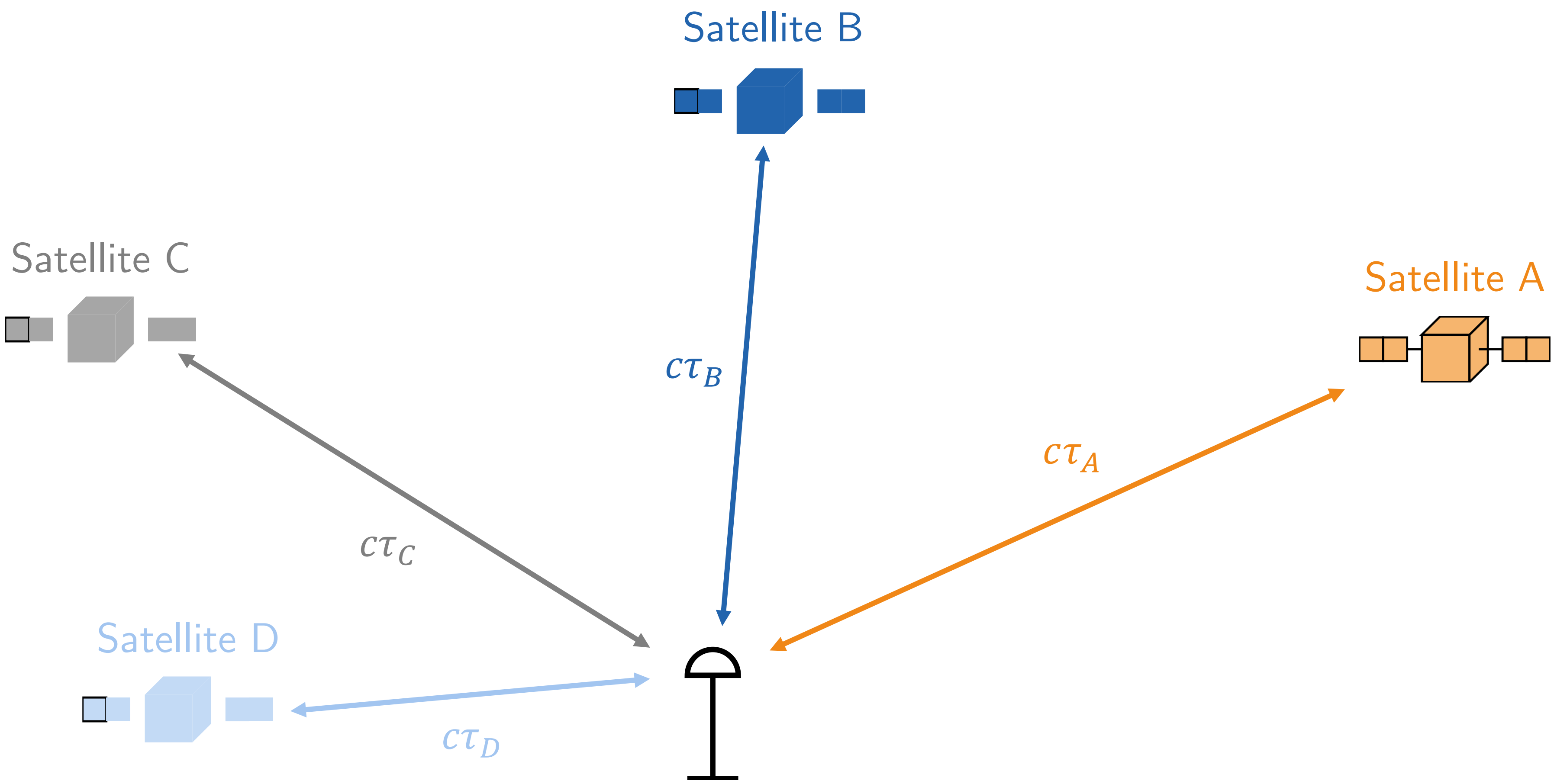

Position Velocity Timing (PVT) solution:
trilateration using three satellites + 1 satellite to estimate the receiver clock bias.

GNSS signal processing

Standard GNSS signal processing:

- range estimation: time-delay estimation,
- cross-correlation.

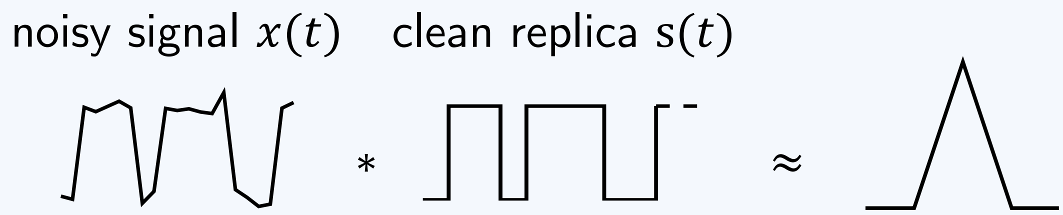

GNSS signal processing

Satellite B

Standard GNSS signal processing:

- range estimation: time-delay estimation,
- cross-correlation.

noisy signal $x(t)$ clean replica $s(t)$

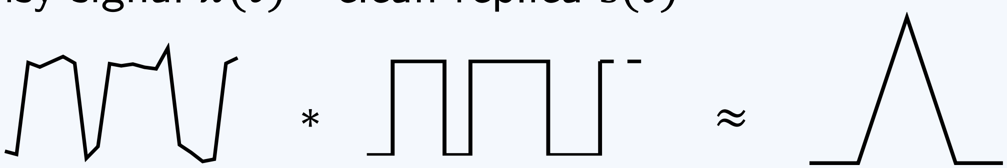

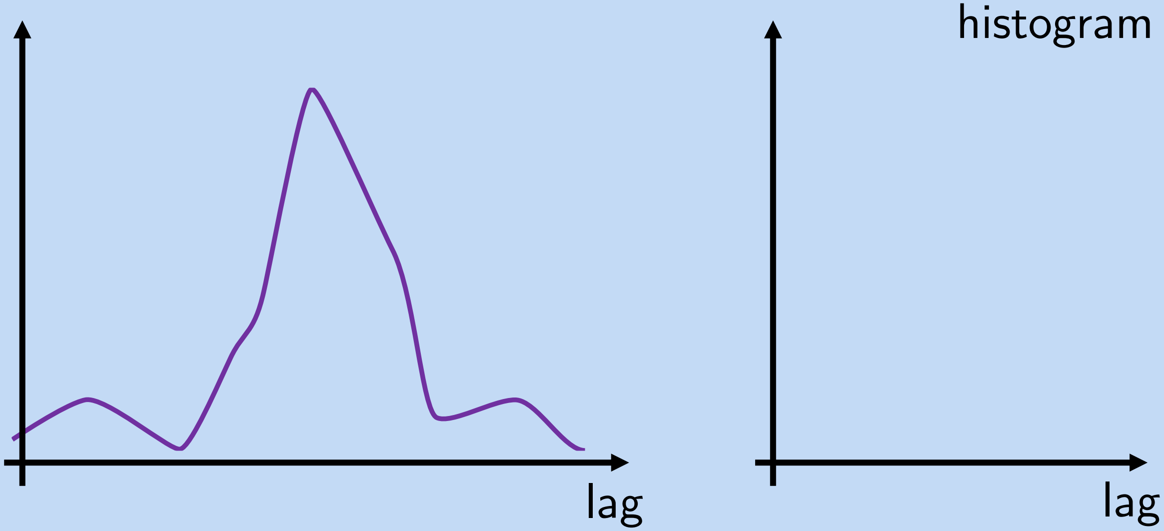

GNSS signal processing

Satellite B

Standard GNSS signal processing:

- range estimation: time-delay estimation,
- cross-correlation.

noisy signal $x(t)$ clean replica $s(t)$

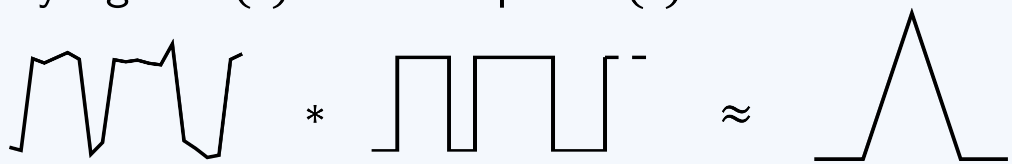

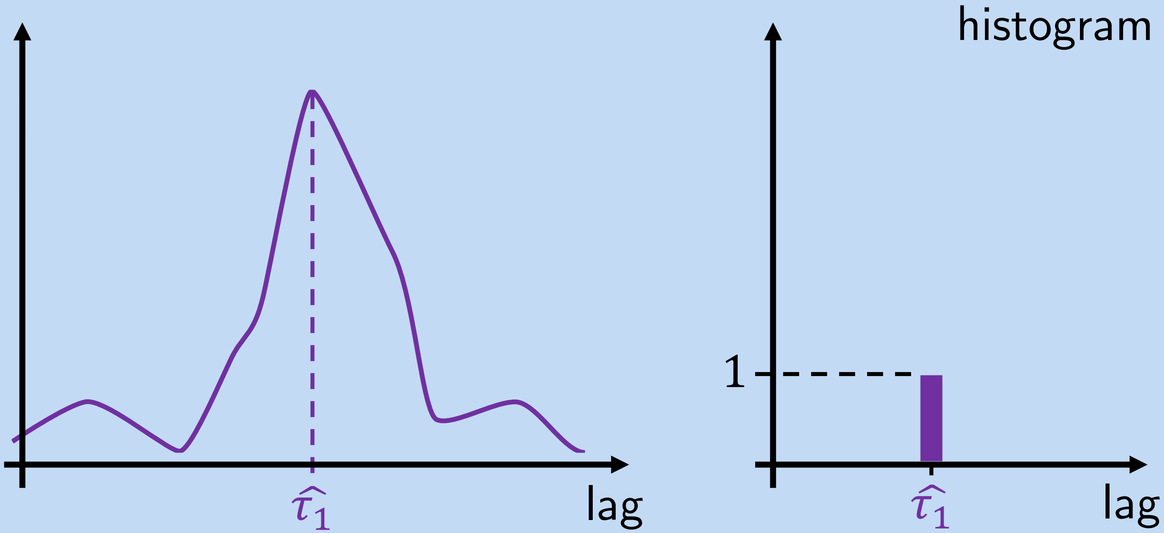

GNSS signal processing

Satellite B

Standard GNSS signal processing:

- range estimation: time-delay estimation,
- cross-correlation.

noisy signal $x(t)$ clean replica $s(t)$

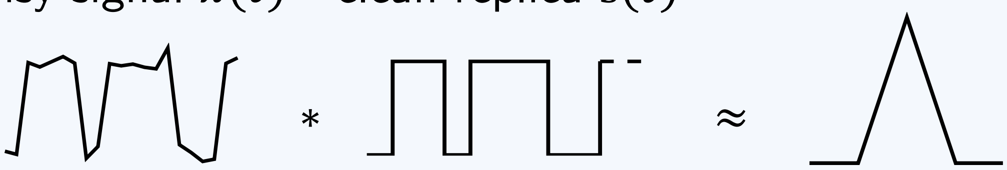

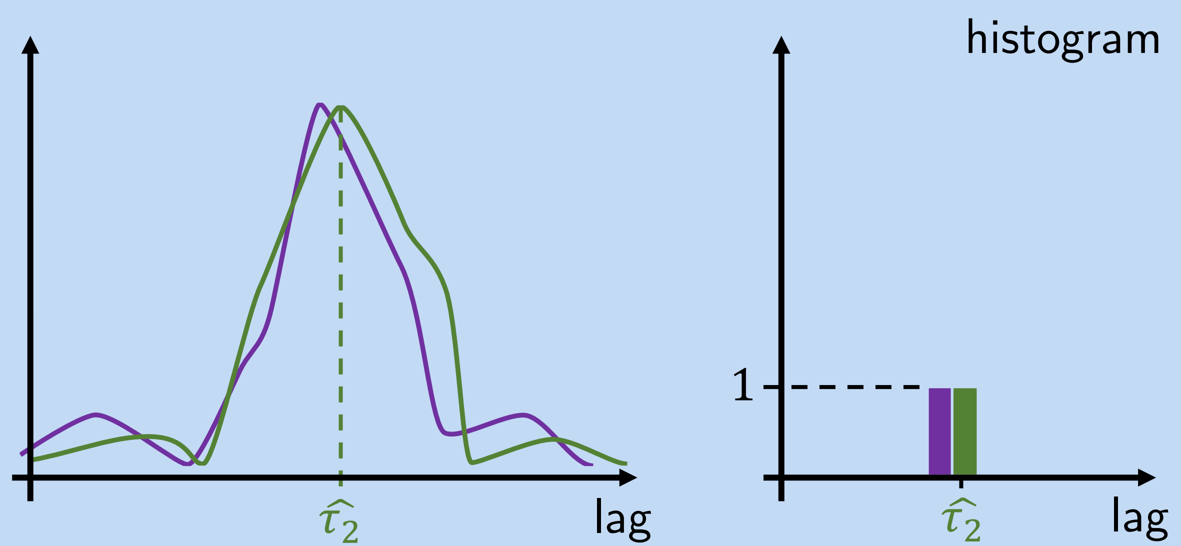

Standard GNSS signal processing:

- range estimation: time-delay estimation,
- cross-correlation.

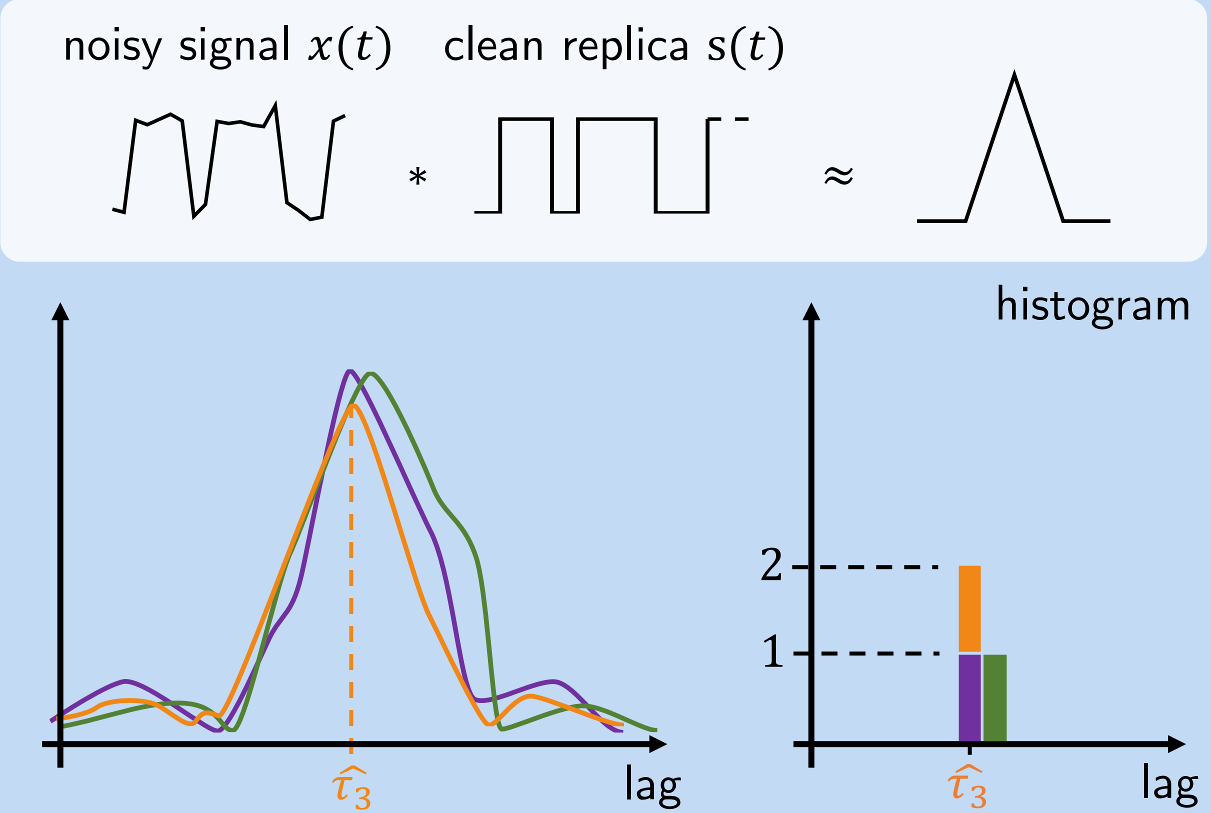

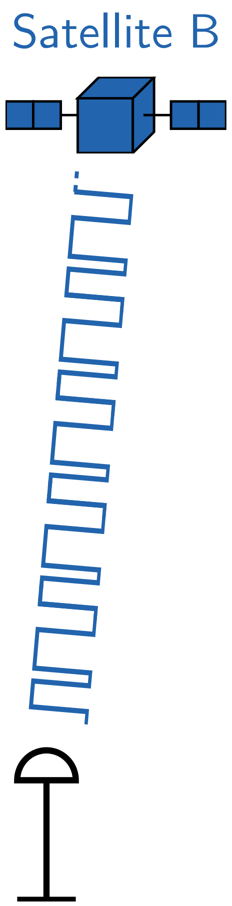

Standard GNSS signal processing:

- range estimation: time-delay estimation,
- cross-correlation.

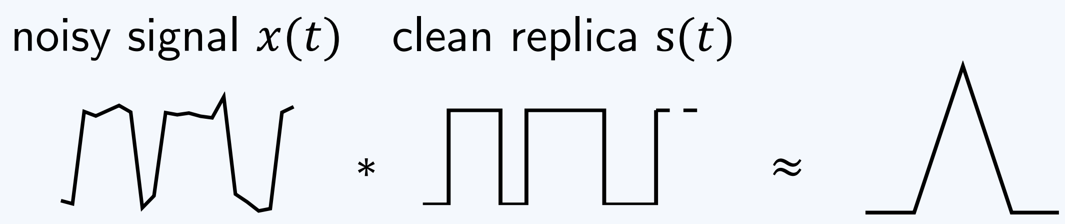

What one expects from an estimator:

- unbiased: $\mu_\tau = \tau_{true}$,
- minimum variance: $\sigma_\tau = \text{CRB}(\tau)$.

CRB: Cramér-Rao bound.

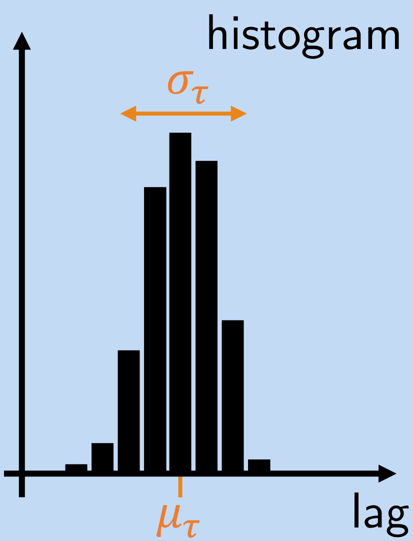

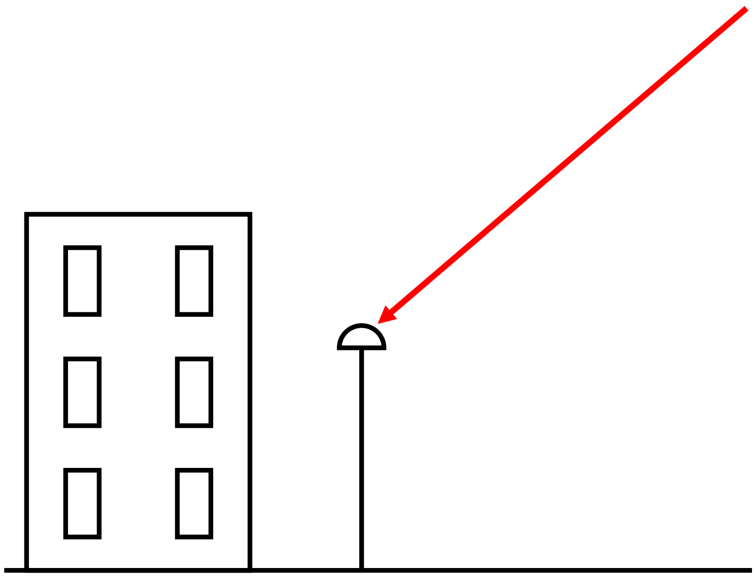

Definition [Kaplan and Hegarty, 2017]: *Multipath is the reception of multiple reflected and diffracted replicas of the desired signal, along with the direct path signal.*

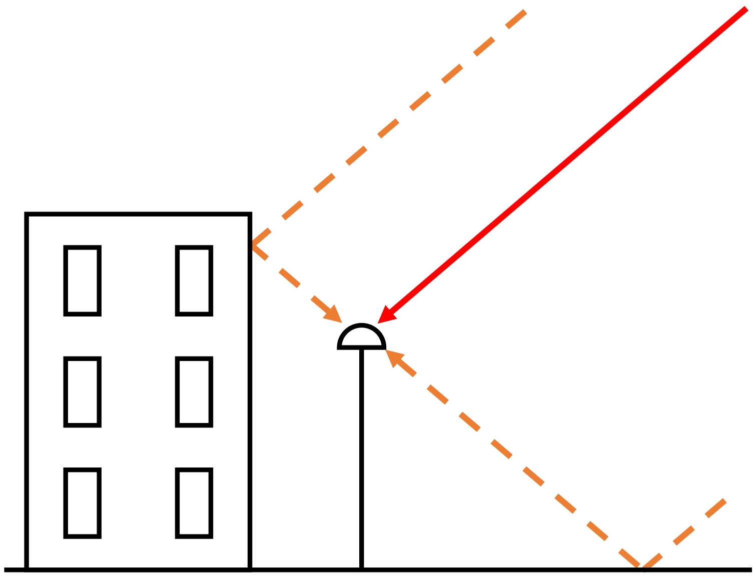

Definition [Kaplan and Hegarty, 2017]:
Multipath is the reception of multiple reflected and diffracted replicas of the desired signal, along with the direct path signal.

GNSS multipath

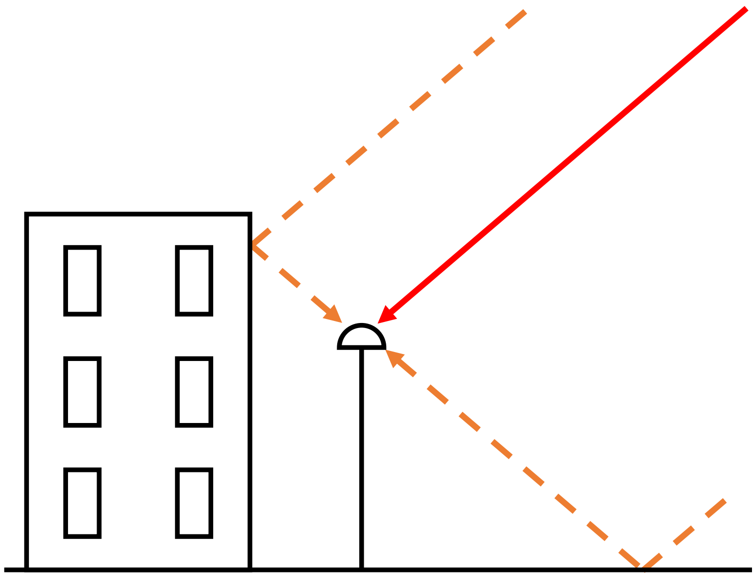

Definition [Kaplan and Hegarty, 2017]: *Multipath is the reception of multiple reflected and diffracted replicas of the desired signal, along with the direct path signal.*

- Degradation of the estimation:
  - bias induced,
  - variance affected.
- In mobile applications: random and dynamic phenomenon.

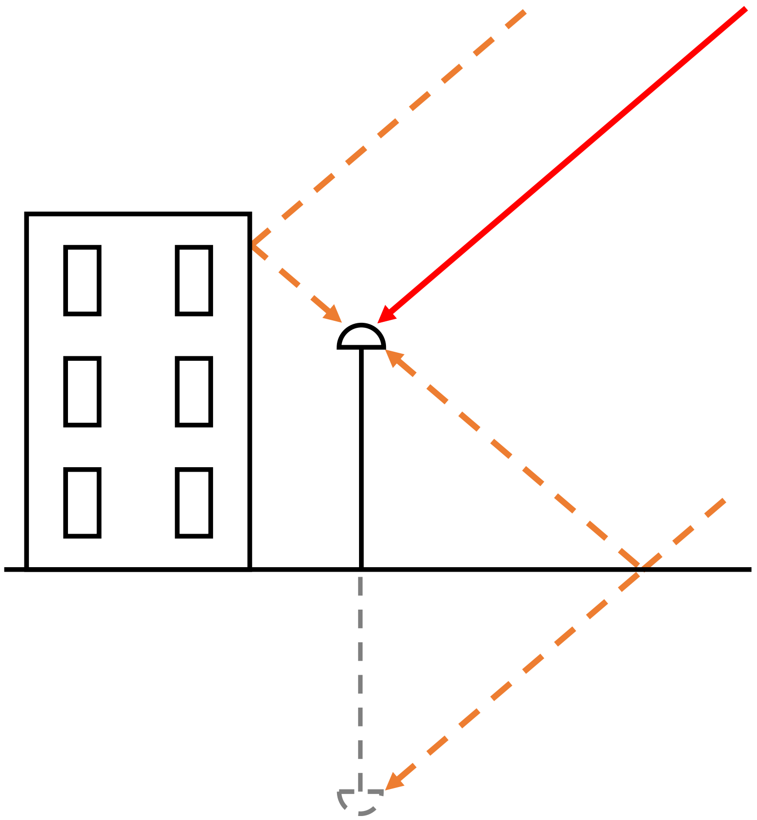

Definition [Kaplan and Hegarty, 2017]: *Multipath is the reception of multiple reflected and diffracted replicas of the desired signal, along with the direct path signal.*

- Degradation of the estimation:
  - bias induced,
  - variance affected.
- In mobile applications: random and dynamic phenomenon.

GNSS multipath

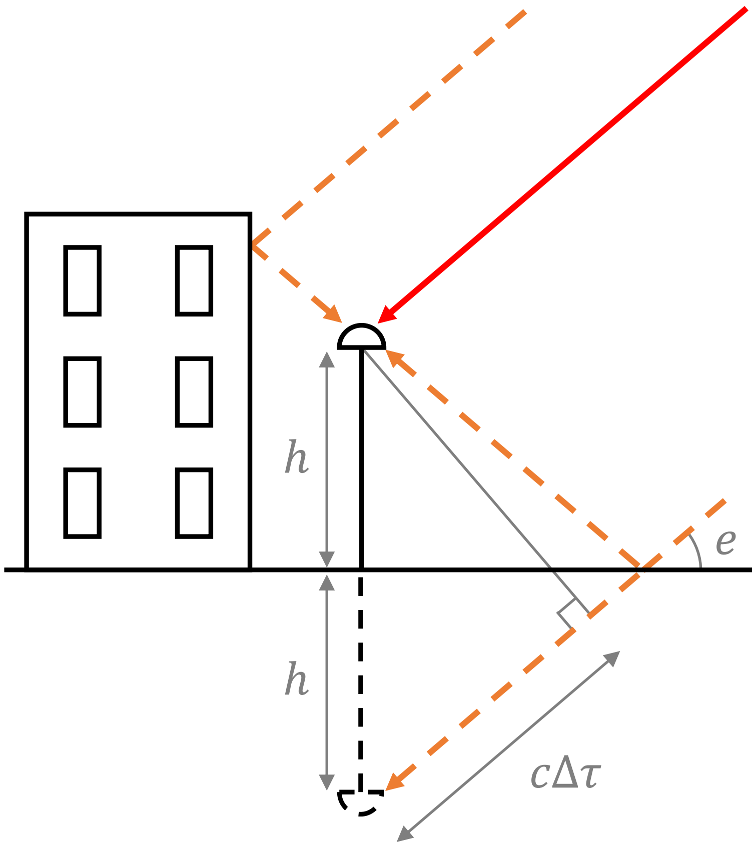

Definition [Kaplan and Hegarty, 2017]:
Multipath is the reception of multiple reflected and diffracted replicas of the desired signal, along with the direct path signal.

- Degradation of the estimation:
  - bias induced
  - variance affected
- In mobile applications: random and dynamic phenomenon
- It contains information!
  - Geometric equation:

$$c\Delta\tau = 2h\sin(e)$$

GNSS reflectometry (GNSS-R)

GNSS-R: study of GNSS signals reflected upon the Earth

- GNSS signals: L-band signals received 24/7 anywhere on Earth: signals of opportunity,
- altimetry and/or reflecting surfaces properties (e.g., reflectivity, roughness).

GNSS reflectometry (GNSS-R)

GNSS-R: study of GNSS signals reflected upon the Earth

- GNSS signals: L-band signals received 24/7 anywhere on Earth: signals of opportunity,
- altimetry and/or reflecting surfaces properties (e.g., reflectivity, roughness).

ground-based

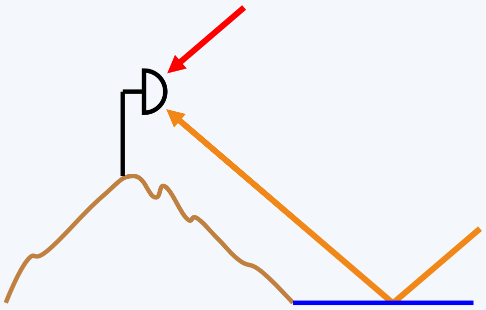

- local coverage
- coherent reflections
- one or two antennas

GNSS reflectometry (GNSS-R)

GNSS-R: study of GNSS signals reflected upon the Earth

- GNSS signals: L-band signals received 24/7 anywhere on Earth: signals of opportunity,
- altimetry and/or reflecting surfaces properties (e.g., reflectivity, roughness).

ground-based

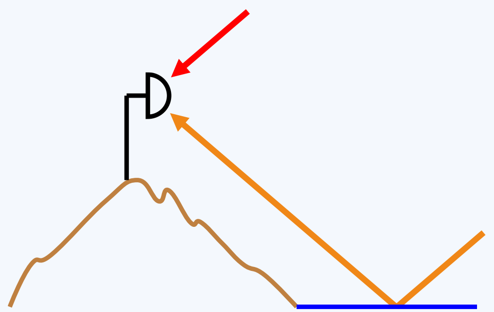

- local coverage
- coherent reflections
- one or two antennas

airborne

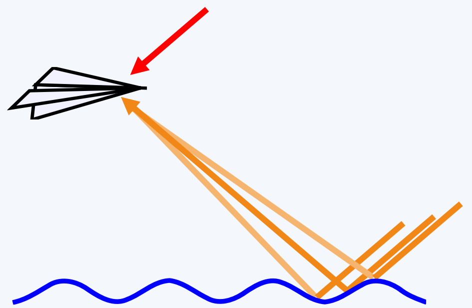

- wide coverage
- coherent and non-coherent reflections
- two antennas

GNSS reflectometry (GNSS-R)

GNSS-R: study of GNSS signals reflected upon the Earth

- GNSS signals: L-band signals received 24/7 anywhere on Earth: signals of opportunity,
- altimetry and/or reflecting surfaces properties (e.g., reflectivity, roughness).

ground-based

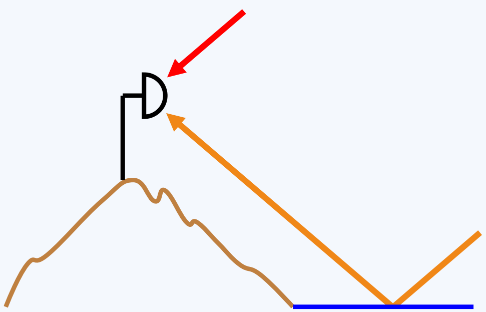

- local coverage
- coherent reflections
- one or two antennas

airborne

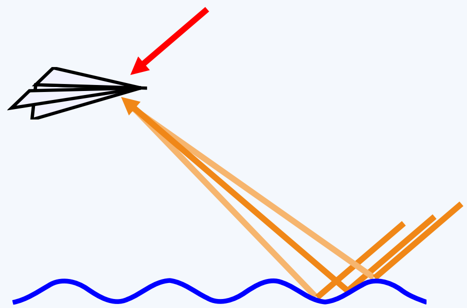

- wide coverage
- coherent and non-coherent reflections
- two antennas

spaceborne

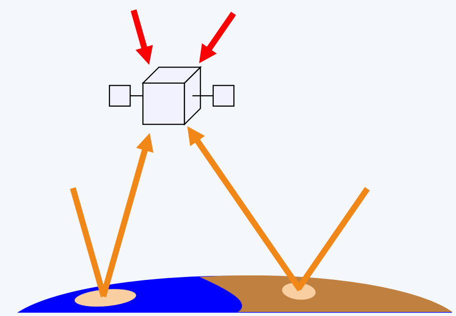

- worldwide coverage
- coherent and non-coherent reflections
- two antennas

GNSS-R: study of GNSS signals reflected upon the Earth

- GNSS signals: L-band signals received 24/7 anywhere on Earth: signals of opportunity,
- altimetry and/or reflecting surfaces properties (e.g., reflectivity, roughness).

ground-based

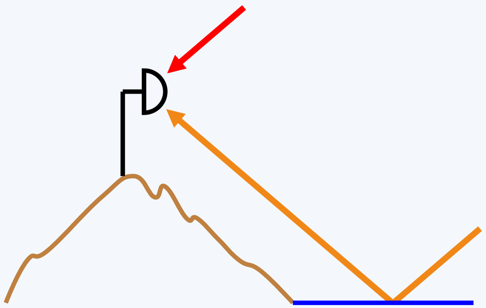

- local coverage
- coherent reflections
- one or two antennas

airborne

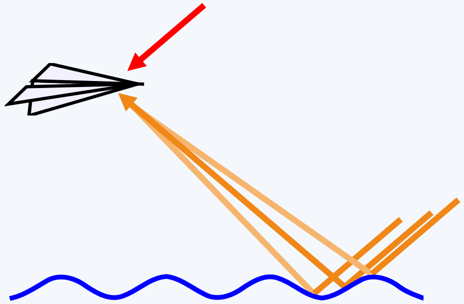

- wide coverage
- coherent and non-coherent reflections
- two antennas

spaceborne

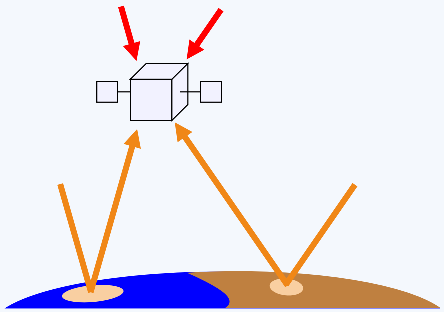

- worldwide coverage
- coherent and non-coherent reflections
- two antennas

GNSS-R: study of GNSS signals reflected upon the Earth

- GNSS signals: L-band signals received 24/7 anywhere on Earth: signals of opportunity,
- altimetry and/or reflecting surfaces properties (e.g., reflectivity, roughness).

ground-based ① ②

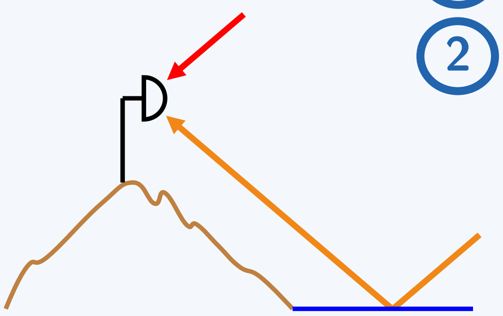

- local coverage
- coherent reflections
- one or two antennas

airborne ③

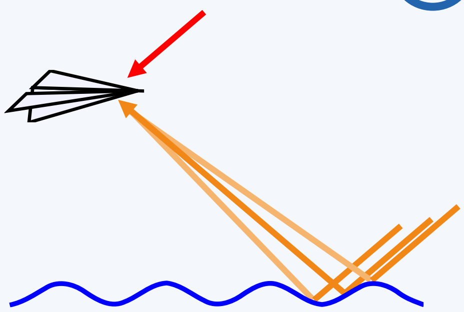

- wide coverage
- coherent and non-coherent reflections
- two antennas

spaceborne

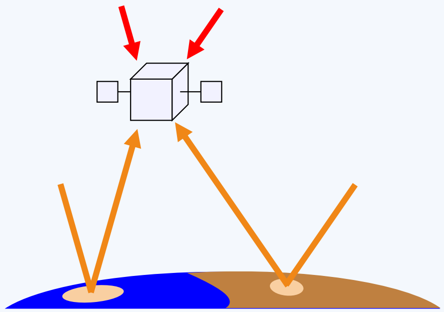

- worldwide coverage
- coherent and non-coherent reflections
- two antennas

Objective of the thesis

Use signal processing and estimation theory tools as a mathematical framework for GNSS-R

Objective of the thesis

Use signal processing and estimation theory tools as a mathematical framework for GNSS-R

1. Dual source signal model:
   - definition,
   - estimation challenge,
   - lower bound.

Objective of the thesis

Use signal processing and estimation theory tools as a mathematical framework for GNSS-R

1. Dual source signal model:
   - definition,
   - estimation challenge,
   - lower bound.
2. Ground-based GNSS-R:
   - data collection campaign,
   - processing example.

Objective of the thesis

Use signal processing and estimation theory tools as a mathematical framework for GNSS-R

1. Dual source signal model:
   - definition,
   - estimation challenge,
   - lower bound.
2. Ground-based GNSS-R:
   - data collection campaign,
   - processing example.
3. Diffuse reflection:
   - definition,
   - estimation and detection challenges.

Objective of the thesis

Use signal processing and estimation theory tools as a mathematical framework for GNSS-R

1. Dual source signal model:
   - definition,
   - estimation challenge,
   - lower bound.
2. Ground-based GNSS-R:
   - data collection campaign,
   - processing example.
3. Diffuse reflection:
   - definition,
   - estimation and detection challenges.

Theoretical approach (1)

Experimental approach (2)

Exploratory approach (3)

1 - Dual source signal model

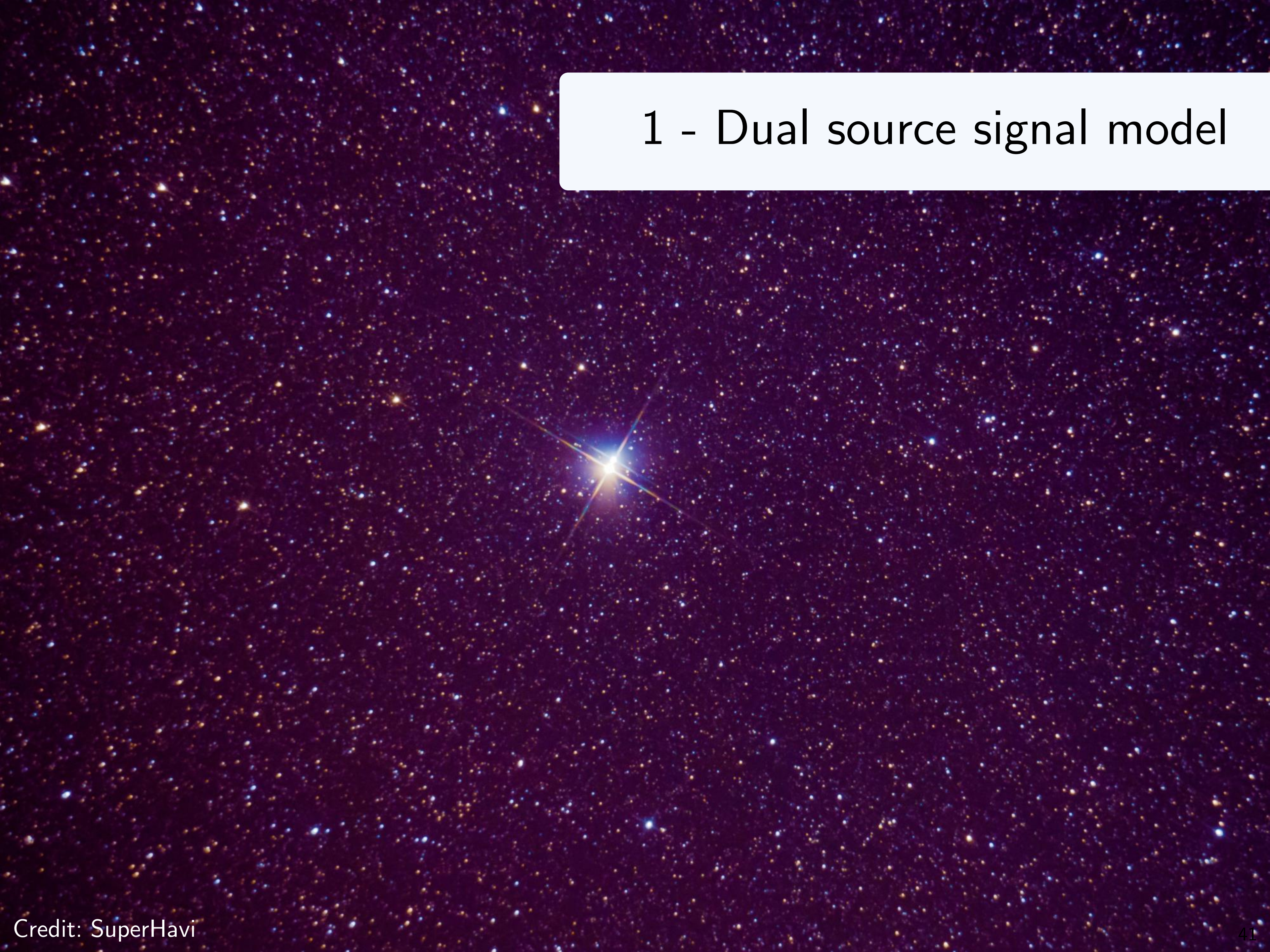

Credit: SuperHavi

Signal model

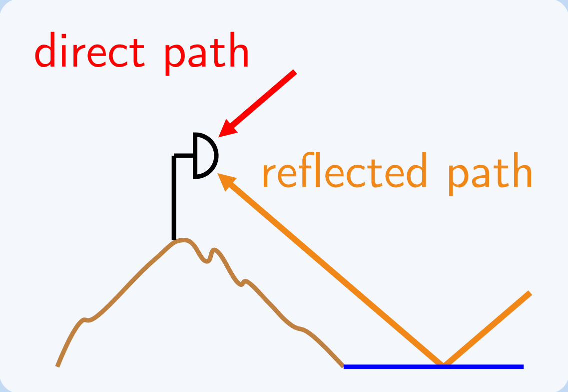

- Dual source signal model with specular reflection:

$$\mathbf{x} = \mathbf{A}(\boldsymbol{\eta}_0, \boldsymbol{\eta}_1)\boldsymbol{\alpha} + \mathbf{w}, \mathbf{w} \sim CN(\mathbf{0}, \sigma_n^2 \mathbf{I}_\mathrm{N}),$$

with N the number of samples and, for $\boldsymbol{\eta}_i^T = \left(\tau_i, F_{d,i}\right)$,

$$\mathbf{A}(\boldsymbol{\eta}_0, \boldsymbol{\eta}_1) = [\mathbf{s}(\boldsymbol{\eta}_0), \mathbf{s}(\boldsymbol{\eta}_1)],$$

$$\mathbf{s}(\boldsymbol{\eta}_i) = (\dots, s(nT_s - \tau_i)e^{-j2\pi F_{d,i}(nT_s - \tau_i)}, \dots),$$

$$\boldsymbol{\alpha}^T = \left(\rho_0 e^{j\phi_0}, \rho_1 e^{j\phi_1}\right).$$

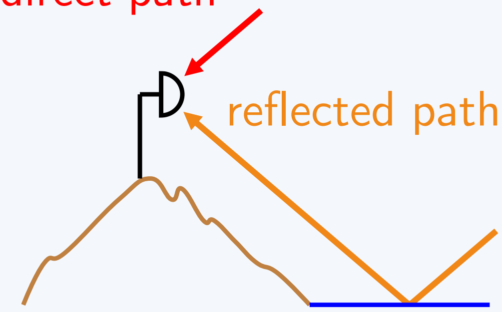

Signal model

- Dual source signal model with specular reflection:

$$\mathbf{x} = \mathbf{A}(\boldsymbol{\eta}_0, \boldsymbol{\eta}_1)\boldsymbol{\alpha} + \mathbf{w}, \mathbf{w} \sim CN(\mathbf{0}, \sigma_n^2 \mathbf{I}_\mathrm{N}),$$

with N the number of samples and, for $\boldsymbol{\eta}_i^T = (\tau_i, F_{d,i})$,

$$\mathbf{A}(\boldsymbol{\eta}_0, \boldsymbol{\eta}_1) = [\mathbf{s}(\boldsymbol{\eta}_0), \mathbf{s}(\boldsymbol{\eta}_1)],$$

$$\mathbf{s}(\boldsymbol{\eta}_i) = (\dots, s(nT_s - \tau_i)e^{-j2\pi F_{d,i}(nT_s - \tau_i)}, \dots),$$

$$\boldsymbol{\alpha}^T = (\rho_0 e^{j\phi_0}, \rho_1 e^{j\phi_1}).$$

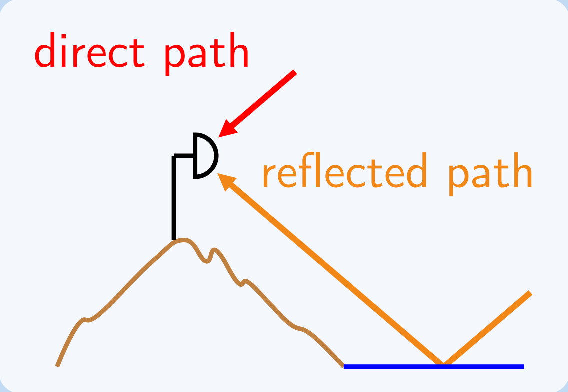

- Deterministic parameters formulation with the following vector of unknowns:

$$\boldsymbol{\epsilon}^T = (\sigma_n^2, \underbrace{\tau_0, F_{d,0}, \rho_0, \phi_0}_{\boldsymbol{\theta}_0^T}, \underbrace{\tau_1, F_{d,1}, \rho_1, \phi_1}_{\boldsymbol{\theta}_1^T}).$$

Cramér-Rao bound (CRB)

- Problem: estimate $\boldsymbol{\epsilon}$. How good can we get?

Cramér-Rao bound (CRB)

- Problem: estimate $\boldsymbol{\epsilon}$. How good can we get?
- Cramér-Rao bound: theoretical lower bound for the variance of any locally unbiased estimator.

Cramér-Rao bound (CRB)

- Problem: estimate $\boldsymbol{\epsilon}$. How good can we get?
- Cramér-Rao bound: theoretical lower bound for the variance of any locally unbiased estimator.
- From the signal model, the Fisher Information Matrix (FIM) can be obtained using the Slepian-Bangs formula [Yau and Bresler, 1992]:

$$\left[\mathbf{F}_{\epsilon|\epsilon}(\boldsymbol{\epsilon})\right]_{k,l} = \frac{2}{\sigma_n^2}\mathrm{Re}\left\{\left(\frac{\partial \mathbf{A}\boldsymbol{\alpha}}{\partial \epsilon_k}\right)^H \left(\frac{\partial \mathbf{A}\boldsymbol{\alpha}}{\partial \epsilon_l}\right)\right\} + \frac{N}{\sigma_n^4}\frac{\partial \sigma_n^2}{\partial \epsilon_k}\frac{\partial \sigma_n^2}{\partial \epsilon_l}.$$

Cramér-Rao bound (CRB)

- Problem: estimate $\boldsymbol{\epsilon}$. How good can we get?
- Cramér-Rao bound: theoretical lower bound for the variance of any locally unbiased estimator.
- From the signal model, the Fisher Information Matrix (FIM) can be obtained using the Slepian-Bangs formula [Yau and Bresler, 1992]:

$$\left[\mathbf{F}_{\epsilon|\epsilon}(\boldsymbol{\epsilon})\right]_{k,l} = \frac{2}{\sigma_n^2} \mathrm{Re}\left\{\left(\frac{\partial \mathbf{A}\boldsymbol{\alpha}}{\partial \epsilon_k}\right)^H \left(\frac{\partial \mathbf{A}\boldsymbol{\alpha}}{\partial \epsilon_l}\right)\right\} + \frac{N}{\sigma_n^4} \frac{\partial \sigma_n^2}{\partial \epsilon_k} \frac{\partial \sigma_n^2}{\partial \epsilon_l}.$$

- The CRB for the estimation of $\boldsymbol{\epsilon}$ is obtained by inverting the FIM:

$$\mathbf{CRB}_{\epsilon|\epsilon}(\boldsymbol{\epsilon}) = \left[\mathbf{F}_{\epsilon|\epsilon}(\boldsymbol{\epsilon})\right]^{-1}.$$

Cramér-Rao bound (CRB)

$$\mathbf{CRB}_{\epsilon|\epsilon}(\epsilon) = \begin{bmatrix} F_{\sigma_n^2|\epsilon} & \mathbf{0} & \mathbf{0} \\ \mathbf{0} & \mathbf{F}_{\theta_0|\epsilon} & \mathbf{F}_{\theta_0,\theta_1|\epsilon} \\ \mathbf{0} & \mathbf{F}_{\theta_1,\theta_0|\epsilon} & \mathbf{F}_{\theta_1|\epsilon} \end{bmatrix}^{-1}.$$

- Closed-form expression that depends on the signal baseband samples.

- $\mathbf{F}_{\theta_i|\epsilon}$: known uncoupled contribution from each signal,
- $\mathbf{F}_{\theta_1,\theta_0|\epsilon} = \mathbf{F}^{\mathbf{T}}_{\theta_0,\theta_1|\epsilon}$: interference terms!

$$\mathbf{CRB}_{\epsilon|\epsilon}(\epsilon) = \begin{bmatrix} F_{\sigma_n^2|\epsilon} & \mathbf{0} & \mathbf{0} \\ \mathbf{0} & \mathbf{F}_{\theta_0|\epsilon} & \mathbf{F}_{\theta_0,\theta_1|\epsilon} \\ \mathbf{0} & \mathbf{F}_{\theta_1,\theta_0|\epsilon} & \mathbf{F}_{\theta_1|\epsilon} \end{bmatrix}^{-1}.$$

- Closed-form expression that depends on the signal baseband samples.

- $\mathbf{F}_{\theta_i|\epsilon}$: known uncoupled contribution from each signal,
- $\mathbf{F}_{\theta_1,\theta_0|\epsilon} = \mathbf{F}_{\theta_0,\theta_1|\epsilon}^{\mathbf{T}}$: interference terms!

- Validation of the expression:
  - implementation of an **efficient estimator** (unbiased and variance equal to the CRB) and check the variance.

Cramér-Rao bound (CRB)

$$\mathbf{CRB}_{\epsilon|\epsilon}(\epsilon) = \begin{bmatrix} F_{\sigma_n^2|\epsilon} & \mathbf{0} & \mathbf{0} \\ \mathbf{0} & \mathbf{F}_{\theta_0|\epsilon} & \mathbf{F}_{\theta_0,\theta_1|\epsilon} \\ \mathbf{0} & \mathbf{F}_{\theta_1,\theta_0|\epsilon} & \mathbf{F}_{\theta_1|\epsilon} \end{bmatrix}^{-1}.$$

- Closed-form expression that depends on the signal baseband samples.
- $\mathbf{F}_{\theta_i|\epsilon}$: known uncoupled contribution from each signal,
- $\mathbf{F}_{\theta_1,\theta_0|\epsilon} = \mathbf{F}^{\mathbf{T}}_{\theta_0,\theta_1|\epsilon}$: interference terms!
- Validation of the expression:
  - implementation of an **efficient estimator** (unbiased and variance equal to the CRB) and check the variance.
  - Such an estimator does not exist for the non-linear problem at hand...
  - Estimator asymptotically efficient (when the number of observations [Stoica and Nehorai, 1990] or the the signal to noise ratio [Renaux *et al.* 2006] become large): the maximum likelihood estimator!

Dual source maximum likelihood estimator (2S-MLE)

- Signal model: $\mathbf{x} = \mathbf{A}(\boldsymbol{\eta}_0, \boldsymbol{\eta}_1)\boldsymbol{\alpha} + \mathbf{w}, \mathbf{w} \sim \mathcal{CN}(\mathbf{0}, \sigma_n^2 \mathbf{I}_{\mathrm{N}}) \Rightarrow \mathbf{x} \sim \boldsymbol{\mathcal{CN}}(\mathbf{A}\boldsymbol{\alpha}, \sigma_n^2 \mathbf{I}_N)$.

- Signal model: $\mathbf{x} = \mathbf{A}(\boldsymbol{\eta}_0, \boldsymbol{\eta}_1)\boldsymbol{\alpha} + \mathbf{w}, \mathbf{w} \sim CN(\mathbf{0}, \sigma_n^2 \mathbf{I}_\mathrm{N}) \Rightarrow \mathbf{x} \sim \boldsymbol{CN}(\mathbf{A}\boldsymbol{\alpha}, \sigma_n^2 \mathbf{I}_N)$.

- **Maximum likelihood estimation**: $\hat{\boldsymbol{\epsilon}}$ maximizes the likelihood $p(\mathbf{x}; \boldsymbol{\epsilon})$ that the process described by the model produced the data $\mathbf{x}$ that was actually observed:

$$\hat{\boldsymbol{\epsilon}} = \arg\max_{\boldsymbol{\epsilon}} \{p(\mathbf{x}; \boldsymbol{\epsilon})\} \text{ where } p(\mathbf{x}; \boldsymbol{\epsilon}) = \frac{1}{(\pi\sigma_n^2)^N} e^{-\frac{1}{\sigma_n^2}\|\mathbf{x}-\mathbf{A}\boldsymbol{\alpha}\|^2}.$$

Dual source maximum likelihood estimator (2S-MLE)

- Signal model: $\mathbf{x} = \mathbf{A}(\boldsymbol{\eta}_0, \boldsymbol{\eta}_1)\boldsymbol{\alpha} + \mathbf{w}, \mathbf{w} \sim CN(\mathbf{0}, \sigma_n^2 \mathbf{I}_\mathrm{N}) \Rightarrow \mathbf{x} \sim \boldsymbol{CN}(\mathbf{A}\boldsymbol{\alpha}, \sigma_n^2 \mathbf{I}_N)$.

- **Maximum likelihood estimation**: $\hat{\boldsymbol{\epsilon}}$ maximizes the likelihood $p(\mathbf{x}; \boldsymbol{\epsilon})$ that the process described by the model produced the data $\mathbf{x}$ that was actually observed:

$$\hat{\boldsymbol{\epsilon}} = \arg\max_{\boldsymbol{\epsilon}} \{p(\mathbf{x}; \boldsymbol{\epsilon})\} \text{ where } p(\mathbf{x}; \boldsymbol{\epsilon}) = \frac{1}{(\pi\sigma_n^2)^N} e^{-\frac{1}{\sigma_n^2}\|\mathbf{x}-\mathbf{A}\boldsymbol{\alpha}\|^2}.$$

- 9-dimensional grid search!

Dual source maximum likelihood estimator (2S-MLE)

- Signal model: $\mathbf{x} = \mathbf{A}(\boldsymbol{\eta}_0, \boldsymbol{\eta}_1)\boldsymbol{\alpha} + \mathbf{w}, \mathbf{w} \sim CN(\mathbf{0}, \sigma_n^2 \mathbf{I}_\mathrm{N}) \Rightarrow \mathbf{x} \sim \boldsymbol{CN}(\mathbf{A}\boldsymbol{\alpha}, \sigma_n^2 \mathbf{I}_N)$.

- **Maximum likelihood estimation**: $\hat{\boldsymbol{\epsilon}}$ maximizes the likelihood $p(\mathbf{x}; \boldsymbol{\epsilon})$ that the process described by the model produced the data $\mathbf{x}$ that was actually observed:

$$\hat{\boldsymbol{\epsilon}} = \arg\max_{\boldsymbol{\epsilon}} \{p(\mathbf{x}; \boldsymbol{\epsilon})\} \text{ where } p(\mathbf{x}; \boldsymbol{\epsilon}) = \frac{1}{(\pi \sigma_n^2)^N} e^{-\frac{1}{\sigma_n^2} \|\mathbf{x} - \mathbf{A}\boldsymbol{\alpha}\|^2}.$$

- 9-dimensional grid search!

$$\max_{\boldsymbol{\epsilon}} \{p(\mathbf{x}; \boldsymbol{\epsilon})\} = \min_{\boldsymbol{\epsilon}} \{\|\mathbf{x} - \mathbf{A}\boldsymbol{\alpha}\|^2\}.$$

Dual source maximum likelihood estimator (2S-MLE)

- Signal model: $\mathbf{x} = \mathbf{A}(\boldsymbol{\eta}_0, \boldsymbol{\eta}_1)\boldsymbol{\alpha} + \mathbf{w}, \mathbf{w} \sim CN(\mathbf{0}, \sigma_n^2 \mathbf{I}_\mathrm{N}) \Rightarrow \mathbf{x} \sim \boldsymbol{CN}(\mathbf{A}\boldsymbol{\alpha}, \sigma_n^2 \mathbf{I}_N)$.

- **Maximum likelihood estimation**: $\hat{\boldsymbol{\epsilon}}$ maximizes the likelihood $p(\mathbf{x}; \boldsymbol{\epsilon})$ that the process described by the model produced the data $\mathbf{x}$ that was actually observed:

$$\hat{\boldsymbol{\epsilon}} = \arg\max_{\boldsymbol{\epsilon}} \{p(\mathbf{x}; \boldsymbol{\epsilon})\} \text{ where } p(\mathbf{x}; \boldsymbol{\epsilon}) = \frac{1}{(\pi\sigma_n^2)^N} e^{-\frac{1}{\sigma_n^2}\|\mathbf{x}-\mathbf{A}\boldsymbol{\alpha}\|^2}.$$

- 9-dimensional grid search!

$$\max_{\boldsymbol{\epsilon}} \{p(\mathbf{x}; \boldsymbol{\epsilon})\} = \min_{\boldsymbol{\epsilon}} \{\|\mathbf{x} - \mathbf{A}\boldsymbol{\alpha}\|^2\}.$$

- Using linear algebra, this problem can be reduced to a 4-dimensional search.

2S-MLE: search grid strategy

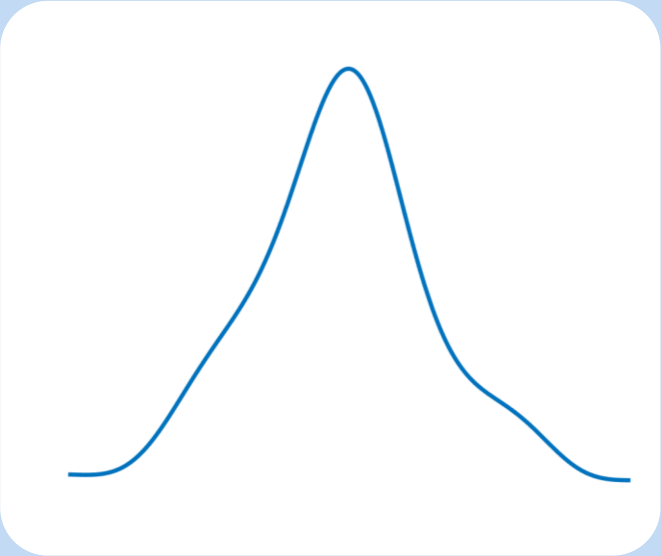

- Iterative search:

2S-MLE: search grid strategy

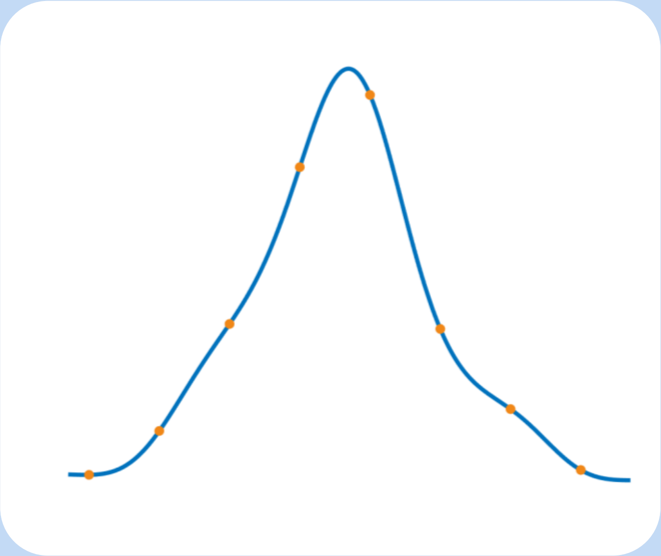

- Iterative search:
  - coarse search,

2S-MLE: search grid strategy

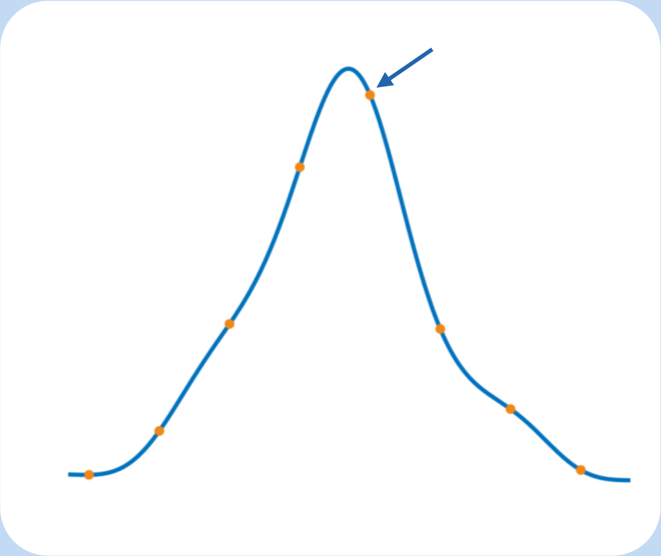

- Iterative search:
  - coarse search,

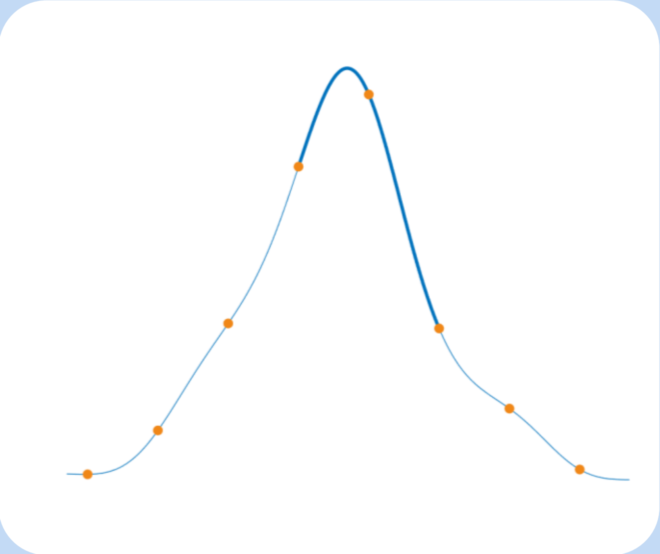

- Iterative search:
  - coarse search,

2S-MLE: search grid strategy

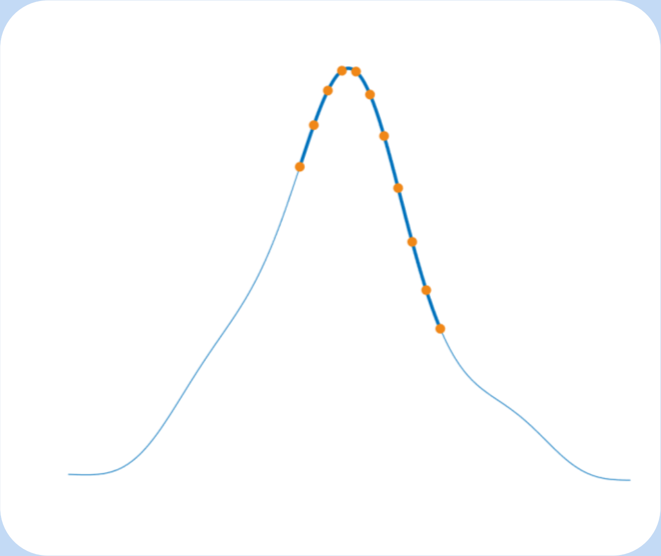

- Iterative search:
  - coarse search,
  - fine search.

2S-MLE: search grid strategy

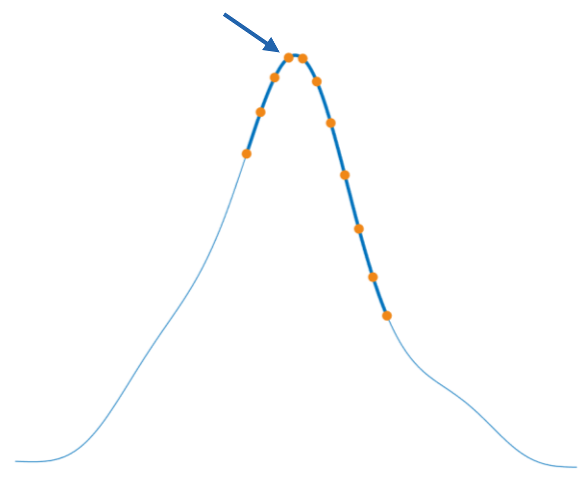

- Iterative search:
  - coarse search,
  - fine search.

2S-MLE: search grid strategy

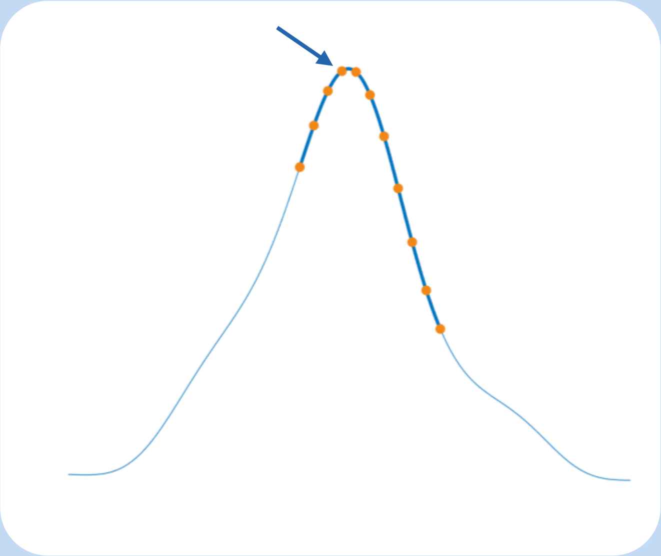

- Iterative search:
  - coarse search,
  - fine search.

- Property of the 2S-MLE:
  asymptotically efficient (large SNR).

2S-MLE: search grid strategy

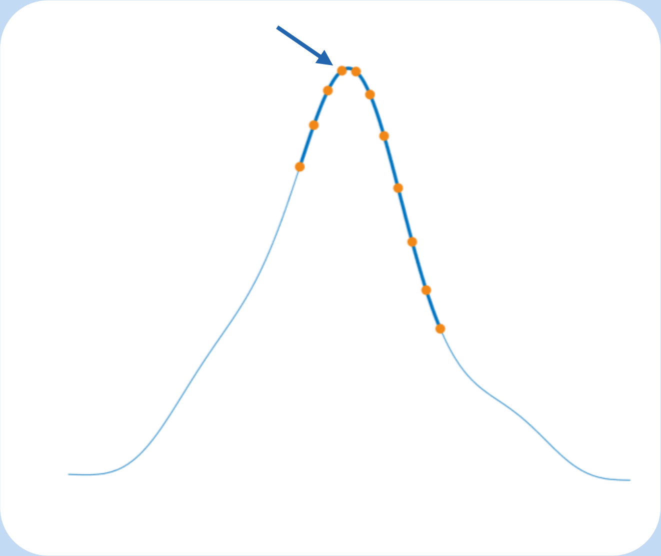

- Iterative search:
  - coarse search,
  - fine search.

- Property of the 2S-MLE: asymptotically efficient (large SNR).

- Simulation set-up:
  - signal: GPS L1 C/A,
  - $c\Delta\tau = 37$ m,
  - $F_{d,0} = 20$ Hz, $F_{d,1} = 20$ Hz,
  - $\rho_1/\rho_0 = 0.5, \Delta\phi = 15^{o}$,
  - 1000 Monte Carlo runs.

2S-MLE: search grid strategy

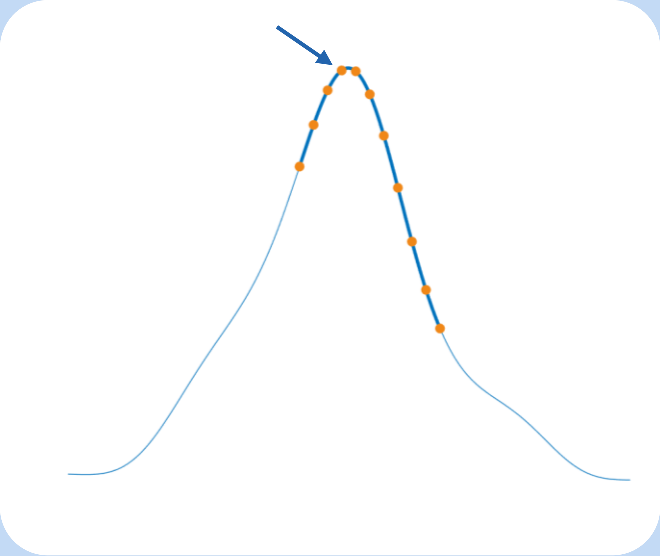

- Iterative search:
  - coarse search,
  - fine search.

- Property of the 2S-MLE: asymptotically efficient (large SNR).

- Simulation set-up:
  - signal: GPS L1 C/A,
  - $c\Delta\tau = 37$ m,
  - $F_{d,0} = 20$ Hz, $F_{d,1} = 20$ Hz,
  - $\rho_1/\rho_0 = 0.5, \Delta\phi = 15^o$,
  - 1000 Monte Carlo runs.

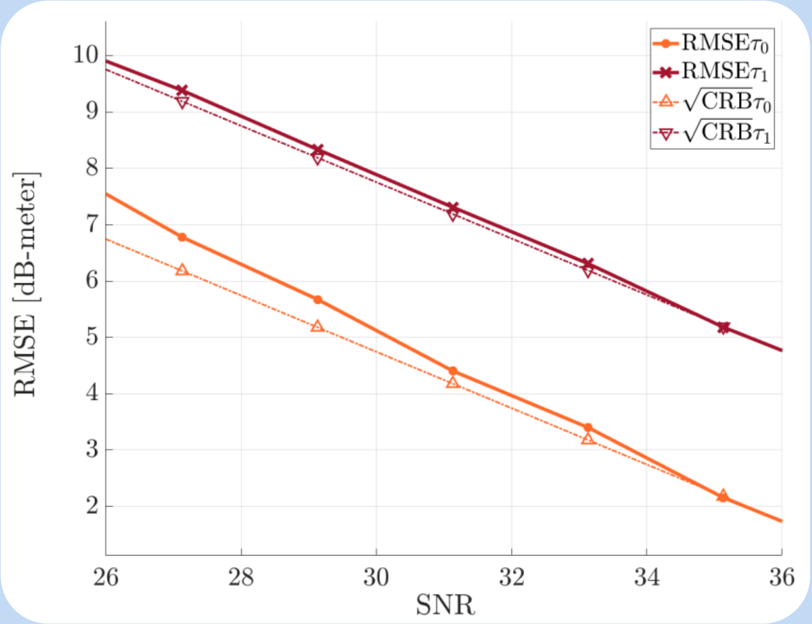

Wrap-up on 2S signal model

In this presentation

- Dual source signal model adapted to the ground-based GNSS-R.
- Derivation of a closed-form CRB and validation using the 2S-MLE.
  - Lubeigt *et al.* 2020, *Remote Sensing*.

Wrap-up on 2S signal model

In this presentation

- Dual source signal model adapted to the ground-based GNSS-R.
- Derivation of a closed-form CRB and validation using the 2S-MLE.
  - Lubeigt *et al.* 2020, *Remote Sensing.*

Related works

- Use of the CRB as a way to assess GNSS multipath effect.
  - Lubeigt *et al.* 2022, *IEEE Aerospace Conference.*
- Proposition of a metric for candidate GNSS signal design based on the CRB.
  - Lubeigt *et al.* 2022, *IEEE Trans. Aerosp. Electron. Syst.*
- Derivation of the Misspecified CRB (MCRB)
  - Lubeigt *et al.* 2023, *Signal Processing.*

2 - Ground-based GNSS-R

Motivation

- Standard GNSS-R processing:
  - 1 channel for the direct path,
  - 1 channel for the reflected path.

Motivation

- Standard GNSS-R processing:
  - 1 channel for the direct path,
  - 1 channel for the reflected path.
- Assumption: channels isolated from one another.

$$\mathbf{x} = \rho e^{j\phi}\mathbf{s}(\boldsymbol{\eta}) + \mathbf{w}, \quad \boldsymbol{\eta} = (\tau, F_d)^{\mathrm{T}}.$$

Motivation

- Standard GNSS-R processing:
  - 1 channel for the direct path,
  - 1 channel for the reflected path.
- Assumption: channels isolated from one another.

$$\mathbf{x} = \rho e^{j\phi}\mathbf{s}(\boldsymbol{\eta}) + \mathbf{w}, \quad \boldsymbol{\eta} = (\tau, F_d)^{\mathrm{T}}.$$

- Crosstalk effect:
  - direct channel processing,
  - SNR during the recording.

Motivation

- Standard GNSS-R processing:
  - 1 channel for the direct path,
  - 1 channel for the reflected path.
- Assumption: channels isolated from one another.

$$\mathbf{x} = \rho e^{j\phi}\mathbf{s}(\boldsymbol{\eta}) + \mathbf{w}, \quad \boldsymbol{\eta} = (\tau, F_d)^{\mathrm{T}}.$$

- Crosstalk effect:
  - direct channel processing,
  - SNR during the recording.

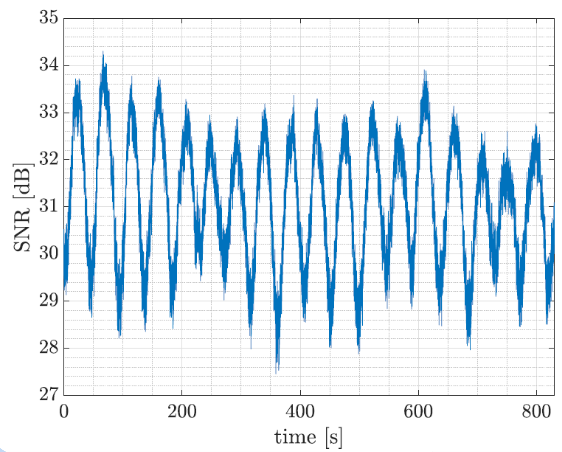

Motivation

- Standard GNSS-R processing:
  - 1 channel for the direct path,
  - 1 channel for the reflected path.

- Assumption: channels isolated from one another.

$$\mathbf{x} = \rho e^{j\phi}\mathbf{s}(\boldsymbol{\eta}) + \mathbf{w}, \quad \boldsymbol{\eta} = (\tau, F_d)^{\mathrm{T}}.$$

- Crosstalk effect:
  - direct channel processing,
  - SNR during the recording.

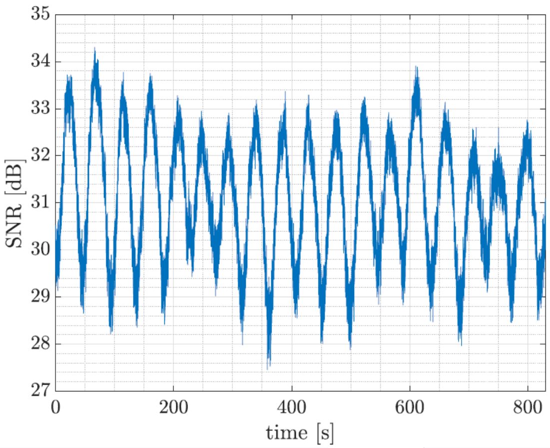

- Oscillations due to changing geometry!
- GNSS-IR or IPT techniques to estimate the height [Ribot *et al.* 2014].

Motivation

- Standard GNSS-R processing:
  - 1 channel for the direct path,
  - 1 channel for the reflected path.
- Assumption: channels isolated from one another.

$$\mathbf{x} = \rho e^{j\phi}\mathbf{s}(\boldsymbol{\eta}) + \mathbf{w}, \quad \boldsymbol{\eta} = (\tau, F_d)^{\mathrm{T}}.$$

- Ground-based GNSS-R is usually put aside because of the signal crosstalk.

- Crosstalk effect:
  - direct channel processing,
  - SNR during the recording.

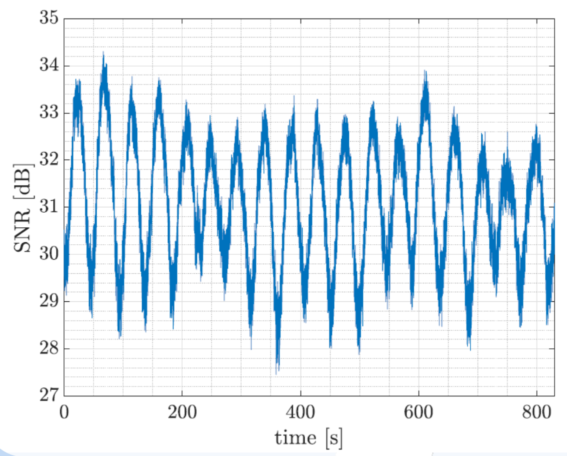

  - Oscillations due to changing geometry!
  - GNSS-IR or IPT techniques to estimate the height [Ribot *et al.* 2014].

Motivation

- Standard GNSS-R processing:
  - 1 channel for the direct path,
  - 1 channel for the reflected path.
- Assumption: channels isolated from one another.

$$\mathbf{x} = \rho e^{j\phi}\mathbf{s}(\boldsymbol{\eta}) + \mathbf{w}, \quad \boldsymbol{\eta} = (\tau, F_d)^{\mathrm{T}}.$$

x

- Ground-based GNSS-R is usually put aside because of the signal crosstalk.
- Challenge: change the signal processing approach to cope with the presence of crosstalk.

$$\mathbf{x} = \rho_0 e^{j\phi_0}\mathbf{s}(\boldsymbol{\eta}_0) + \rho_1 e^{j\phi_1}\mathbf{s}(\boldsymbol{\eta}_1) + \mathbf{w}.$$

- Crosstalk effect:
  - direct channel processing,
  - SNR during the recording.

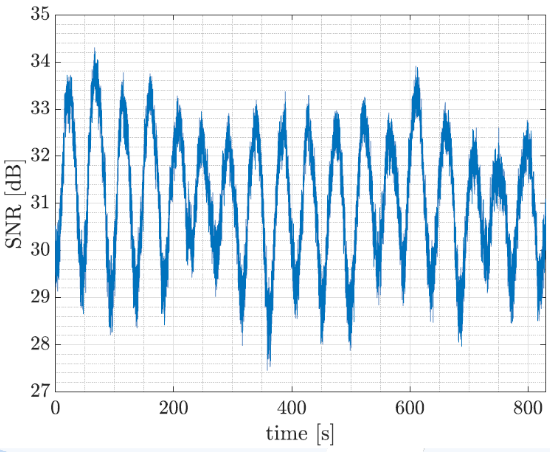

- Oscillations due to changing geometry!
- GNSS-IR or IPT techniques to estimate the height [Ribot *et al.* 2014].

Gruissan experiment

Experiment planning

- Site modeling: definition of a mask.

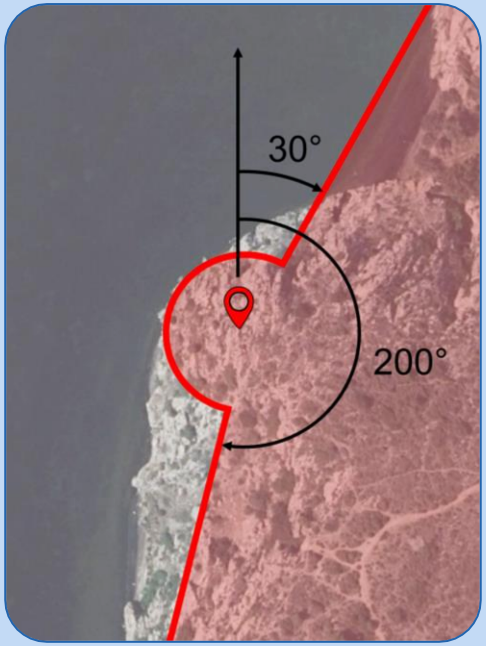

- Site modeling: definition of a mask.
- Satellite visibility: orbit propagation based on TLE.

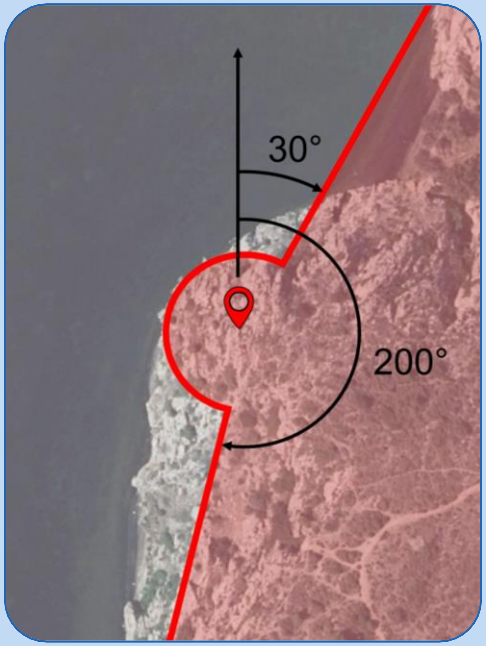

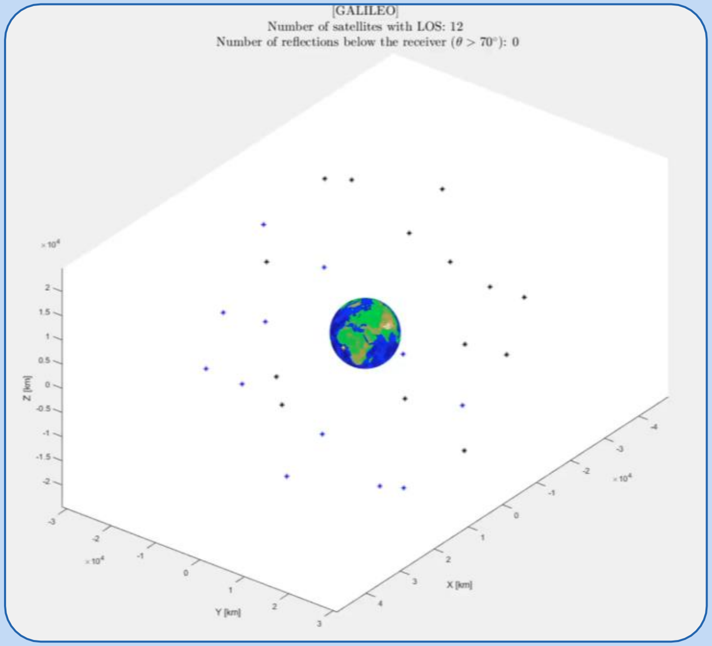

- Site modeling: definition of a mask.
- Satellite visibility: orbit propagation based on TLE.

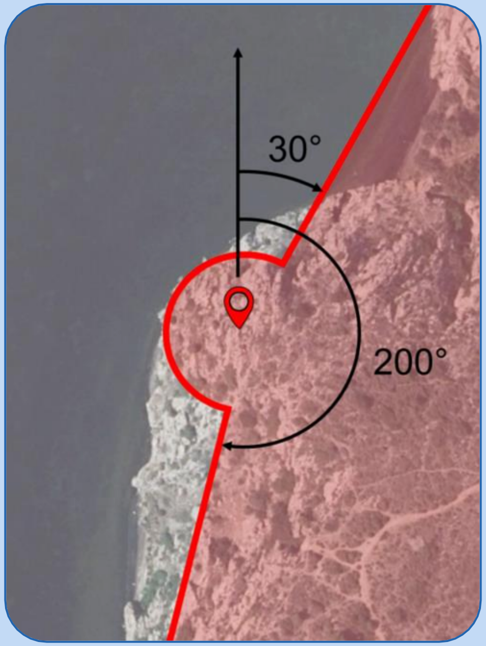

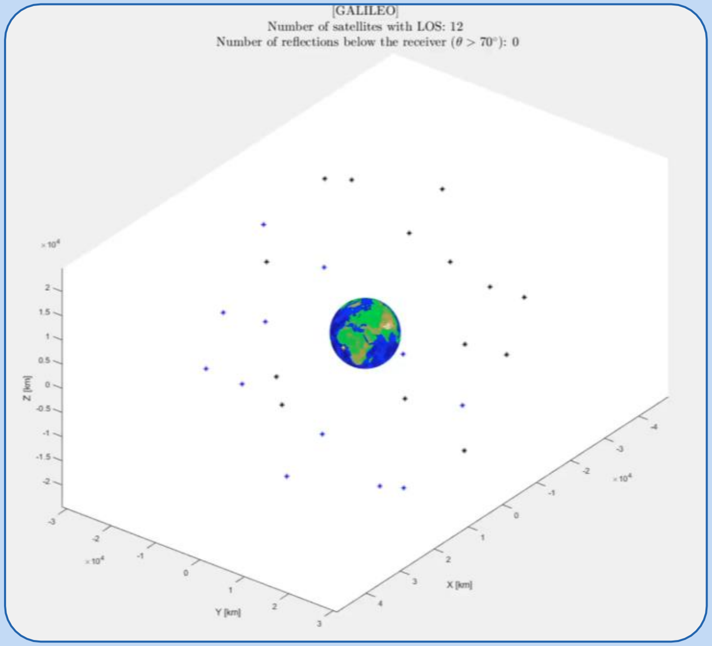

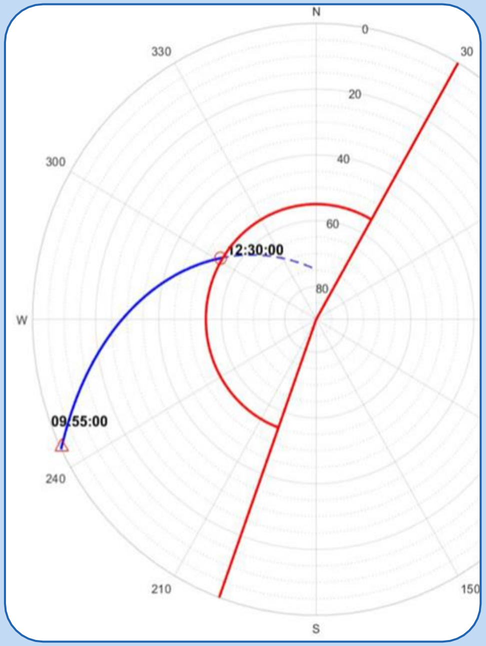

Experiment planning

- Site modeling: definition of a mask.
- Satellite visibility: orbit propagation based on TLE.
- Experiment: July 27, 2021!

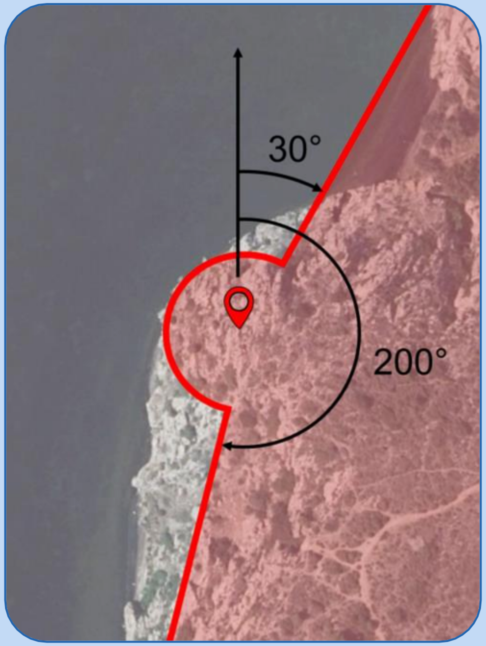

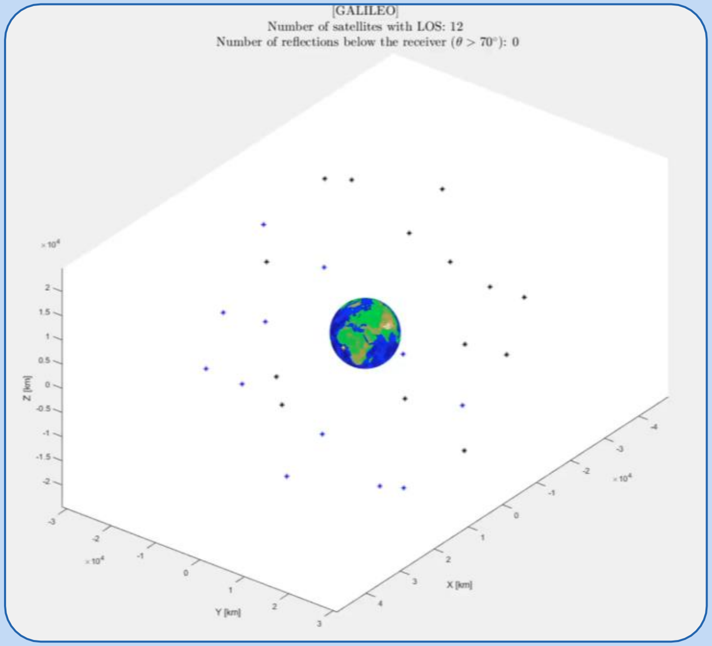

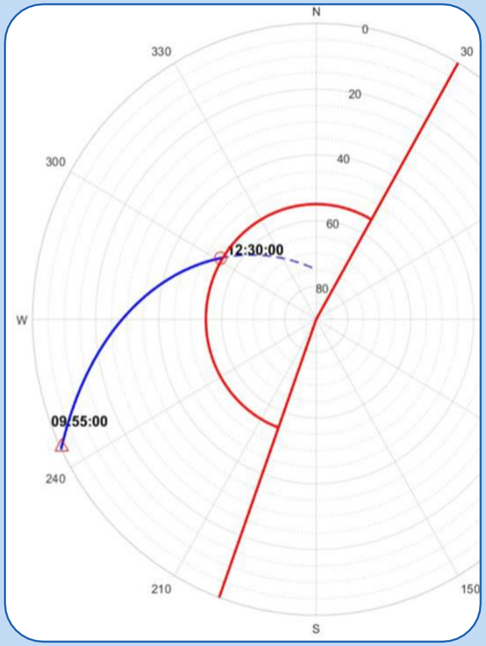

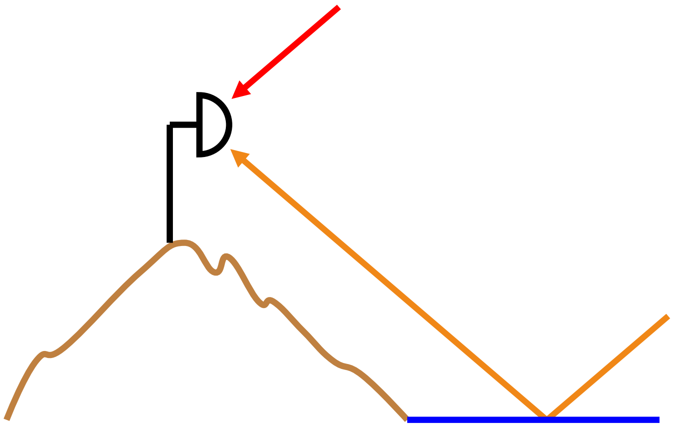

Gruissan experiment particulars

- Equipment:
  - RHCP and LHCP antenna,
  - 4 synchronized channels:
    - 2 L1/E1 at 6.144 Msps,
    - 2 L5/E5A at 61.440 Msps.

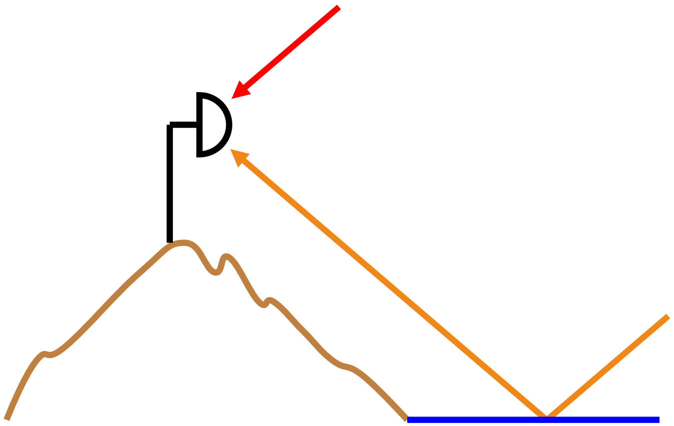

Gruissan experiment particulars

- Equipment:
  - RHCP and LHCP antenna,
  - 4 synchronized channels:
    - 2 L1/E1 at 6.144 Msps,
    - 2 L5/E5A at 61.440 Msps.
- Geometry:
  - ground truth: $h = 23.40$ m,

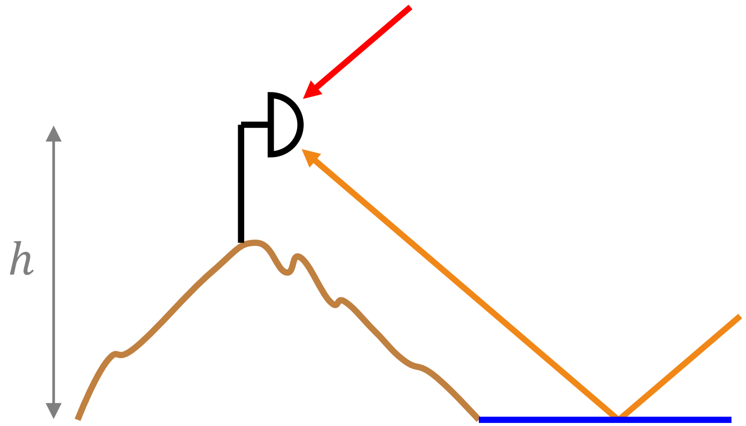

Gruissan experiment particulars

- Equipment:
  - RHCP and LHCP antenna,
  - 4 synchronized channels:
    - 2 L1/E1 at 6.144 Msps,
    - 2 L5/E5A at 61.440 Msps.
- Geometry:
  - ground truth: $h = 23.40$ m,
  - expected time delay:

$$c\Delta\tau = 2h\sin(e).$$

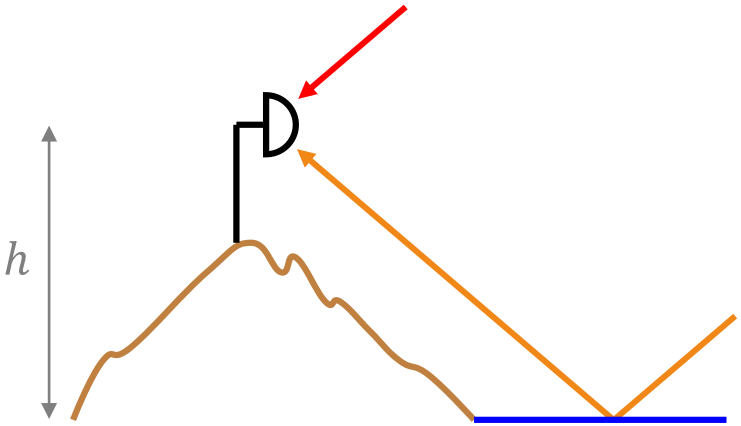

Gruissan experiment particulars

- Equipment:
  - RHCP and LHCP antenna,
  - 4 synchronized channels:
    - 2 L1/E1 at 6.144 Msps,
    - 2 L5/E5A at 61.440 Msps.
- Geometry:
  - ground truth: $h = 23.40$ m,
  - expected time delay:

$$c\Delta\tau = 2h\sin(e).$$

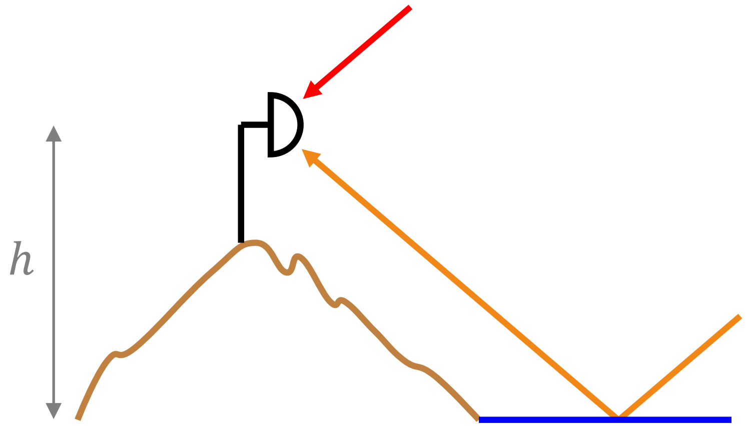

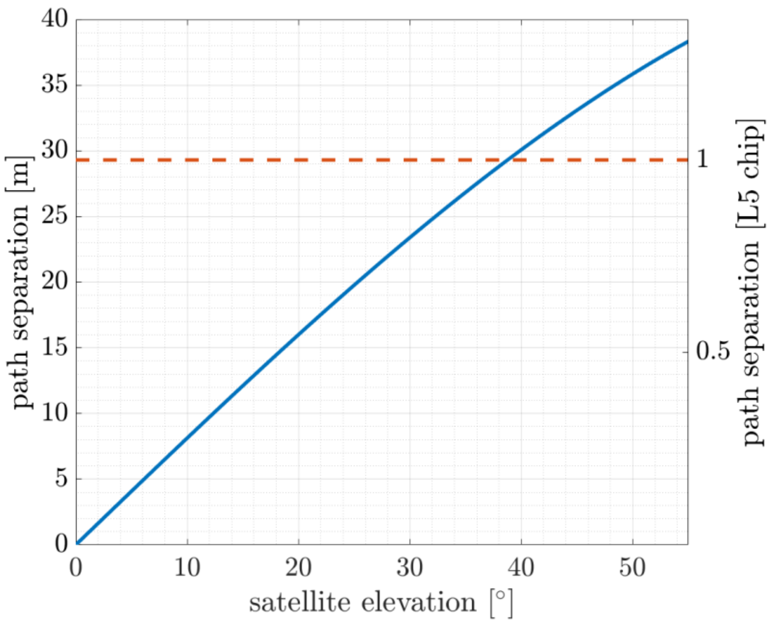

Gruissan experiment particulars

- Equipment:
  - RHCP and LHCP antenna,
  - 4 synchronized channels:
    - 2 L1/E1 at 6.144 Msps,
    - 2 L5/E5A at 61.440 Msps.
- Geometry:
  - ground truth: $h = 23.40$ m,
  - expected time delay:

$$c\Delta\tau = 2h\sin(e).$$

- Challenges:

L1/E1
(L1 chip ≈ 300 m)

Strong interference
→ approximations

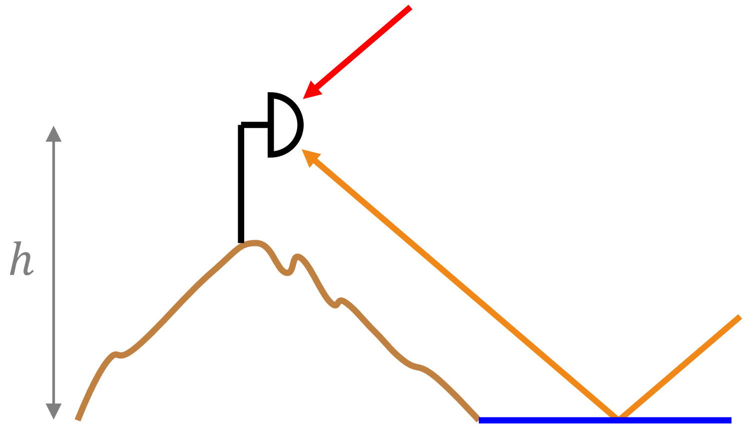

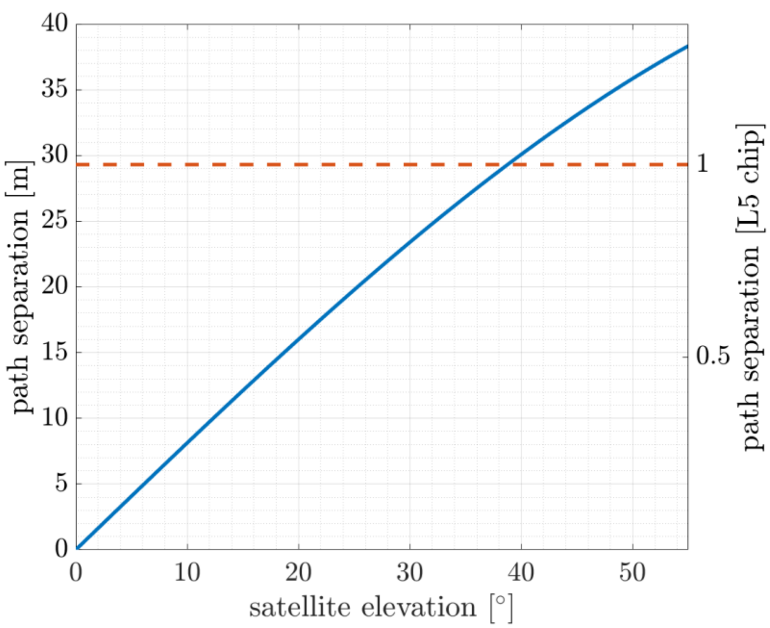

Gruissan experiment particulars

- Equipment:
  - RHCP and LHCP antenna,
  - 4 synchronized channels:
    - 2 L1/E1 at 6.144 Msps,
    - 2 L5/E5A at 61.440 Msps.
- Geometry:
  - ground truth: $h = 23.40$ m,
  - expected time delay:

$$c\Delta\tau = 2h\sin(e).$$

- Challenges:

L1/E1 (L1 chip ≈ 300 m)	L5/E5A (L5 chip ≈ 30 m)
Strong interference → approximations	Weak interference → 2S processing

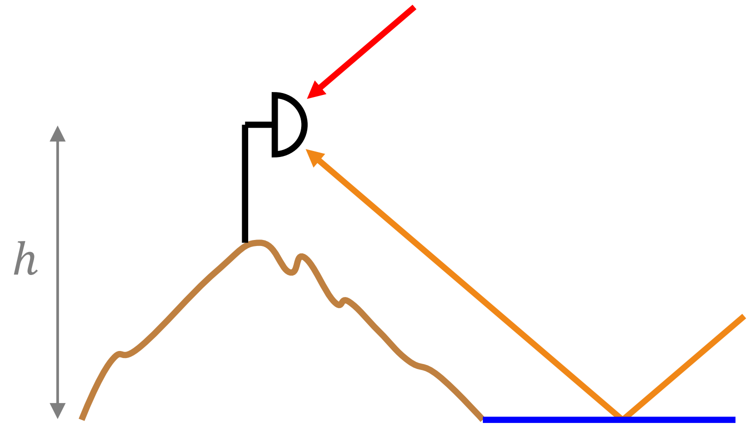

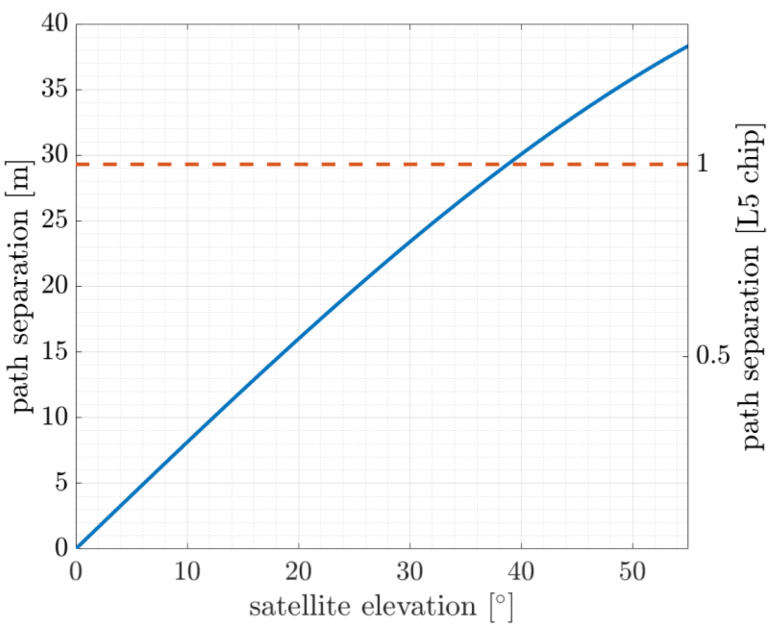

Gruissan experiment particulars

- Equipment:
  - RHCP and LHCP antenna,
  - 4 synchronized channels:
    - 2 L1/E1 at 6.144 Msps,
    - 2 L5/E5A at 61.440 Msps.
- Geometry:
  - ground truth: $h = 23.40$ m,
  - expected time delay:

$$c\Delta\tau = 2h\sin(e).$$

- Challenges:

L1/E1 (L1 chip ≈ 300 m)	L5/E5A (L5 chip ≈ 30 m)
Strong interference → approximations	Weak interference → 2S processing

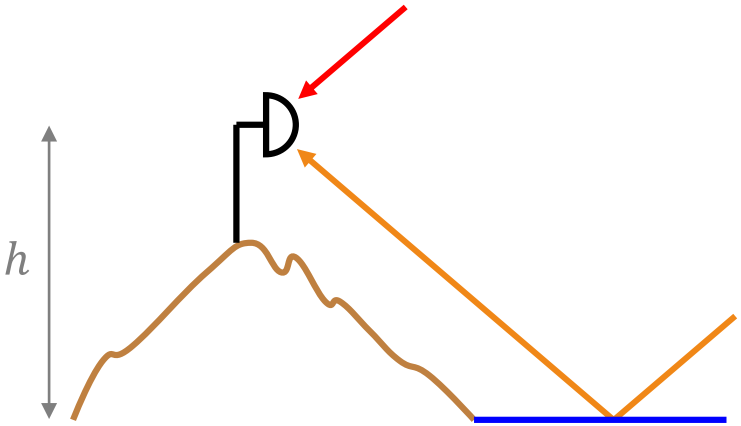

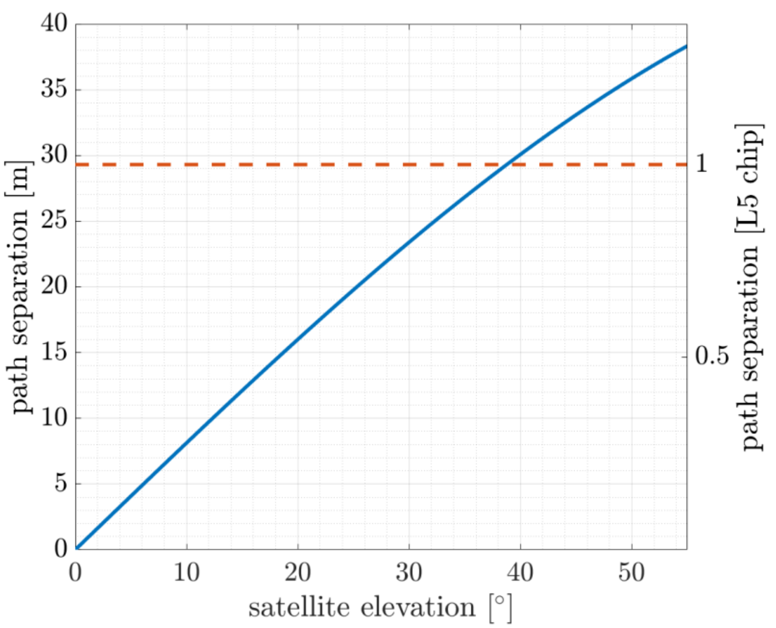

Assuming no crosstalk: single source processing (Maximum Likelihood estimator):

- RHCP antenna: $\hat{\tau}_0$.
- LHCP antenna: $\hat{\tau}_1$.

$$\hat{h} = \frac{c(\hat{\tau}_1 - \hat{\tau}_0)}{2\sin(e)}$$

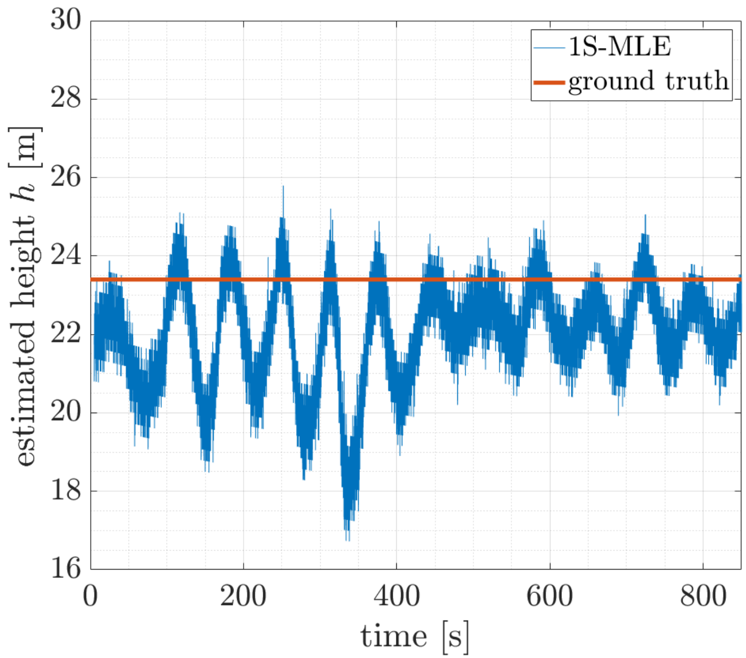

Assuming crosstalk: dual source processing (CLEAN-RELAX estimator):

- RHCP antenna: $\hat{\tau}_0^{\text{RHCP}}, \hat{\tau}_1^{\text{RHCP}}$.
- LHCP antenna: $\hat{\tau}_0^{\text{LHCP}}, \hat{\tau}_1^{\text{LHCP}}$.

$$\hat{h} = \frac{c\left(\hat{\tau}_1^{\text{LHCP}} - \hat{\tau}_0^{\text{RHCP}}\right)}{2\sin(e)}$$

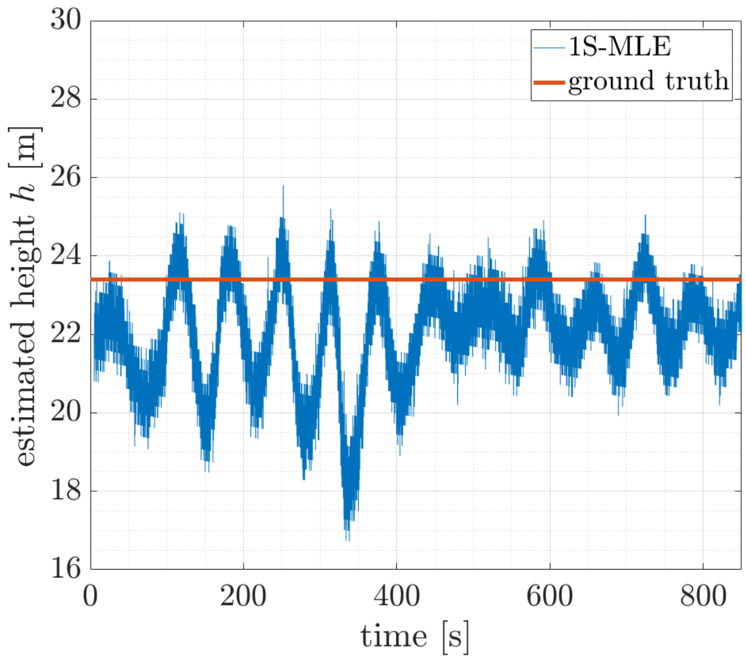

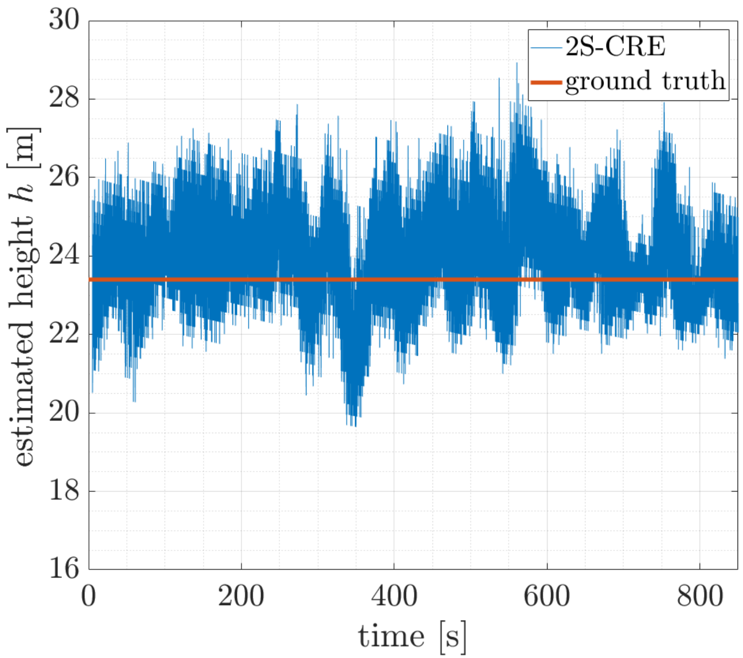

Wrap-up on ground-based GNSS-R

In this presentation

- Presentation of the Gruissan experiment.
- First results using a simple dual source signal processing scheme.
  - Lubeigt *et al.* 2022, *GRETSI*.

Wrap-up on ground-based GNSS-R

In this presentation

- Presentation of the Gruissan experiment.
- First results using a simple dual source signal processing scheme.
  - Lubeigt *et al.* 2022, *GRETSI*.

Related works

- Use of the 2S-CRB to assess signal crosstalk impact on standard GNSS-R processings.
  - Lubeigt *et al.* 2021, *Remote Sensing*.
- Signal antenna close-to-ground GNSS-R:
  - Taylor approximation of the 2S-MLE to reduce its complexity.
  - Validation with simulations and comparison with 2S-MLE performance.
  - Lubeigt *et al.* 2022, *NAVITEC*.
  - Lubeigt *et al.* (under review after major revision), *Signal Processing*.

3 – Diffuse reflection

Credit: Xavier Lubeigt

Specular reflection

Specular vs diffuse reflections

Specular reflection

- smooth surface (mirror-like),
- coherent reflection,

Specular reflection

- smooth surface (mirror-like),
- coherent reflection,
- simple signal model.

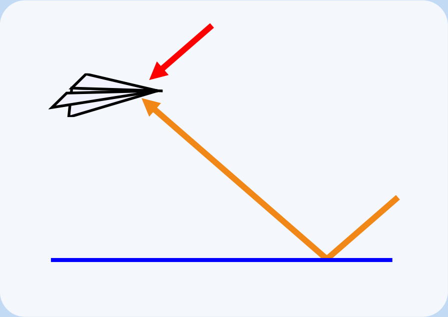

Specular vs diffuse reflections

Specular reflection

- smooth surface (mirror-like),
- coherent reflection,
- simple signal model.

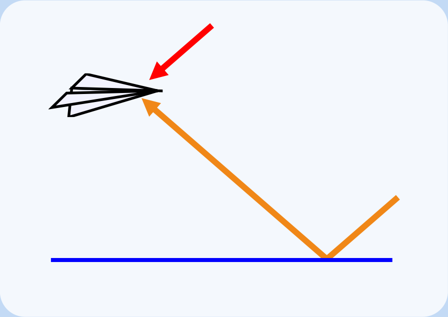

Diffuse reflection

Specular vs diffuse reflections

Specular reflection

- smooth surface (mirror-like),
- coherent reflection,
- simple signal model.

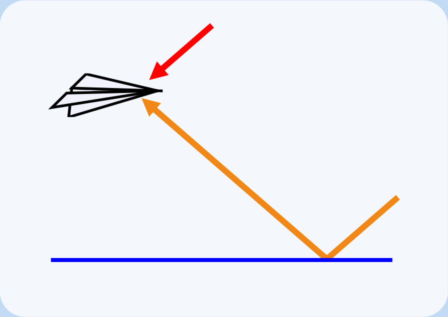

Diffuse reflection

- rough surface,
- coherent and non-coherent reflection,

Specular vs diffuse reflections

Specular reflection

- smooth surface (mirror-like),
- coherent reflection,
- simple signal model.

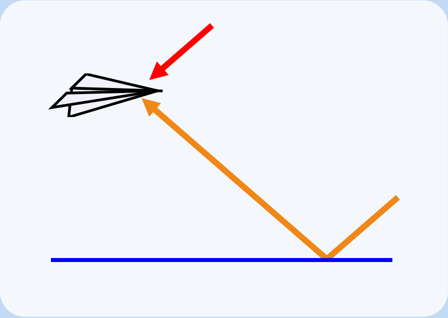

Diffuse reflection

- rough surface,
- coherent and non-coherent reflection,
- signal model?

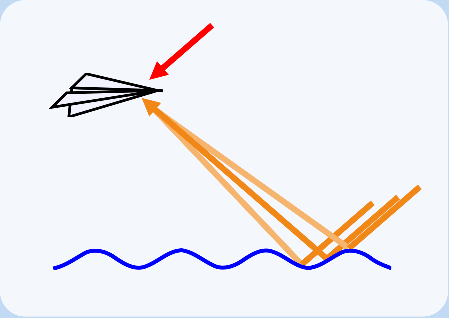

Towards the impulse response signal model

- Specular reflection:
  - symmetric cross-correlation function.

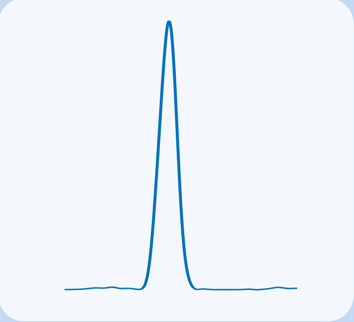

- Specular reflection:
  - symmetric cross-correlation function.

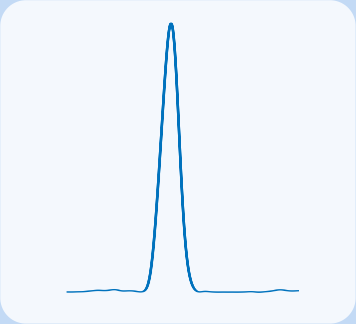

- Diffuse reflection:
  - distorted cross-correlation function,

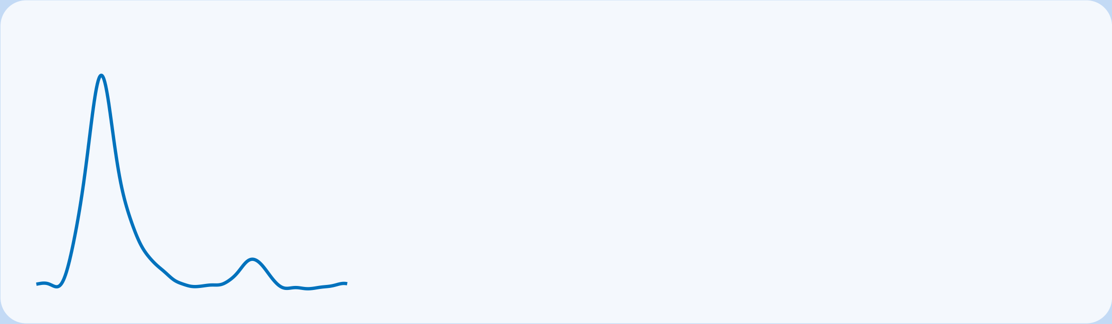

Towards the impulse response signal model

- Specular reflection:
  - symmetric cross-correlation function.

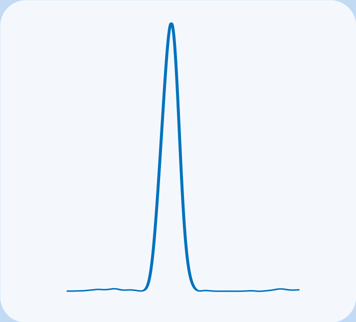

- Diffuse reflection:
  - distorted cross-correlation function,
  - convolution product?

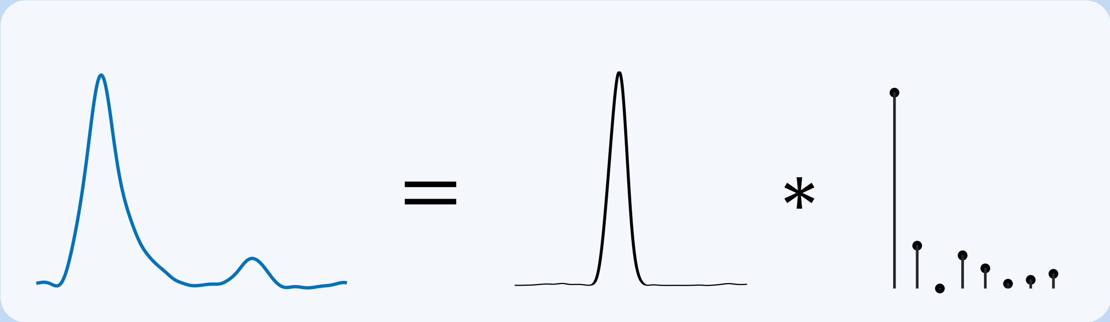

Towards the impulse response signal model

- Specular reflection:
  - symmetric cross-correlation function.

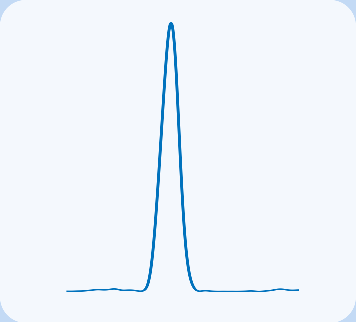

- Diffuse reflection:
  - distorted cross-correlation function,
  - convolution product?

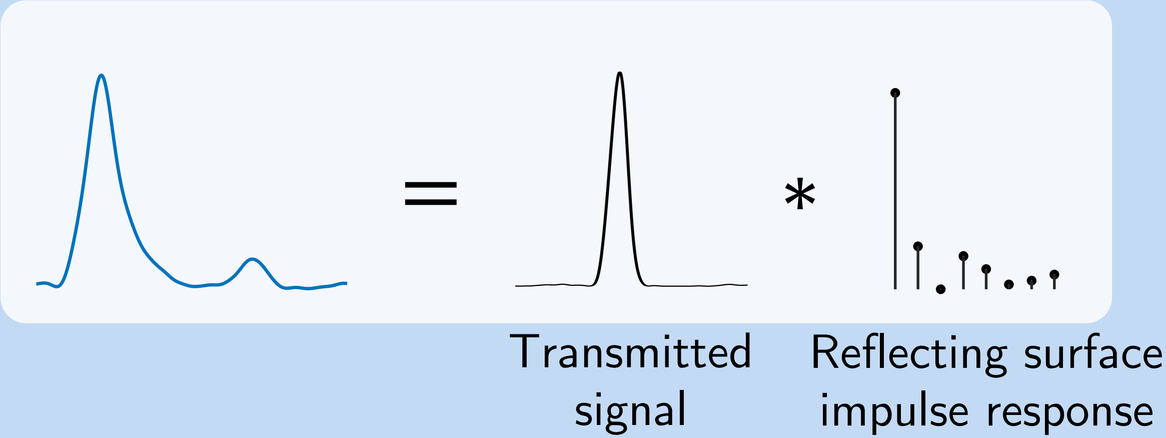

Reflecting surface IR estimation challenges

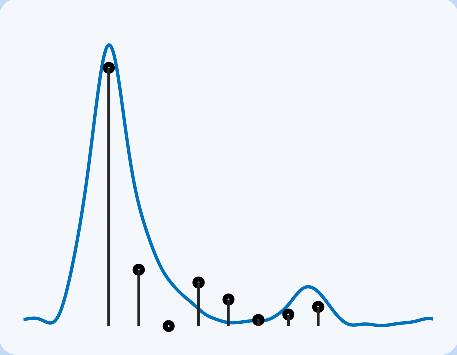

- Impulse response signal model (with P sources):

$$\mathbf{x} = \mathbf{h} * \mathbf{s}_0(\boldsymbol{\eta}) + \mathbf{w} = \mathbf{A}_P(\boldsymbol{\eta})\boldsymbol{\alpha} + \mathbf{w}, \mathbf{w} \sim CN(\mathbf{0}, \sigma_n^2 \mathbf{I}_\mathrm{N}),$$

with, for $\boldsymbol{\eta}^T = (\tau, F_d)$, $\mathbf{h} = \sum_{p=0}^{P-1} \alpha_p \delta_{pT_s}$,

$$\boldsymbol{\alpha}^T = (\dots, \alpha_p, \dots), \mathbf{A}_\mathrm{P}(\boldsymbol{\eta}) = [\dots, \mathbf{s}_p(\boldsymbol{\eta}), \dots],$$

$$\mathbf{s}_p(\boldsymbol{\eta}) = (\dots, s(nT_s - \tau - pT_s)e^{-j2\pi F_d(nT_s - \tau - pT_s)}, \dots).$$

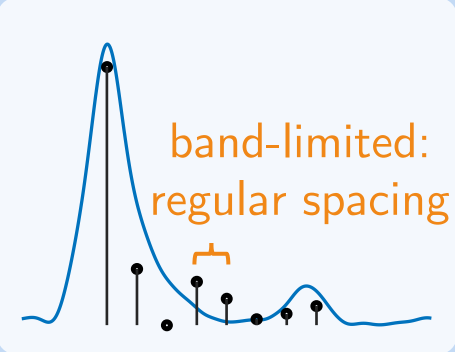

- Impulse response signal model (with P sources):

$$\mathbf{x} = \mathbf{h} * \mathbf{s}_0(\boldsymbol{\eta}) + \mathbf{w} = \mathbf{A}_P(\boldsymbol{\eta})\boldsymbol{\alpha} + \mathbf{w}, \mathbf{w} \sim CN(\mathbf{0}, \sigma_n^2 \mathbf{I}_\mathrm{N}),$$

with, for $\boldsymbol{\eta}^T = (\tau, F_d)$, $\mathbf{h} = \sum_{p=0}^{P-1} \alpha_p \delta_{pT_s}$,

$$\boldsymbol{\alpha}^T = (\dots, \alpha_p, \dots), \mathbf{A}_\mathrm{P}(\boldsymbol{\eta}) = [\dots, \mathbf{s}_p(\boldsymbol{\eta}), \dots],$$

$$\mathbf{s}_p(\boldsymbol{\eta}) = (\dots, s(nT_s - \tau - pT_s)e^{-j2\pi F_d(nT_s - \tau - pT_s)}, \dots).$$

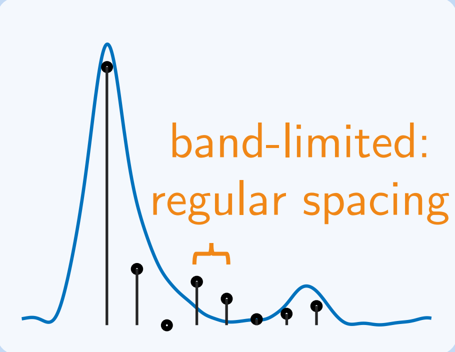

- Motivations: impulse response characterization, reflecting surface roughness (sea state inference), classification of reflecting surface, etc.

Reflecting surface IR estimation challenges

- Impulse response signal model (with P sources):

$$\mathbf{x} = \mathbf{h} * \mathbf{s}_0(\boldsymbol{\eta}) + \mathbf{w} = \mathbf{A}_P(\boldsymbol{\eta})\boldsymbol{\alpha} + \mathbf{w}, \mathbf{w} \sim CN(\mathbf{0}, \sigma_n^2 \mathbf{I}_\mathrm{N}),$$

with, for $\boldsymbol{\eta}^T = (\tau, F_d)$, $\mathbf{h} = \sum_{p=0}^{P-1} \alpha_p \delta_{pT_s}$,

$$\boldsymbol{\alpha}^T = (\dots, \alpha_p, \dots), \mathbf{A}_\mathrm{P}(\boldsymbol{\eta}) = [\dots, \mathbf{s}_p(\boldsymbol{\eta}), \dots],$$

$$\mathbf{s}_p(\boldsymbol{\eta}) = (\dots, s(nT_s - \tau - pT_s)e^{-j2\pi F_d(nT_s - \tau - pT_s)}, \dots).$$

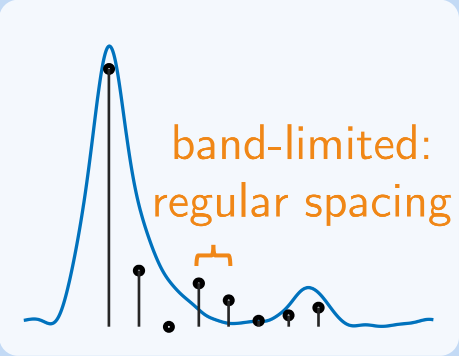

- Motivations: impulse response characterization, reflecting surface roughness (sea state inference), classification of reflecting surface, etc.
- Challenge: determining the number of sources P to describe the impulse response.

Reflecting surface IR estimation challenges

- Impulse response signal model (with P sources):

$$\mathbf{x} = \mathbf{h} * \mathbf{s}_0(\boldsymbol{\eta}) + \mathbf{w} = \mathbf{A}_P(\boldsymbol{\eta})\boldsymbol{\alpha} + \mathbf{w}, \mathbf{w} \sim CN(\mathbf{0}, \sigma_n^2 \mathbf{I}_\mathrm{N}),$$

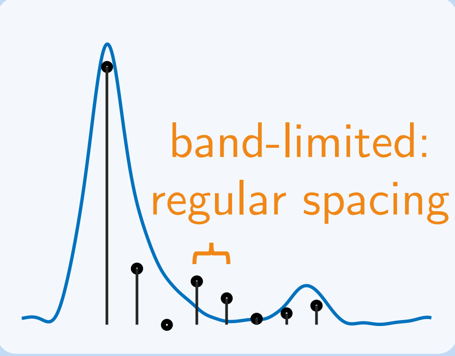

with, for $\boldsymbol{\eta}^T = (\tau, F_d)$, $\mathbf{h} = \sum_{p=0}^{P-1} \alpha_p \delta_{pT_s}$,

$$\boldsymbol{\alpha}^T = (\dots, \alpha_p, \dots), \mathbf{A}_\mathrm{P}(\boldsymbol{\eta}) = [\dots, \mathbf{s}_p(\boldsymbol{\eta}), \dots],$$

$$\mathbf{s}_p(\boldsymbol{\eta}) = (\dots, s(nT_s - \tau - pT_s)e^{-j2\pi F_d(nT_s - \tau - pT_s)}, \dots).$$

- Motivations: impulse response characterization, reflecting surface roughness (sea state inference), classification of reflecting surface, etc.
- Challenge: determining the number of sources P to describe the impulse response.
- Undershoot:

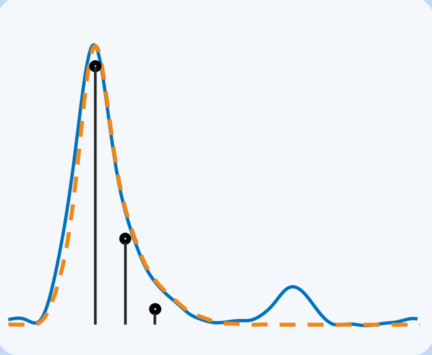

Reflecting surface IR estimation challenges

- Impulse response signal model (with P sources):

$$\mathbf{x} = \mathbf{h} * \mathbf{s}_0(\boldsymbol{\eta}) + \mathbf{w} = \mathbf{A}_P(\boldsymbol{\eta})\boldsymbol{\alpha} + \mathbf{w}, \mathbf{w} \sim CN(\mathbf{0}, \sigma_n^2 \mathbf{I}_\mathrm{N}),$$

with, for $\boldsymbol{\eta}^T = (\tau, F_d)$, $\mathbf{h} = \sum_{p=0}^{P-1} \alpha_p \delta_{pT_s}$,

$$\boldsymbol{\alpha}^T = (\dots, \alpha_p, \dots), \mathbf{A}_\mathrm{P}(\boldsymbol{\eta}) = [\dots, \mathbf{s}_p(\boldsymbol{\eta}), \dots],$$

$$\mathbf{s}_p(\boldsymbol{\eta}) = (\dots, s(nT_s - \tau - pT_s)e^{-j2\pi F_d(nT_s - \tau - pT_s)}, \dots).$$

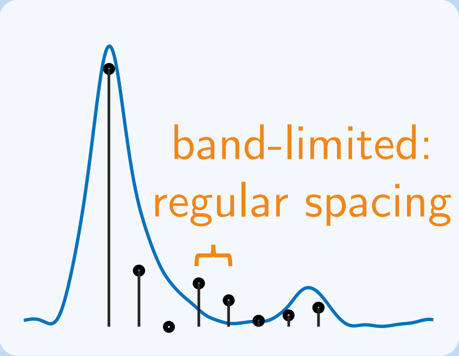

- Motivations: impulse response characterization, reflecting surface roughness (sea state inference), classification of reflecting surface, etc.
- Challenge: determining the number of sources P to describe the impulse response.

- Undershoot:
  - missed information,
  - bias estimates.

Reflecting surface IR estimation challenges

- Impulse response signal model (with P sources):

$$\mathbf{x} = \mathbf{h} * \mathbf{s}_0(\boldsymbol{\eta}) + \mathbf{w} = \mathbf{A}_P(\boldsymbol{\eta})\boldsymbol{\alpha} + \mathbf{w}, \mathbf{w} \sim CN(\mathbf{0}, \sigma_n^2 \mathbf{I}_\mathrm{N}),$$

with, for $\boldsymbol{\eta}^T = (\tau, F_d)$, $\mathbf{h} = \sum_{p=0}^{P-1} \alpha_p \delta_{pT_s}$,

$$\boldsymbol{\alpha}^T = (\dots, \alpha_p, \dots), \mathbf{A}_\mathrm{P}(\boldsymbol{\eta}) = [\dots, \mathbf{s}_p(\boldsymbol{\eta}), \dots],$$

$$\mathbf{s}_p(\boldsymbol{\eta}) = (\dots, s(nT_s - \tau - pT_s)e^{-j2\pi F_d(nT_s - \tau - pT_s)}, \dots).$$

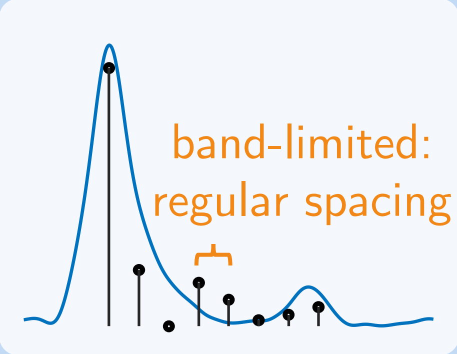

- Motivations: impulse response characterization, reflecting surface roughness (sea state inference), classification of reflecting surface, etc.
- Challenge: determining the number of sources P to describe the impulse response.

- Undershoot:
  - missed information,
  - bias estimates.
- Overshoot:

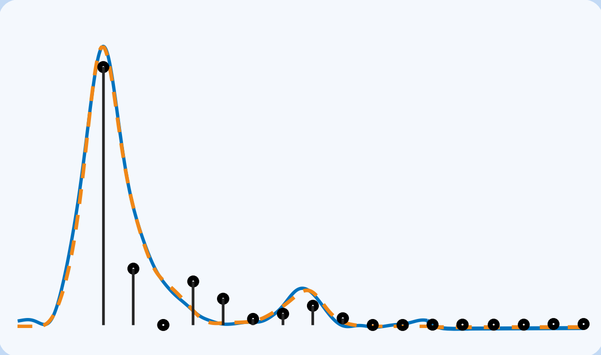

Reflecting surface IR estimation challenges

- Impulse response signal model (with P sources):

$$\mathbf{x} = \mathbf{h} * \mathbf{s}_0(\boldsymbol{\eta}) + \mathbf{w} = \mathbf{A}_P(\boldsymbol{\eta})\boldsymbol{\alpha} + \mathbf{w}, \mathbf{w} \sim \mathcal{CN}(\mathbf{0}, \sigma_n^2 \mathbf{I}_\mathrm{N}),$$

with, for $\boldsymbol{\eta}^T = (\tau, F_d)$, $\mathbf{h} = \sum_{p=0}^{P-1} \alpha_p \delta_{pT_s}$,

$$\boldsymbol{\alpha}^T = (\dots, \alpha_p, \dots), \mathbf{A}_\mathrm{P}(\boldsymbol{\eta}) = [\dots, \mathbf{s}_p(\boldsymbol{\eta}), \dots],$$

$$\mathbf{s}_p(\boldsymbol{\eta}) = (\dots, s(nT_s - \tau - pT_s)e^{-j2\pi F_d(nT_s - \tau - pT_s)}, \dots).$$

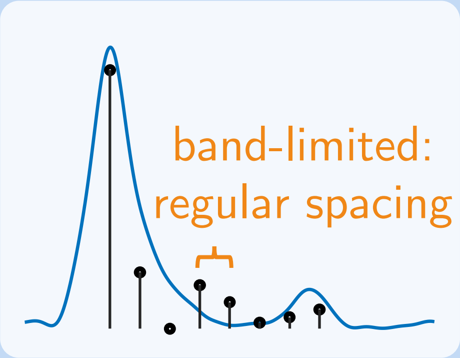

- Motivations: impulse response characterization, reflecting surface roughness (sea state inference), classification of reflecting surface, etc.
- Challenge: determining the number of sources P to describe the impulse response.

- Undershoot:
  - missed information,
  - bias estimates.
- Overshoot:
  - correct but not optimal,
  - overkill...

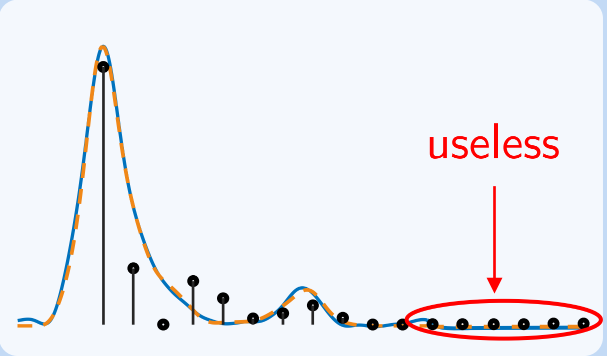

Reflecting surface IR size determination

Iterative procedure

Iterative procedure

- Assume P sources, $P < P_{\text{true}}$,
- test statistic for source $P+1$ based on the likelihood criterion:

$$T_{P+\text{next}} = \left| \left(\mathbf{P}^{\perp}_{\mathbf{A}_P} \mathbf{x} \right)^H s_{P+1}\left(\hat{\tau}, \widehat{F_d}\right) \right|^2$$

Reflecting surface IR size determination

Iterative procedure

- Assume P sources, $P < P_{\text{true}}$,
- test statistic for source $P+1$ based on the likelihood criterion:

$$T_{P+\text{next}} = \left| \left(\mathbf{P}^{\perp}_{\mathbf{A}_P} \mathbf{x} \right)^H s_{P+1}\left(\hat{\tau}, \widehat{F_d}\right) \right|^2$$

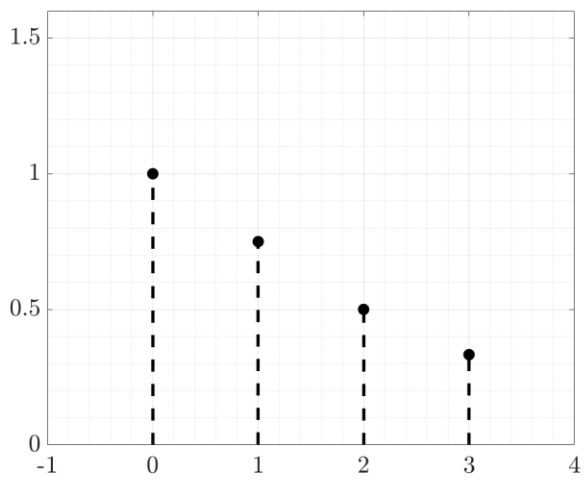

Iterative procedure

- Assume P sources, $P < P_{\text{true}}$,
- test statistic for source $P+1$ based on the likelihood criterion:

$$T_{P+\text{next}} = \left| \left(\mathbf{P}_{\mathbf{A}_P}^{\perp} \mathbf{x} \right)^H s_{P+1}\left(\hat{\tau}, \widehat{F_d}\right) \right|^2$$

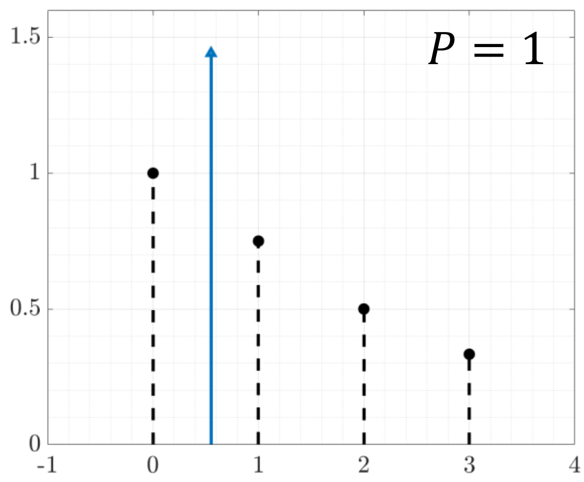

Iterative procedure

- Assume P sources, $P < P_{\text{true}}$,
- test statistic for source $P+1$ based on the likelihood criterion:

$$T_{P+\text{next}} = \left| \left(\mathbf{P}^{\perp}_{\mathbf{A}_P} \mathbf{x} \right)^H s_{P+1}\left(\hat{\tau}, \widehat{F_d}\right) \right|^2$$

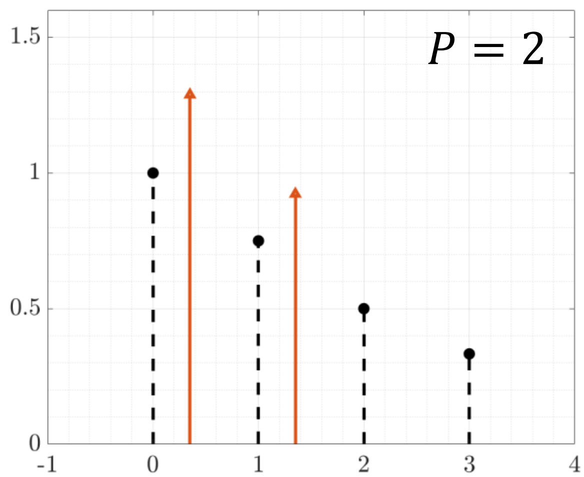

Iterative procedure

- Assume P sources, $P < P_{\text{true}}$,
- test statistic for source $P+1$ based on the likelihood criterion:

$$T_{P+\text{next}} = \left| \left(\mathbf{P}^{\perp}_{\mathbf{A}_P} \mathbf{x} \right)^H s_{P+1}\left(\hat{\tau}, \widehat{F_d}\right) \right|^2$$

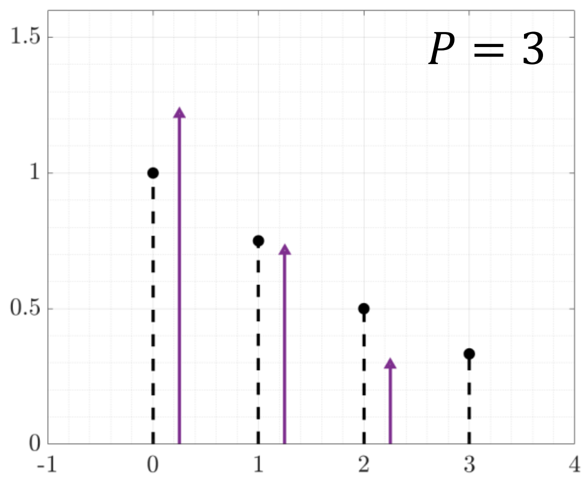

Iterative procedure

- Assume P sources, $P < P_{\text{true}}$,
- test statistic for source $P+1$ based on the likelihood criterion:

$$T_{P+\text{next}} = \left| \left(\mathbf{P}^{\perp}_{\mathbf{A}_P} \mathbf{x} \right)^H s_{P+1}(\hat{\tau}, \widehat{F_d}) \right|^2$$

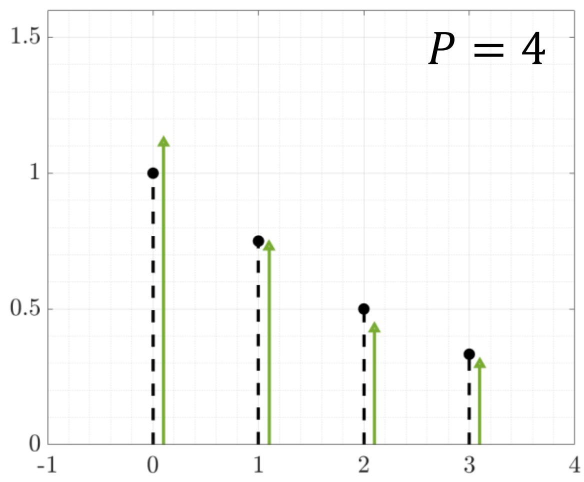

Iterative procedure

- Assume P sources, $P < P_{\text{true}}$,
- test statistic for source $P+1$ based on the likelihood criterion:

$$T_{P+\text{next}} = \left| \left(\mathbf{P}^{\perp}_{\mathbf{A}_P} \mathbf{x} \right)^H s_{P+1}\left(\hat{\tau}, \widehat{F_d}\right) \right|^2$$

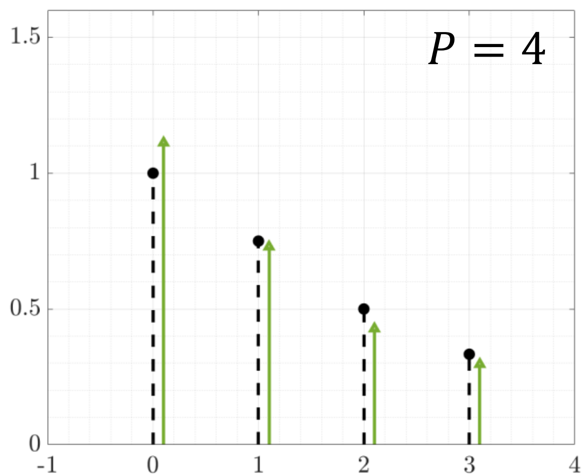

Overshoot-and-decimate procedure

Reflecting surface IR size determination

Iterative procedure

- Assume P sources, $P < P_{\text{true}}$,
- test statistic for source $P+1$ based on the likelihood criterion:

$$T_{P+\text{next}} = \left| \left(\mathbf{P}^{\perp}_{\mathbf{A}_P} \mathbf{x} \right)^H s_{P+1}\left(\hat{\tau}, \widehat{F_d}\right) \right|^2$$

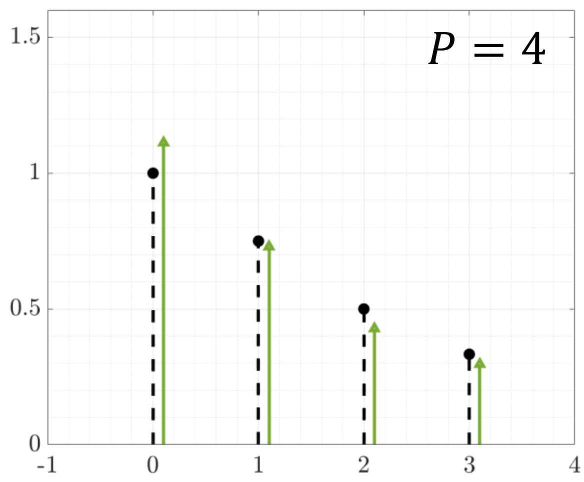

Overshoot-and-decimate procedure

- Assume M sources, $M > P_{\text{true}}$,
- test statistic for the M candidates based on a likelihood ratio LR:

$$LR_m = \left\| \mathbf{P}^{\perp}_{\mathbf{A}_M} \mathbf{x} \right\|^2 / \left\| \mathbf{P}^{\perp}_{\mathbf{A}_{M-1,m}} \mathbf{x} \right\|^2$$

Reflecting surface IR size determination

Iterative procedure

- Assume P sources, $P < P_{\text{true}}$,
- test statistic for source $P+1$ based on the likelihood criterion:

$$T_{P+\text{next}} = \left| \left(\mathbf{P}^{\perp}_{\mathbf{A}_P} \mathbf{x} \right)^H s_{P+1}\left(\hat{\tau}, \widehat{F_d}\right) \right|^2$$

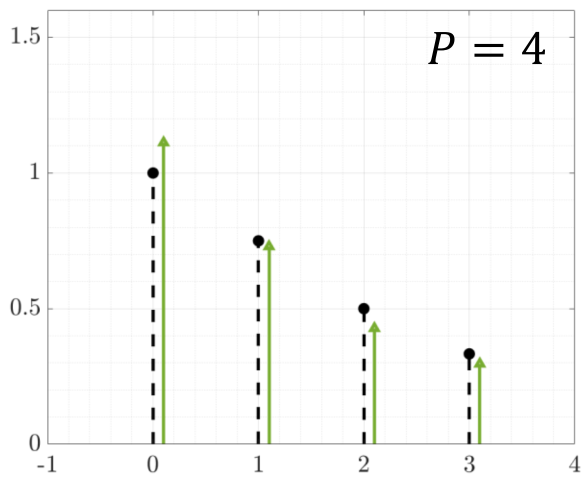

Overshoot-and-decimate procedure

- Assume M sources, $M > P_{\text{true}}$,
- test statistic for the M candidates based on a likelihood ratio LR:

$$LR_m = \left\| \mathbf{P}^{\perp}_{\mathbf{A}_M} \mathbf{x} \right\|^2 / \left\| \mathbf{P}^{\perp}_{\mathbf{A}_{M-1,m}} \mathbf{x} \right\|^2$$

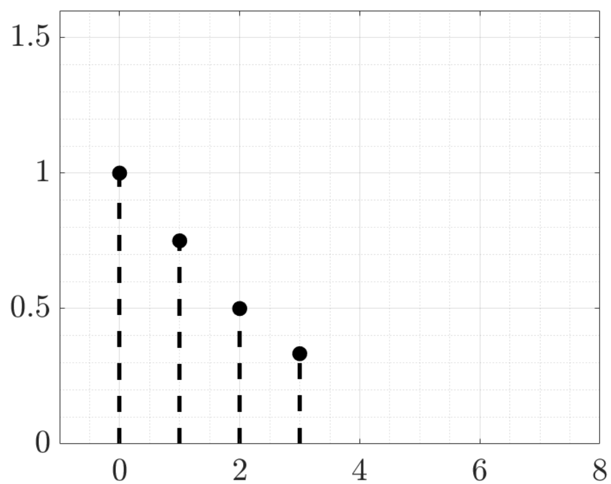

Iterative procedure

- Assume P sources, $P < P_{\text{true}}$,
- test statistic for source $P+1$ based on the likelihood criterion:

$$T_{P+\text{next}} = \left| \left(\mathbf{P}^{\perp}_{\mathbf{A}_P} \mathbf{x} \right)^H s_{P+1}\left(\hat{\tau}, \widehat{F_d}\right) \right|^2$$

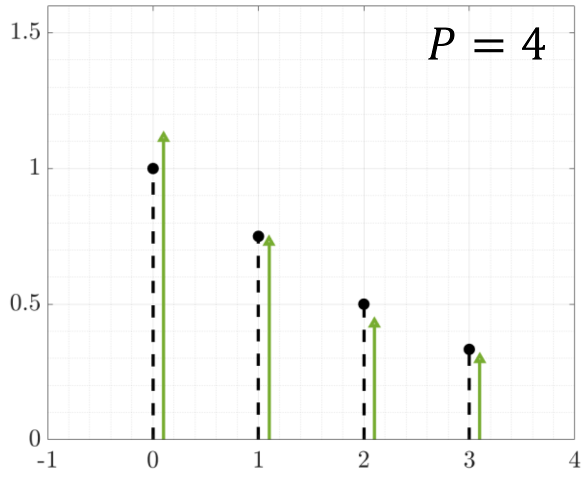

Overshoot-and-decimate procedure

- Assume M sources, $M > P_{\text{true}}$,
- test statistic for the M candidates based on a likelihood ratio LR:

$$LR_m = \left\| \mathbf{P}^{\perp}_{\mathbf{A}_M} \mathbf{x} \right\|^2 \Big/ \left\| \mathbf{P}^{\perp}_{\mathbf{A}_{M-1,m}} \mathbf{x} \right\|^2$$

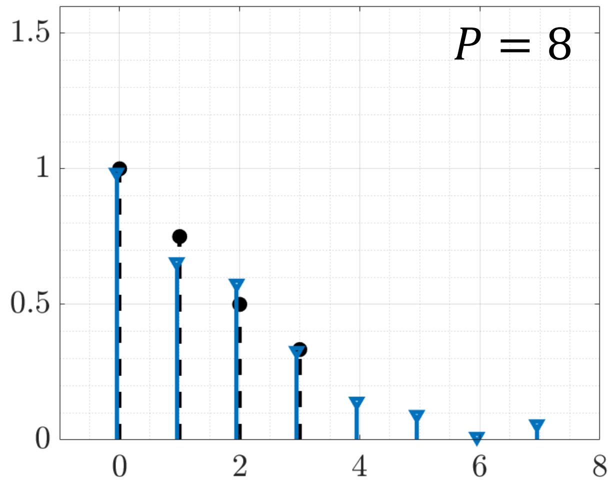

Iterative procedure

- Assume P sources, $P < P_{\text{true}}$,
- test statistic for source $P+1$ based on the likelihood criterion:

$$T_{P+\text{next}} = \left| \left(\mathbf{P}^{\perp}_{\mathbf{A}_P} \mathbf{x} \right)^H s_{P+1}(\hat{\tau}, \widehat{F_d}) \right|^2$$

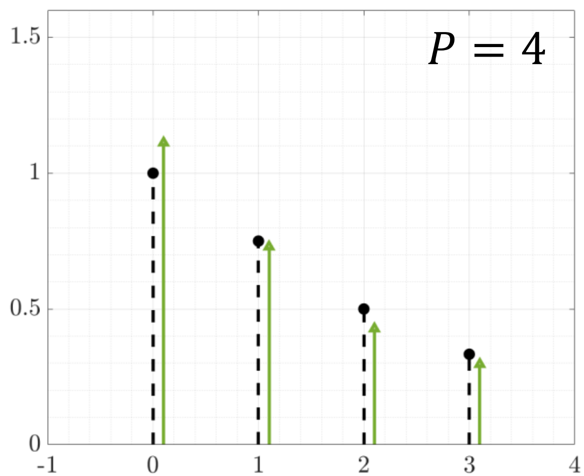

Overshoot-and-decimate procedure

- Assume M sources, $M > P_{\text{true}}$,
- test statistic for the M candidates based on a likelihood ratio LR:

$$LR_m = \left\| \mathbf{P}^{\perp}_{\mathbf{A}_M} \mathbf{x} \right\|^2 / \left\| \mathbf{P}^{\perp}_{\mathbf{A}_{M-1,m}} \mathbf{x} \right\|^2$$

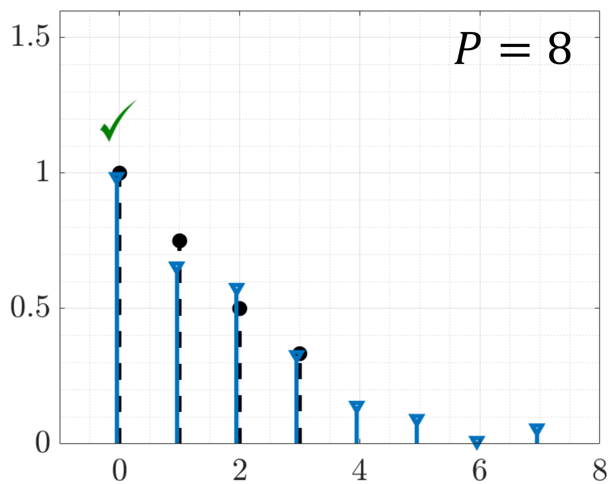

Reflecting surface IR size determination

Iterative procedure

- Assume P sources, $P < P_{\text{true}}$,
- test statistic for source $P+1$ based on the likelihood criterion:

$$T_{P+\text{next}} = \left| \left(\mathbf{P}^{\perp}_{\mathbf{A}_P} \mathbf{x} \right)^H s_{P+1}(\hat{\tau}, \widehat{F_d}) \right|^2$$

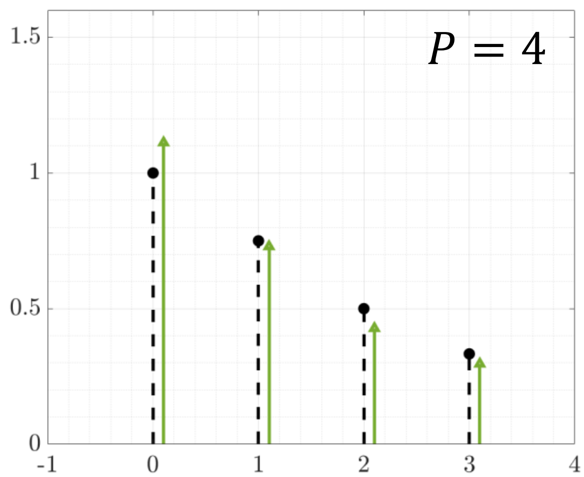

Overshoot-and-decimate procedure

- Assume M sources, $M > P_{\text{true}}$,
- test statistic for the M candidates based on a likelihood ratio LR:

$$LR_m = \left\| \mathbf{P}^{\perp}_{\mathbf{A}_M} \mathbf{x} \right\|^2 / \left\| \mathbf{P}^{\perp}_{\mathbf{A}_{M-1,m}} \mathbf{x} \right\|^2$$

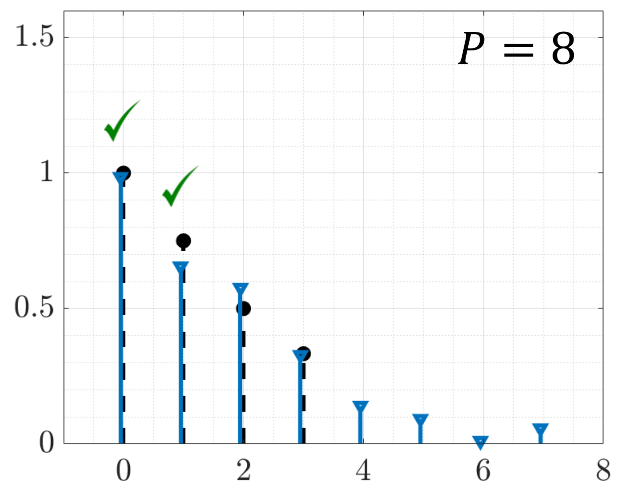

Reflecting surface IR size determination

Iterative procedure

- Assume P sources, $P < P_{\text{true}}$,
- test statistic for source $P+1$ based on the likelihood criterion:

$$T_{P+\text{next}} = \left| \left(\mathbf{P}^{\perp}_{\mathbf{A}_P} \mathbf{x} \right)^H s_{P+1}(\hat{\tau}, \widehat{F_d}) \right|^2$$

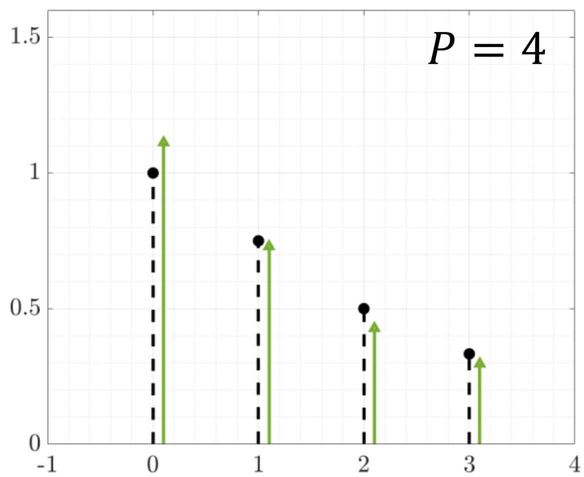

Overshoot-and-decimate procedure

- Assume M sources, $M > P_{\text{true}}$,
- test statistic for the M candidates based on a likelihood ratio LR:

$$LR_m = \left\| \mathbf{P}^{\perp}_{\mathbf{A}_M} \mathbf{x} \right\|^2 / \left\| \mathbf{P}^{\perp}_{\mathbf{A}_{M-1,m}} \mathbf{x} \right\|^2$$

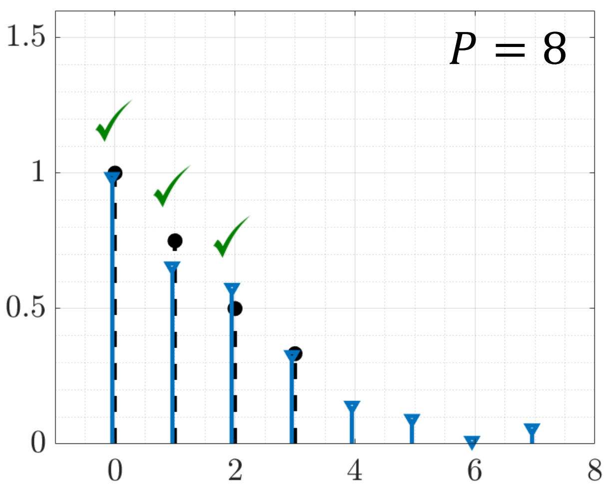

Iterative procedure

- Assume P sources, $P < P_{\text{true}}$,
- test statistic for source $P+1$ based on the likelihood criterion:

$$T_{P+\text{next}} = \left|\left(\mathbf{P}^{\perp}_{\mathbf{A}_P}\mathbf{x}\right)^H s_{P+1}(\hat{\tau}, \widehat{F_d})\right|^2$$

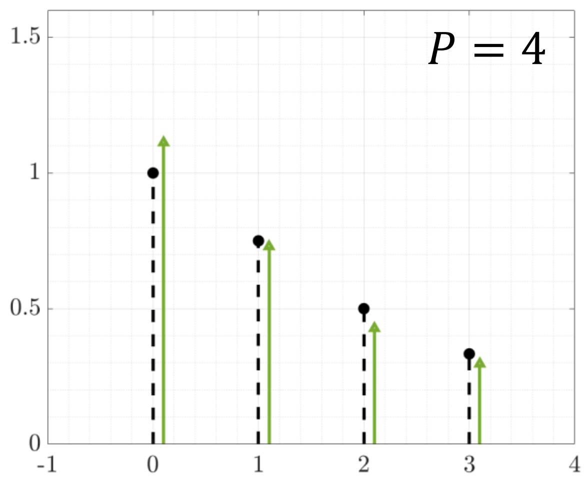

Overshoot-and-decimate procedure

- Assume M sources, $M > P_{\text{true}}$,
- test statistic for the M candidates based on a likelihood ratio LR:

$$LR_m = \left\|\mathbf{P}^{\perp}_{\mathbf{A}_M}\mathbf{x}\right\|^2 / \left\|\mathbf{P}^{\perp}_{\mathbf{A}_{M-1,m}}\mathbf{x}\right\|^2$$

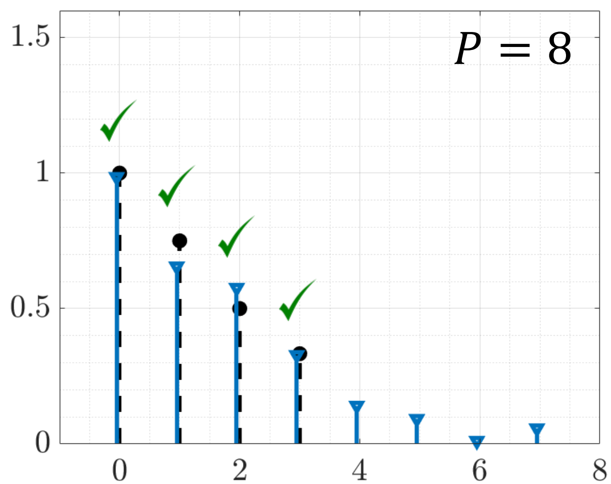

Iterative procedure

- Assume P sources, $P < P_{\text{true}}$,
- test statistic for source $P+1$ based on the likelihood criterion:

$$T_{P+\text{next}} = \left|\left(\mathbf{P}^{\perp}_{\mathbf{A}_P}\mathbf{x}\right)^H s_{P+1}\left(\hat{\tau}, \widehat{F_d}\right)\right|^2$$

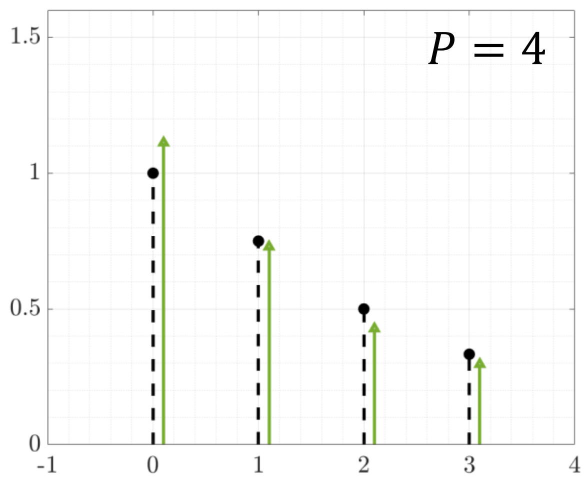

Overshoot-and-decimate procedure

- Assume M sources, $M > P_{\text{true}}$,
- test statistic for the M candidates based on a likelihood ratio LR:

$$LR_m = \left\|\mathbf{P}^{\perp}_{\mathbf{A}_M}\mathbf{x}\right\|^2 / \left\|\mathbf{P}^{\perp}_{\mathbf{A}_{M-1,m}}\mathbf{x}\right\|^2$$

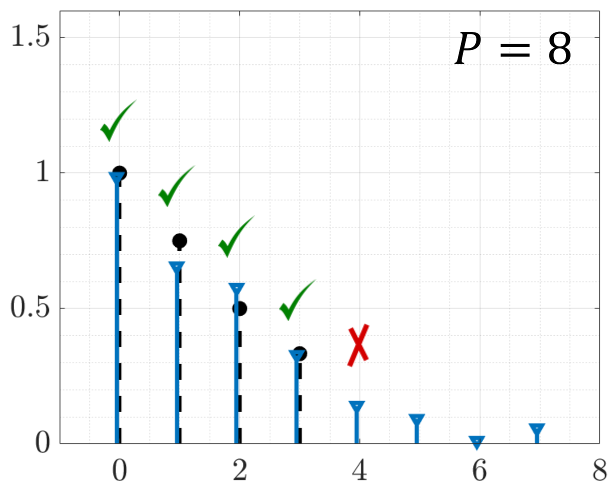

Iterative procedure

- Assume P sources, $P < P_{\text{true}}$,
- test statistic for source $P+1$ based on the likelihood criterion:

$$T_{P+\text{next}} = \left| \left(\mathbf{P}^{\perp}_{\mathbf{A}_P} \mathbf{x} \right)^H s_{P+1}(\hat{\tau}, \widehat{F_d}) \right|^2$$

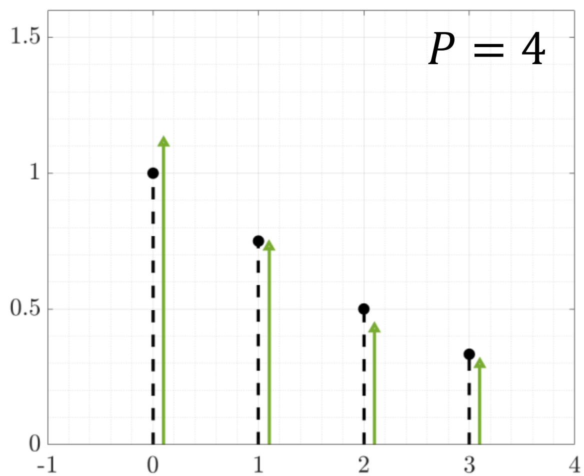

Overshoot-and-decimate procedure

- Assume M sources, $M > P_{\text{true}}$,
- test statistic for the M candidates based on a likelihood ratio LR:

$$LR_m = \left\| \mathbf{P}^{\perp}_{\mathbf{A}_M} \mathbf{x} \right\|^2 / \left\| \mathbf{P}^{\perp}_{\mathbf{A}_{M-1,m}} \mathbf{x} \right\|^2$$

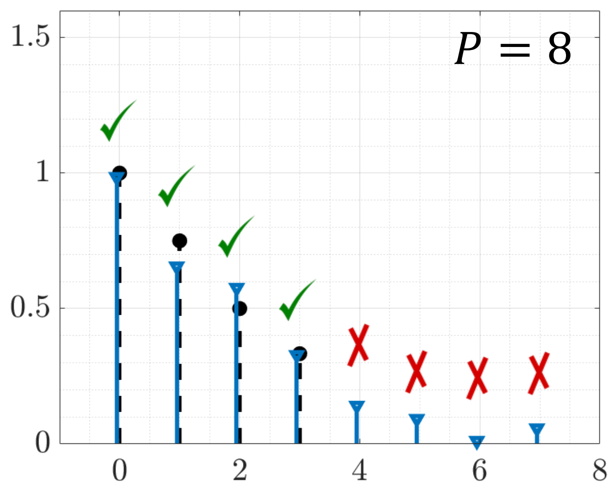

Reflecting surface IR size determination

Iterative procedure

- Assume P sources, $P < P_{\text{true}}$,
- test statistic for source $P+1$ based on the likelihood criterion:

$$T_{P+\text{next}} = \left| \left(\mathbf{P}_{\mathbf{A}_P}^{\perp} \mathbf{x} \right)^H s_{P+1}\left(\hat{\tau}, \widehat{F_d}\right) \right|^2$$

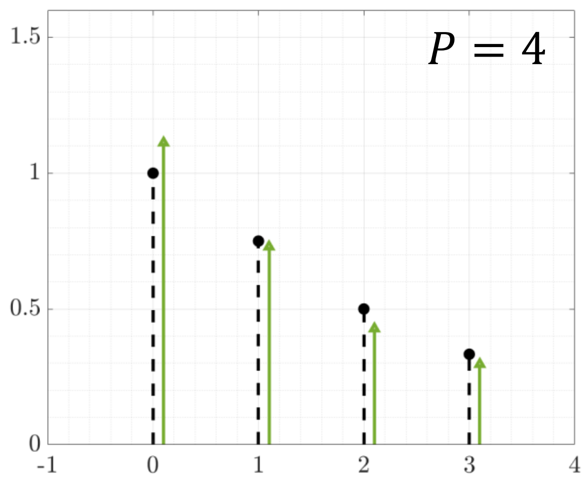

Overshoot-and-decimate procedure

- Assume M sources, $M > P_{\text{true}}$,
- test statistic for the M candidates based on a likelihood ratio LR:

$$LR_m = \left\| \mathbf{P}_{\mathbf{A}_M}^{\perp} \mathbf{x} \right\|^2 / \left\| \mathbf{P}_{\mathbf{A}_{M-1,m}}^{\perp} \mathbf{x} \right\|^2$$

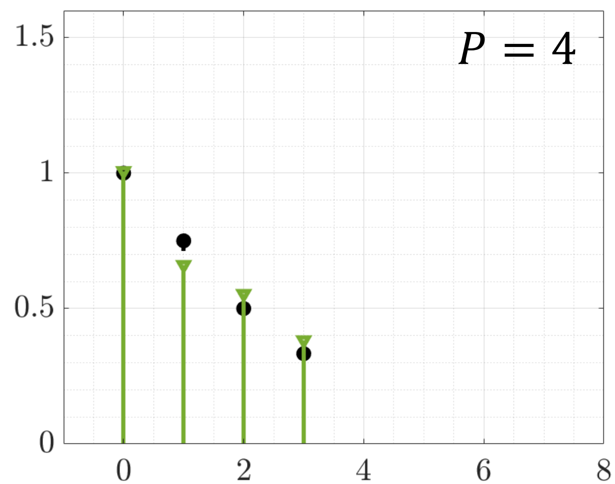

Wrap-up on diffuse reflection

In this presentation

- Differences between specular and diffuse reflections.
- Introduction to reflecting surface impulse response signal model.
- Determination of the impulse response size.

  Lubeigt *et al.* (under review after major revision), *Signal Processing.*

Wrap-up on diffuse reflection

In this presentation

- Differences between specular and diffuse reflections.
- Introduction to reflecting surface impulse response signal model.
- Determination of the impulse response size.

  Lubeigt *et al.* (under review after major revision), *Signal Processing*.

Related works

Signal coherence study with ICE in Barcelona:

- Mallorca's Puig Major experiment data.
- Detection of coherent-to-non-coherent transition based on the phase observation.
- Glistening zone size computation based on geometry.

Conclusion

Credit: Ronan Lambert

GNSS Multipath

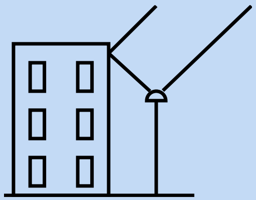

Theoretical approach:

- Dual source signal model.
- Derivation of the Cramér-Rao bound.
- Validation using the properties of the MLE.

GNSS Multipath

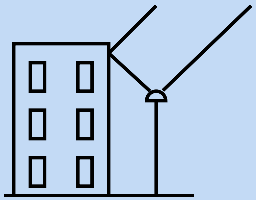

Theoretical approach:

- Dual source signal model.
- Derivation of the Cramér-Rao bound.
- Validation using the properties of the MLE.

Ground-based GNSS-R

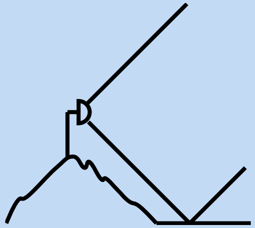

Experimental approach:

- Limits of current ground-based GNSS-R processing techniques.
- Gruissan experiment preparation.
- Dual source processing for weak crosstalk scenarios.

Conclusion

GNSS Multipath

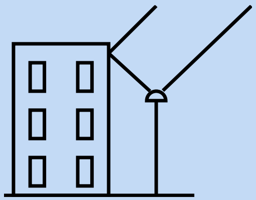

Theoretical approach:

- Dual source signal model.
- Derivation of the Cramér-Rao bound.
- Validation using the properties of the MLE.

Ground-based GNSS-R

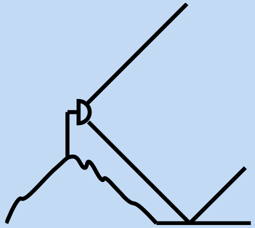

Experimental approach:

- Limits of current ground-based GNSS-R processing techniques.
- Gruissan experiment preparation.
- Dual source processing for weak crosstalk scenarios.

Diffuse reflection

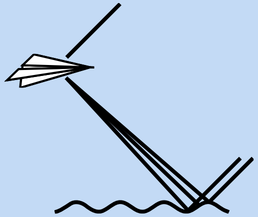

Exploratory approach:

- Specular / Diffuse reflection main differences.
- Reflecting surface impulse response signal model.
- Size of the reflecting surface impulse response.

Perspectives

GNSS Multipath

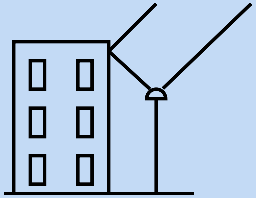

- Extension of MCRB to GNSS interferences (jamming, spoofing).

  Ortega *et al.* (under review), *Navigation.*

- Semiparametric signal models [Fortunati *et al.* 2019].

Perspectives

GNSS Multipath

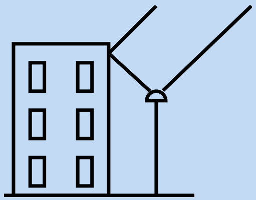

- Extension of MCRB to GNSS interferences (jamming, spoofing).
  - Ortega *et al.* (under review), *Navigation.*
- Semiparametric signal models [Fortunati *et al.* 2019].

Ground-based GNSS-R

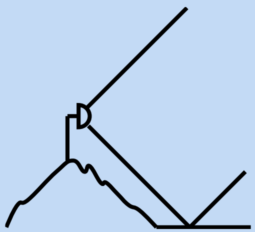

- Exploitation of wide bandwidth signals such as GALILEO E5 AltBOC or GNSS meta-signals [Ortega *et al.* 2020].
- Carrier phase [Lestarquit *et al.* 2016], [Medina *et al.* 2020].

Perspectives

GNSS Multipath

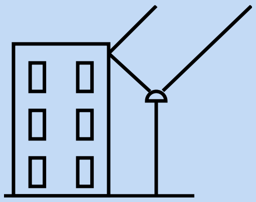

- Extension of MCRB to GNSS interferences (jamming, spoofing).
  - Ortega *et al.* (under review), *Navigation.*
- Semiparametric signal models [Fortunati *et al.* 2019].

Ground-based GNSS-R

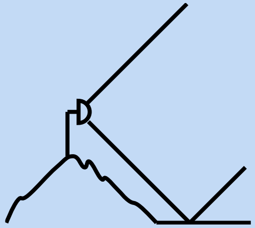

- Exploitation of wide bandwidth signals such as GALILEO E5 AltBOC or GNSS meta-signals [Ortega *et al.* 2020].
- Carrier phase [Lestarquit *et al.* 2016], [Medina *et al.* 2020].

Diffuse reflection

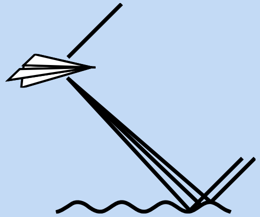

- Reflecting surfaces are random objects:
  - unconditional signal models [Stoica and Nehorai, 1990],
  - sparsity-based models [Zhang *et al.* 2022].
- CNES SAFIRE experiment (airborne GNSS-R).

Acknowledgements / Remerciements

Encadrement de thèse

Eric, Jordi, Lorenzo, pour une équipe (trop) bien huilée.

CNES

Laurent pour l'expertise technique en GNSS et GNSS-R,
FX et Jean-Louis pour deux belles journées à Gruissan.

TéSA

Corinne pour sa bienveillance inconditionnelle,
tout le monde à TéSA, un environnement sain où il fait bon vivre.

ISAE

François pour ses idées géniales,
Benoit pour son expérience et son précieux logiciel.

ICE

Estel and Weiqiang for their (very) precious time and experience!

References

[Martín-Neira, 1993] Martín-Neira, Manuel "A Passive Reflectometry and Interferometry System (PARIS): Application to Ocean Altimetry." *ESA Journal* 17, **1993**.

[Lowe *et al*, 2002] Lowe, Stephen T., *et al.* "First Spaceborne Observation of an Earth-reflected GPS Signal." *Radio Science*, vol. 37, no. 1, pp. 1–28, **2002**.

[Kaplan and Hegarty, 2017] Kaplan, Elliott D. and Hegarty, Christopher J. "Understanding GPS/GNSS: Principle and Applications." 3rd edition, *Artech House*, **2017**.

[Yau and Bresler, 1992] Yau, Sze Fong and Bresler, Yoram "A Compact Cramér-Rao Bound Expression for Parametric Estimation of Superimposed Signals." *IEEE Transactions on Signal Processing*, vol. 50, no. 5, pp. 1226-1230, **1992**.

[Stoica and Nehorai, 1990] Stoica, Petr and Nehorai Arye "Performance Study of Conditional and Unconditional Direction of Arrival Estimation." *IEEE Transactions on Acoustic, Speech, and Signal Processing*, vol. 38, no. 10, pp. 1783-1795, **1990**.

[Renaux *et al.* 2006] Renaux, Alexandre, *et al.* "On the high-SNR conditional maximum-likelihood estimator full statistical characterization." *IEEE Transactions on Signal Processing*, vol. 54, no. 12, pp. 4840-4843, **2006**.

[Ribot *et al.* 2014] Ribot, Miguel Angel, *et al.* "Normalized GNSS Interference Pattern Technique for Altimetry." *Sensors*, vol. 14, no. 6, pp. 10234-10257, **2014**.

[Fortunati *et al.* 2019] Fortunati, Stefano, *et al.* "Semiparametric CRB and Slepian-Bangs Formulas for Complex Elliptically Symmetric Distributions." *IEEE Transactions on Signal Processing*, vol. 67, no. 20, pp. 5352-5364, **2019**.

[Ortega *et al.* 2020] Ortega, Lorenzo, *et al.* "Positioning Performance Limits of GNSS Meta-Signals and HO-BOC Signals." *Sensors*, vol. 20, no. 12 p. 3586, **2020**.

[Lestarquit *et al.* 2016] Lestarquit, Laurent *et al.* "Reflectometry With an Open-Source Software GNSS Receiver: Use Case With Carrier Phase Altimetry." *IEEE Journal of Selected Topics in Applied Earth Observations and Remote Sensing*, vol. 9, no. 10, pp. 4843-4853, **2016**.

[Medina *et al.* 2020] Medina, Daniel, *et al.* "A New Compact CRB for Delay, Doppler and Phase Estimation - Application to GNSS SPP & RTK Performance Characterization." *IET Radar, Sonar & Navigation*, vol. 14, no. 10, pp. 1537-1549, **2020**.

[Zhang *et al.* 2022] Zhang, Yuxuan, *et al.* "Sparsity-Based Time Delay Estimation Through the Matched Filter Outputs." *IEEE Signal Processing Letters* 29, pp. 1769-1773, **2022**.

PhD contributions - Journals

- Corentin Lubeigt, *et al*. "Joint Delay-Doppler Estimation Performance in a Dual Source Context." *Remote Sensing*, vol. 12, no. 23, 3894, **2020**.
- Corentin Lubeigt, *et al*. "On the Impact and Mitigation of Signal Crosstalk in Ground-Based and Low Altitude Airborne GNSS-R." *Remote Sensing*, vol. 13, no. 6, 1085, **2021**.
- Corentin Lubeigt, *et al*. "Clean-to-Composite Bound Ratio: A Multipath Criterion for GNSS Signal Design and Analysis." *IEEE Transactions on Aerospace and Electronic Systems*, vol. 58, no. 6, pp. 5412–5424, **2022**.
- Corentin Lubeigt, *et al*. "Untangling First and Second Order Statistics Contributions in Multipath Scenarios." *Signal Processing*, vol.205, 108868, **2023**.
- Corentin Lubeigt, *et al*. "Band-Limited Impulse Response Estimation Performance," submitted after major revision to *Signal Processing.*
- Corentin Lubeigt, *et al*. "Approximate Maximum Likelihood Time-Delay Estimation for Two Closely Spaced Sources," submitted after major revision to *Signal Processing.*
- Lorenzo Ortega, *et al*. "On the GNSS Synchronization Performance Degradation under Interference Scenarios: Bias and Misspecified CRB," submitted to *Navigation.*

PhD contributions - Conferences

- Corentin Lubeigt, *et al.* "Multipath Estimating Techniques Performance Analysis." *IEEE Aerospace Conference* (March 2022): 1–6.
- Corentin Lubeigt, *et al.* "Close-to-Ground Single Antenna GNSS-R." *NAVITEC* (April 2022).
- Corentin Lubeigt, *et al.* "Les Signaux à Bande Large au Service de la Réflectométrie par GNSS à Site Bas." *GRETSI* (September 2022).
- Lorenzo Ortega, *et al.* "GNSS L5/E5 Maximum Likelihood Synchronization Performance Degradation Under DME Interferences." *IEEE/ION Position, Location and Navigation Symposium* (April 2023).

Back-up: CRB calculation steps

- Slepian-Bangs formula:

$$\left[\mathbf{F}_{\epsilon|\epsilon}(\boldsymbol{\epsilon})\right]_{k,l} = \frac{2}{\sigma_n^2}\mathrm{Re}\left\{\left(\frac{\partial \mathbf{A}\boldsymbol{\alpha}}{\partial \epsilon_k}\right)^H \left(\frac{\partial \mathbf{A}\boldsymbol{\alpha}}{\partial \epsilon_l}\right)\right\} + \frac{N}{\sigma_n^4}\frac{\partial \sigma_n^2}{\partial \epsilon_k}\frac{\partial \sigma_n^2}{\partial \epsilon_l}.$$

- $\mathbf{A}\boldsymbol{\alpha} = \rho_0 e^{j\phi_0}\mathbf{s}(\tau_0, b_0) + \rho_1 e^{j\phi_1}\mathbf{s}(\tau_1, b_1)$.
- After derivating and rearranging the terms:

$$\mathbf{F}_{\epsilon|\epsilon}(\boldsymbol{\epsilon}) = \frac{2F_s}{\sigma_n^2} Re\left\{\mathbf{Q}\begin{bmatrix}\mathbf{W} & (\mathbf{W}^\Delta)^{\mathrm{H}} \\ \mathbf{W}^\Delta & \mathbf{W}\end{bmatrix}\mathbf{Q}^{\mathrm{H}}\right\} \text{ where } \mathbf{W}^\Delta = \begin{bmatrix} W_{1,1}^\Delta & W_{1,2}^\Delta & W_{1,3}^\Delta \\ W_{2,1}^\Delta & W_{2,2}^\Delta & W_{2,3}^\Delta \\ W_{3,1}^\Delta & W_{3,2}^\Delta & W_{3,3}^\Delta \end{bmatrix}.$$

- Example for $W_{1,1}^\Delta$: $W_{1,1}^\Delta = e^{j\omega_c \Delta b \tau_0}\int_R s(t-\tau_0)s(t-\tau_1)^* e^{-j2\pi f_c \Delta b t}\mathrm{d}t$

$u \leftarrow t - \tau_1$

$$= \int_R s(u-\Delta\tau)\left(s(u)e^{\mathrm{j}2\pi f_c \Delta b u}\right)^* \mathrm{d}u$$

FT over an hermitian product

$$= \int_{-\frac{F_s}{2}}^{\frac{F_s}{2}} \left(S(f)e^{-j2\pi f \Delta\tau}\right) S(f - f_c\Delta b)^* \mathrm{d}f$$

Back-up: CRB calculation steps

- Fourier transform of a band-limited signal of band $B = F_s$, for $f \in \left[-\frac{F_s}{2}, \frac{F_s}{2}\right]$:

$$S(f) = \frac{1}{F_s}\sum_{n=0}^{N-1} s(nT_s)e^{-j2\pi f n T_s} = \frac{1}{F_s}\mathbf{s}^{\mathrm{T}}\boldsymbol{\nu}(f)^* \text{ where } \begin{cases} \mathbf{s} = (\dots, s(nT_s), \dots)^{\mathrm{T}}, \\ \boldsymbol{\nu}(f) = \left(\dots, e^{j2\pi f n}, \dots\right)^{\mathrm{T}}. \end{cases}$$

$$W_{1,1}^{\Delta} = \int_{-\frac{F_s}{2}}^{\frac{F_s}{2}} S(f)e^{-j2\pi f\Delta\tau}S(f - f_c\Delta b)^*\mathrm{d}f$$

$$f \leftarrow \frac{f}{F_s}$$

$$= \frac{1}{F_s}\int_{-\frac{1}{2}}^{\frac{1}{2}}\left(\mathbf{s}^{\mathrm{T}}\boldsymbol{\nu}(f)^*\right)e^{-j2\pi f\frac{\Delta\tau}{T_s}}\left(\mathbf{s}^{\mathrm{H}}\mathbf{U}\left(\frac{\Delta b f_c}{F_s}\right)\boldsymbol{\nu}(f)\right)\mathrm{d}f$$

$$= \frac{1}{F_s}\mathbf{s}^{\mathrm{H}}\mathbf{U}\left(\frac{\Delta b f_c}{F_s}\right)\underbrace{\left(\int_{-\frac{1}{2}}^{\frac{1}{2}}\boldsymbol{\nu}(f)\boldsymbol{\nu}(f)^{\mathrm{H}}e^{-j2\pi f\frac{\Delta\tau}{T_s}}\mathrm{d}f\right)}_{\mathbf{V}^{\Delta,0}\left(\frac{\Delta\tau}{T_s}\right)}\mathbf{s} = \frac{1}{\mathrm{F_s}}\mathbf{s}^{\mathrm{H}}\mathbf{U}\left(\frac{\Delta b f_c}{F_s}\right)\mathbf{V}^{\Delta,0}\left(\frac{\Delta\tau}{T_s}\right)\mathbf{s},$$

where $\mathbf{U}(q) = \mathrm{diag}\left(\dots, e^{-j2\pi q n}, \dots\right), \left[\mathbf{V}^{\Delta,0}(p)\right]_{k,l} = \mathrm{sinc}(k - l - p).$

Back-up: Misspecified Cramér-Rao bounds (MCRB)

- True signal model: dual source signal model, with $\boldsymbol{\theta}^T = (\boldsymbol{\eta}^T, \rho, \phi)$ and $\boldsymbol{\eta}^T = (\tau, b)$,

$$p_{\mathbf{x}}(\mathbf{x}; \boldsymbol{\theta}_0, \boldsymbol{\theta}_1) = \mathcal{CN}(\alpha_0 \mathbf{a}(\boldsymbol{\eta}_0) + \alpha_1 \mathbf{a}(\boldsymbol{\eta}_1), \sigma_n^2 \mathbf{I}_N).$$

- Misspecified signal model: single source signal model, pt: pseudotrue,

$$f_{\mathbf{x}}\left(\mathbf{x}; \boldsymbol{\theta}_{pt}\right) = \mathcal{CN}\left(\alpha_{pt} \mathbf{a}\left(\boldsymbol{\eta}_{pt}\right), \sigma_n^2 \mathbf{I}_N\right).$$

- Misspecified Maximum Likelihood Estimator (MMLE): MLE of the misspecified model. The MMLE is biased but it is asymptotically misspecified-unbiased: it concentrates to a mean with a given variance that can be characterized:
  - Mean: pseudotrue estimate that minimizes the Kullback-Leibler Divergence:

$$\boldsymbol{\theta}_{pt} = \arg\min_{\boldsymbol{\theta}} \{D(p_{\mathbf{x}} || f_{\mathbf{x}})\}.$$

  - Variance: misspeciefied Cramér-Rao bound (MCRB):

$$\mathbf{MCRB}(\boldsymbol{\theta}_{pt}) = \mathbf{A}\left(\boldsymbol{\theta}_{pt}\right)^{-1} \mathbf{B}\left(\boldsymbol{\theta}_{pt}\right) \mathbf{A}\left(\boldsymbol{\theta}_{pt}\right)^{-1}.$$

    - $\mathbf{A}\left(\boldsymbol{\theta}_{pt}\right)$ accounts for the model misspecification.
    - $\mathbf{B}\left(\boldsymbol{\theta}_{pt}\right)$ is the FIM of the single source signal model (known).

Back-up: Misspecified Cramér-Rao bounds (MCRB)

- Simulation set-up:
  - signal: GPS L1 C/A,
  - 2000 Monte Carlo runs.

	$\boldsymbol{\theta}_0$	$\boldsymbol{\theta}_1$	$\boldsymbol{\theta}_{pt}$
τ [m]	0	73.26	7
F_d [Hz]	0	100	24
ρ [-]	1	0.5	1.23
ϕ [deg]	0	15	2

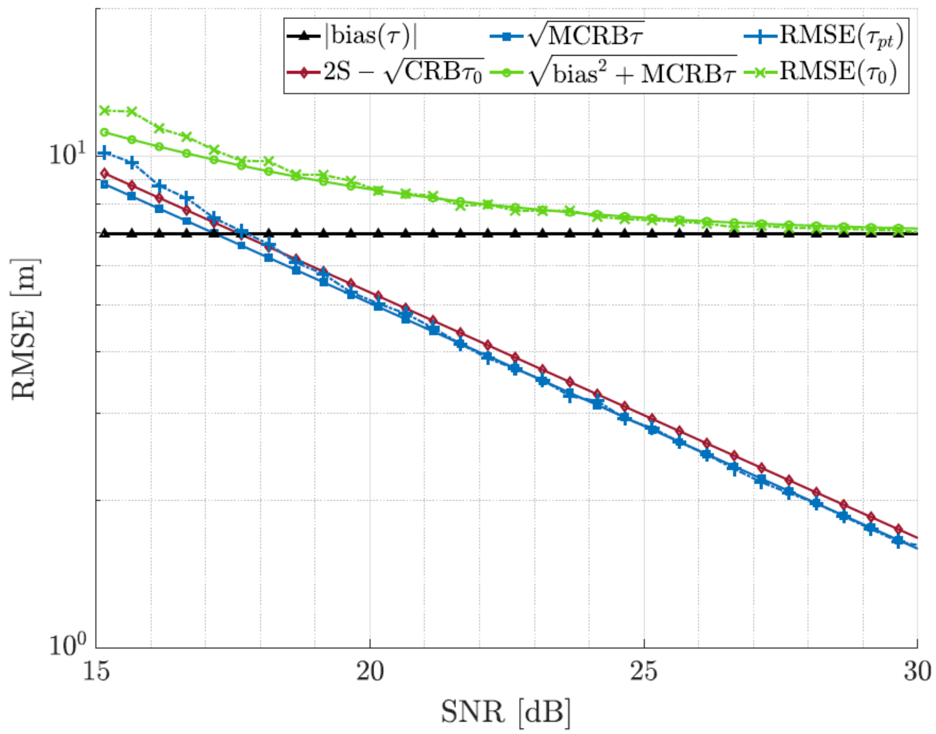

Back-up: 2S-MLE dimensionality reduction

- Signal model: $\mathbf{x} = \mathbf{A}(\boldsymbol{\eta}_0, \boldsymbol{\eta}_1)\boldsymbol{\alpha} + \mathbf{w}, \mathbf{w} \sim CN(\mathbf{0}, \sigma_n^2\mathbf{I}_\mathrm{N}) \Rightarrow \mathbf{x} \sim \boldsymbol{CN}(\mathbf{A}\boldsymbol{\alpha}, \sigma_n^2\mathbf{I}_N)$.

$$\hat{\boldsymbol{\epsilon}} = \arg\max_{\boldsymbol{\epsilon}}\{p(\mathbf{x}; \boldsymbol{\epsilon})\} \text{ where } p(\mathbf{x}; \boldsymbol{\epsilon}) = \frac{1}{(\pi\sigma_n^2)^N} e^{-\frac{1}{\sigma_n^2}\|\mathbf{x}-\mathbf{A}\boldsymbol{\alpha}\|^2}.$$

- Maximizing $p(\mathbf{x};\boldsymbol{\epsilon})$ is equivalent to minizing $\|\mathbf{x} - \mathbf{A}\boldsymbol{\alpha}\|^2$:

$$\max_{\boldsymbol{\epsilon}}\{p(\mathbf{x}; \boldsymbol{\epsilon})\} = \min_{\boldsymbol{\epsilon}}\{\|\mathbf{x} - \mathbf{A}\boldsymbol{\alpha}\|^2\},$$

- and with the projector $\mathbf{P_A} = \mathbf{A}\left(\mathbf{A}^\mathrm{H}\mathbf{A}\right)^{-\mathbf{1}}\mathbf{A}^\mathbf{H}$,

$$\begin{aligned}\|\mathbf{x} - \mathbf{A}\boldsymbol{\alpha}\|^2 &= \|\mathbf{P_A}(\mathbf{x} - \mathbf{A}\boldsymbol{\alpha})\|^2 + \left\|\mathbf{P_A^\perp}(\mathbf{x} - \mathbf{A}\boldsymbol{\alpha})\right\|^2 \\ &= \underbrace{\left\|\mathbf{A}\left(\left(\mathbf{A}^\mathrm{H}\mathbf{A}\right)^{-\mathbf{1}}\mathbf{A}^\mathrm{H}\mathbf{x} - \boldsymbol{\alpha}\right)\right\|^2}_{\text{null for } \boldsymbol{\alpha} \text{ well chosen}} + \left\|\mathbf{P_A^\perp x}\right\|^2.\end{aligned}$$

$$\hat{\boldsymbol{\epsilon}} = \min_{\boldsymbol{\epsilon}}\{\|\mathbf{x} - \mathbf{A}\boldsymbol{\alpha}\|^2\} \Leftrightarrow \min_{\boldsymbol{\eta}_0,\boldsymbol{\eta}_1}\left\{\left\|\mathbf{P_A^\perp x}\right\|^2\right\} \text{ and } \hat{\boldsymbol{\alpha}} = \left(\mathbf{A}^\mathrm{H}\mathbf{A}\right)^{-\mathbf{1}}\mathbf{A}^\mathrm{H}\mathbf{x}.$$

Back-up: CLEAN-RELAX estimator

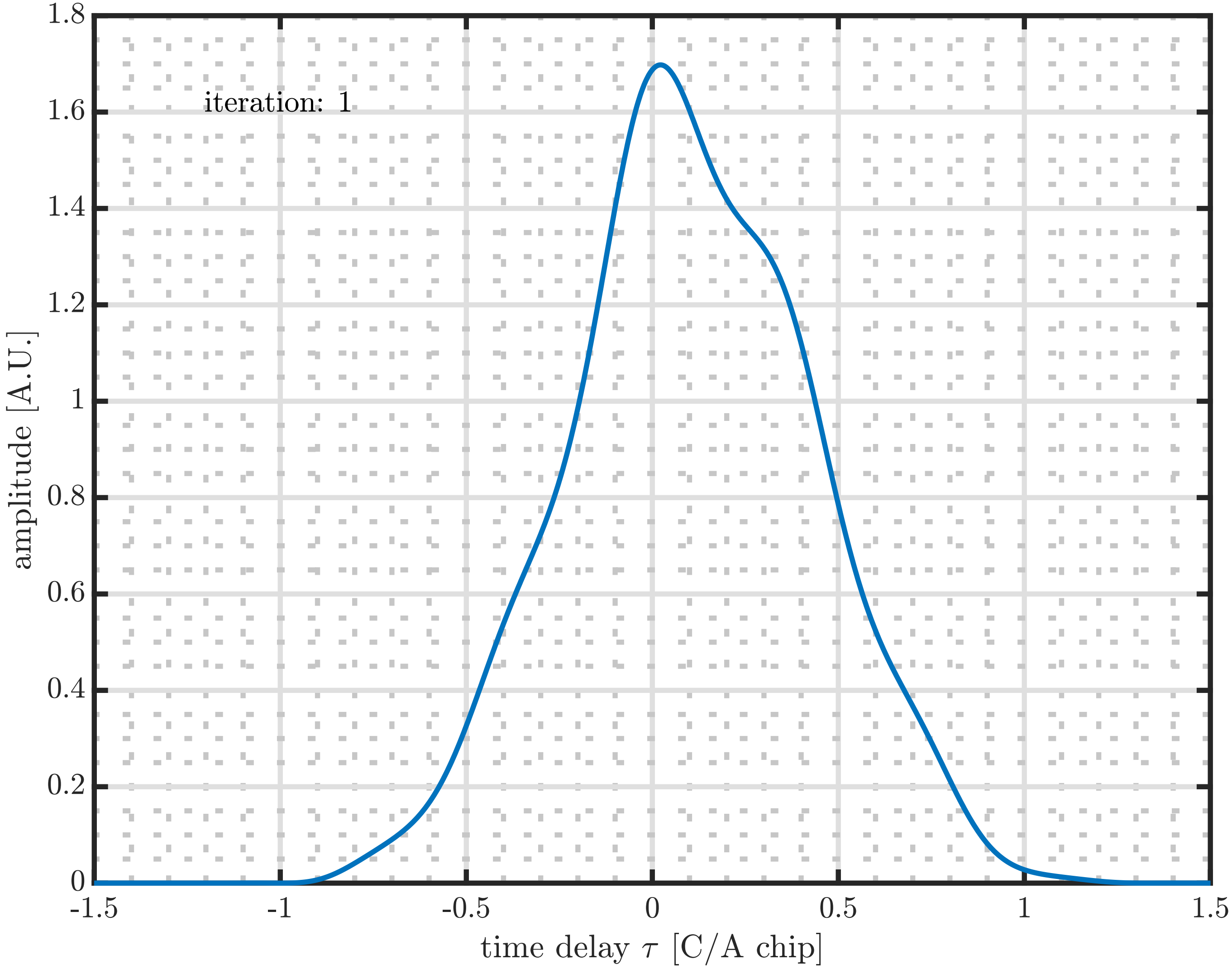

Back-up: CLEAN-RELAX estimator

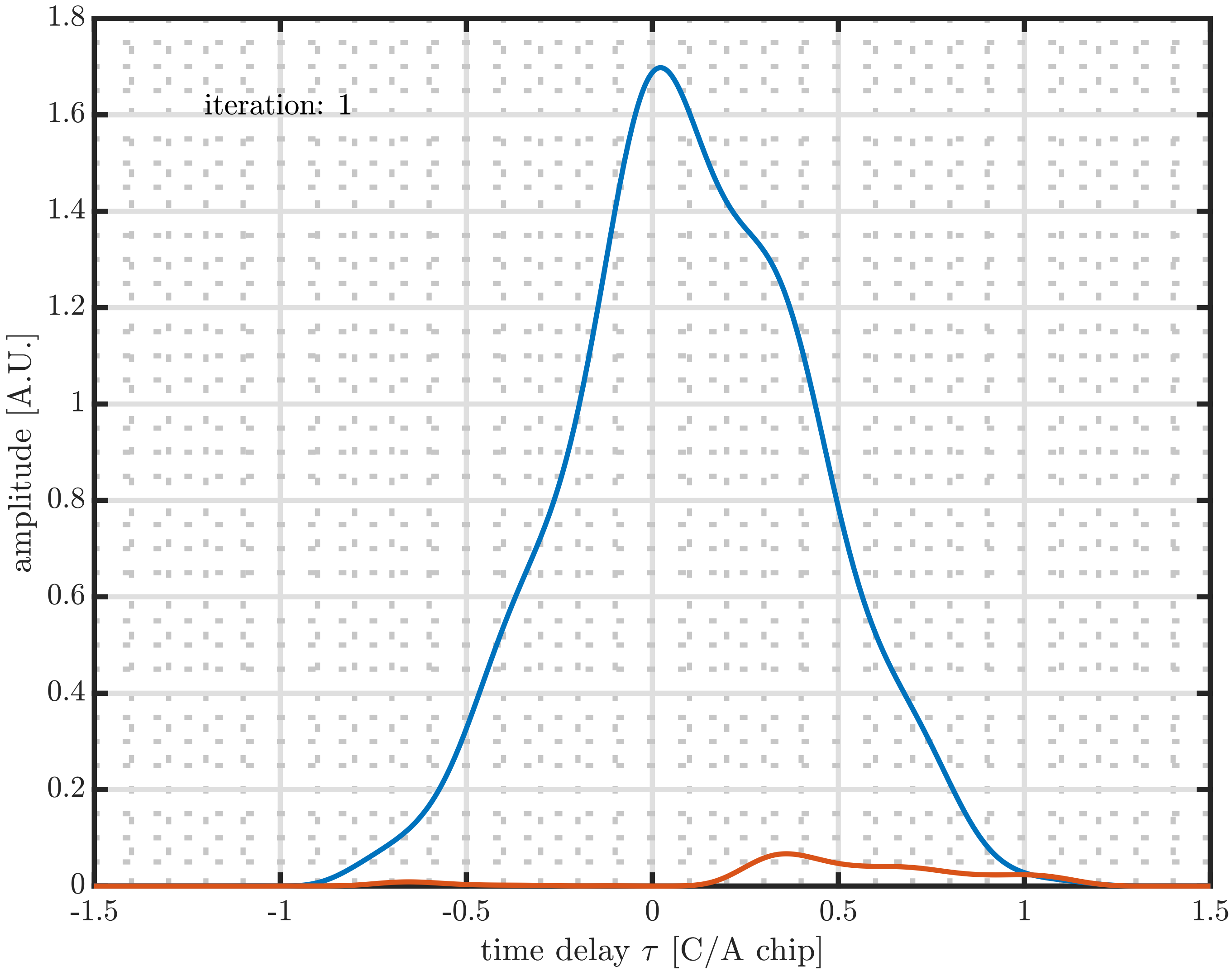

Back-up: CLEAN-RELAX estimator

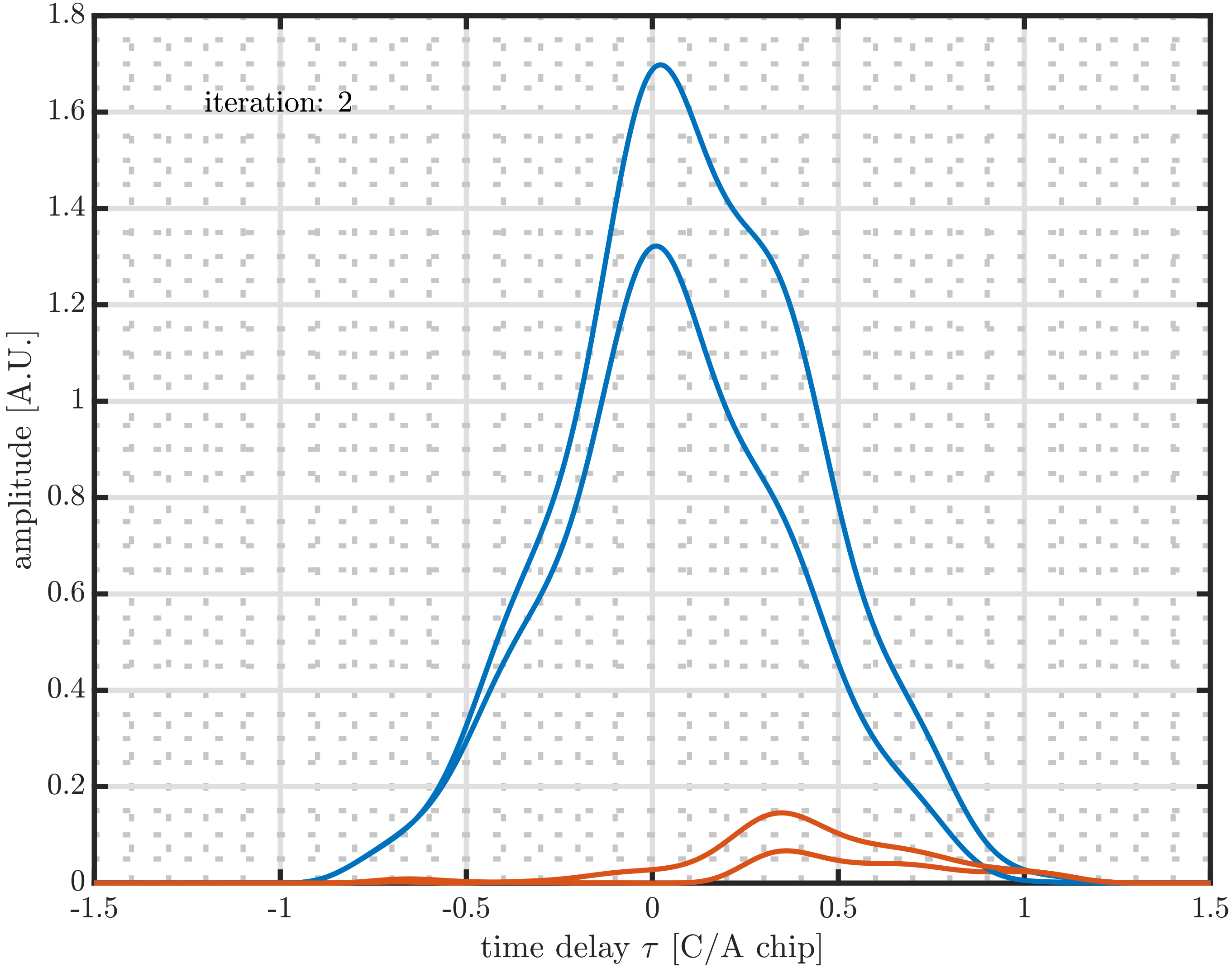

Back-up: CLEAN-RELAX estimator

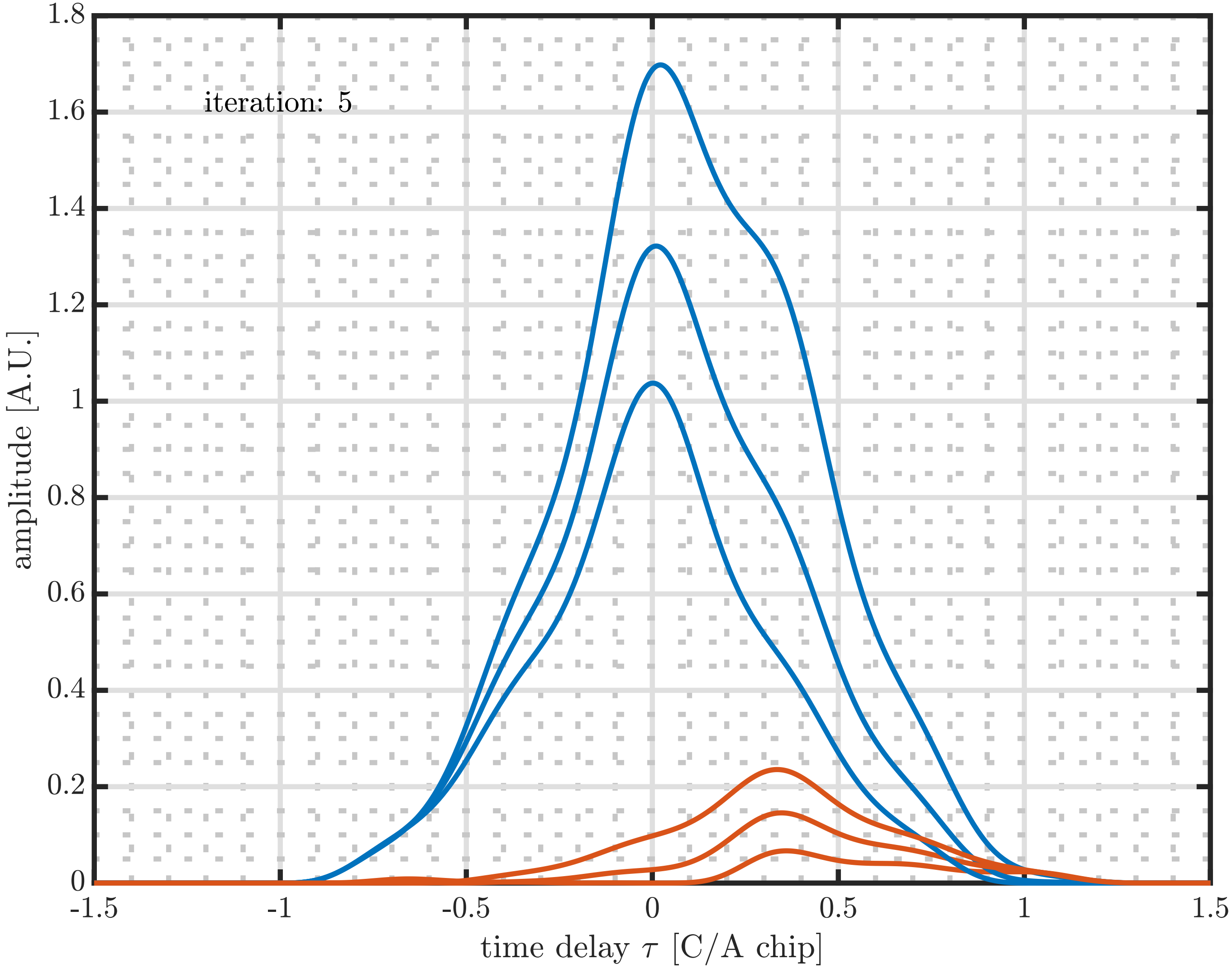

Back-up: CLEAN-RELAX estimator

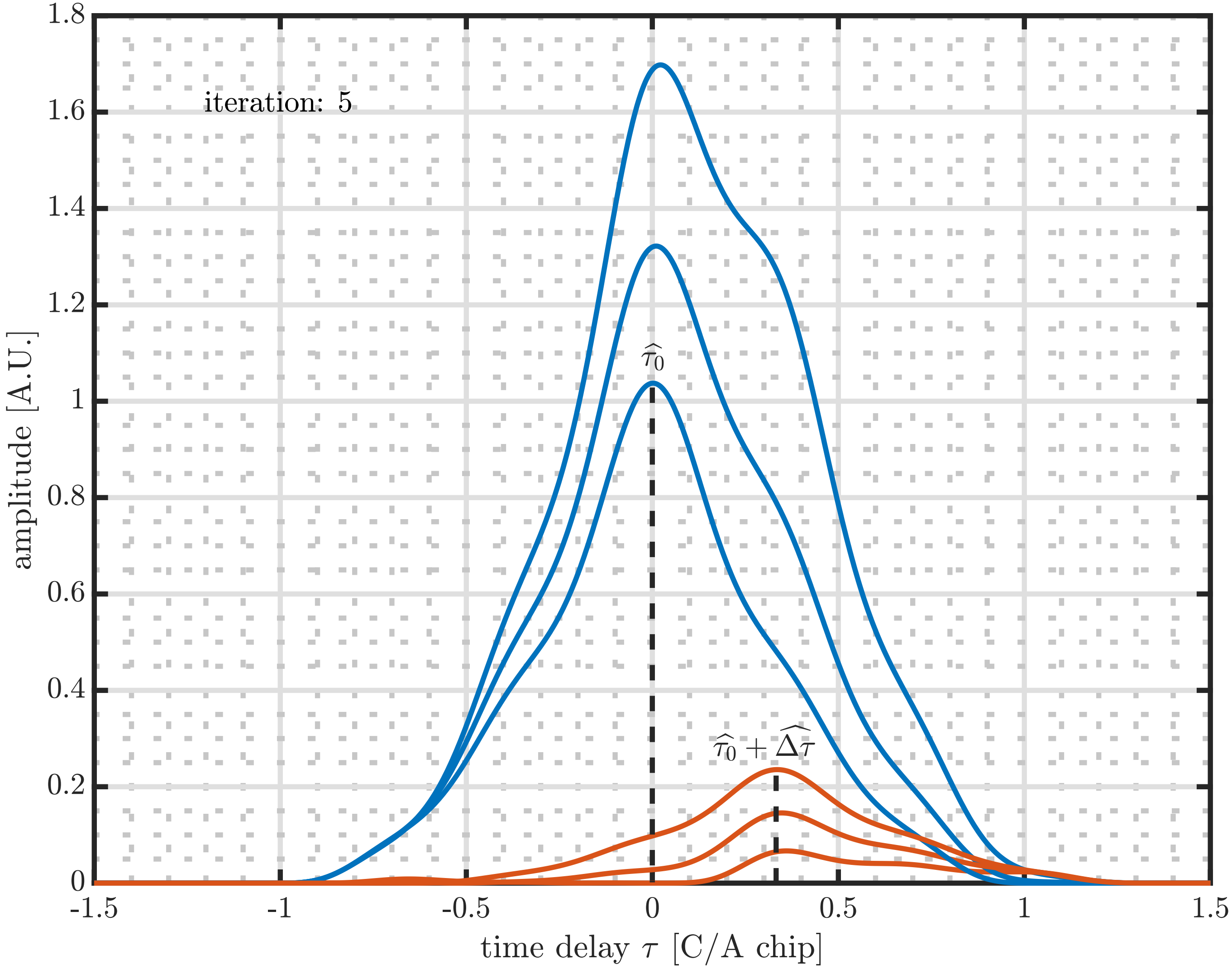

Back-up: Alternate Projection estimator

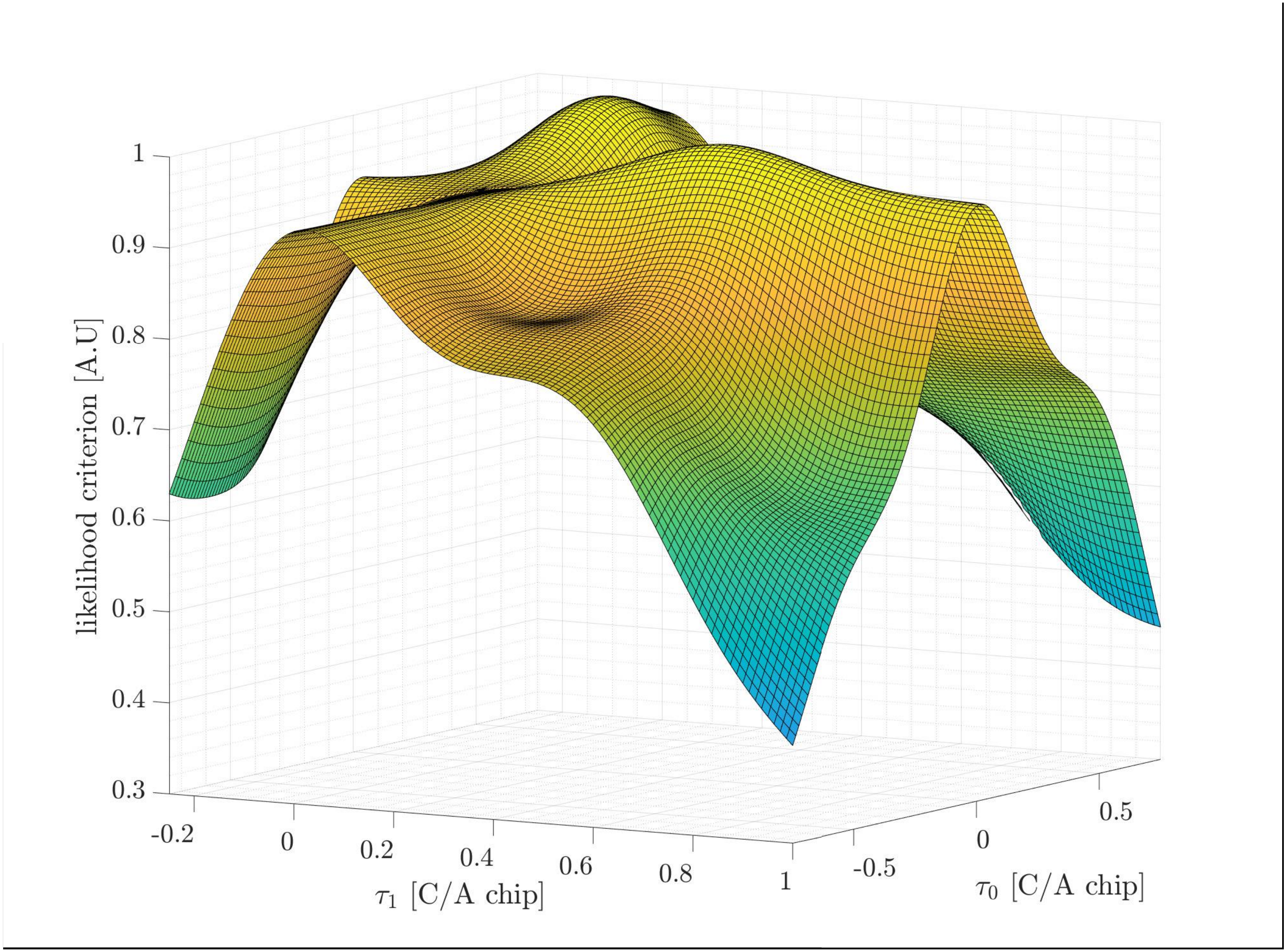

Back-up: Alternate Projection estimator

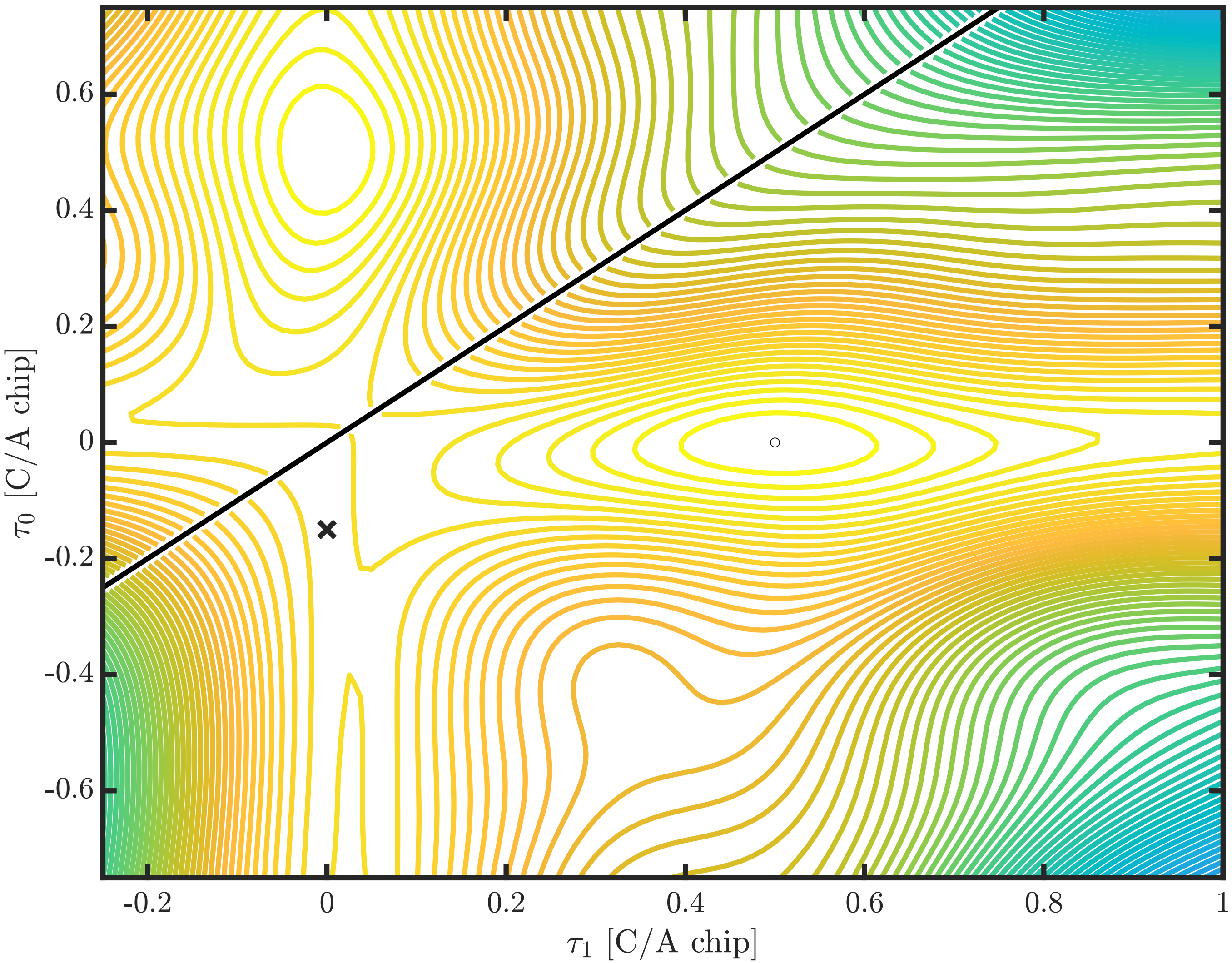

Back-up: Alternate Projection estimator

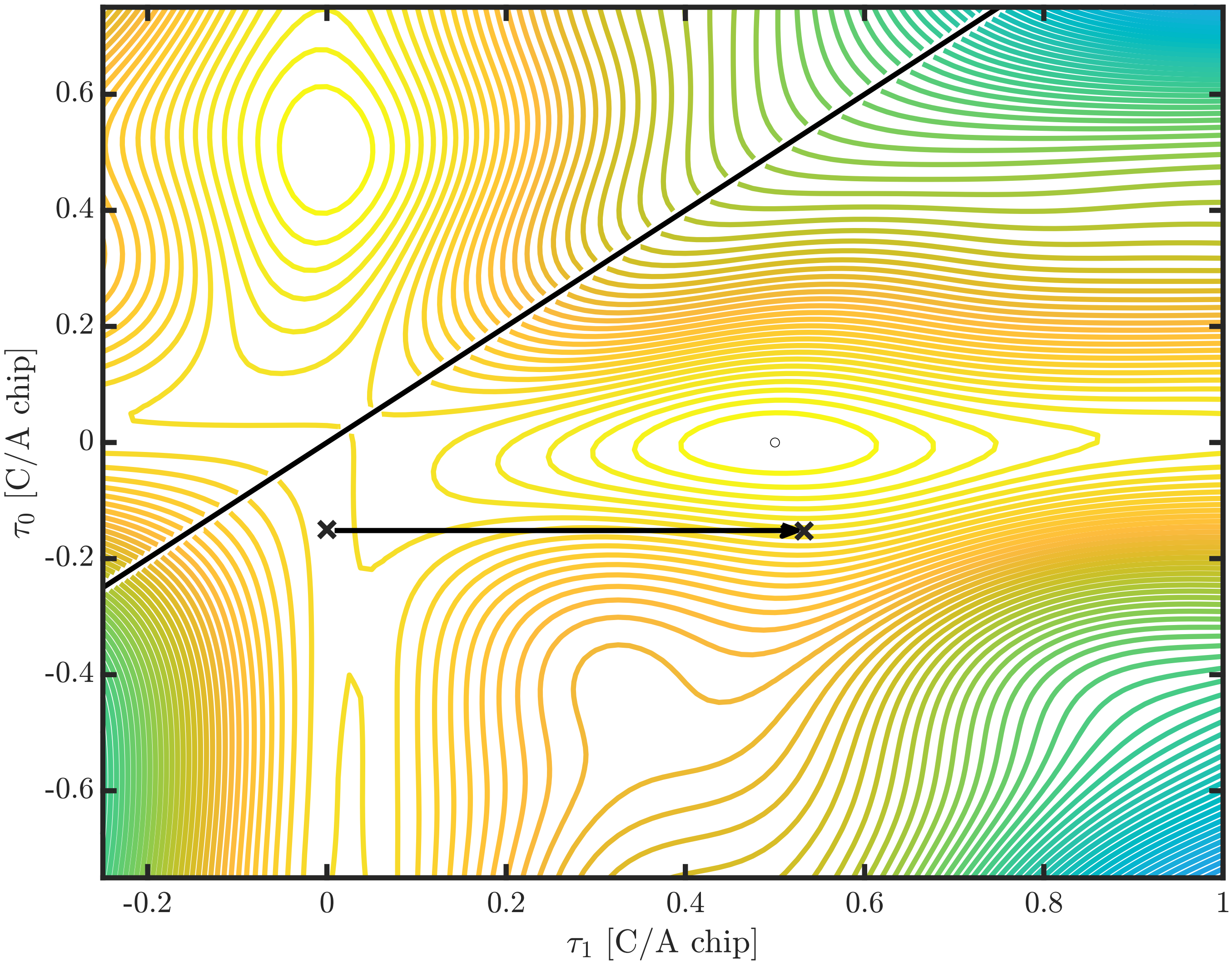

Back-up: Alternate Projection estimator

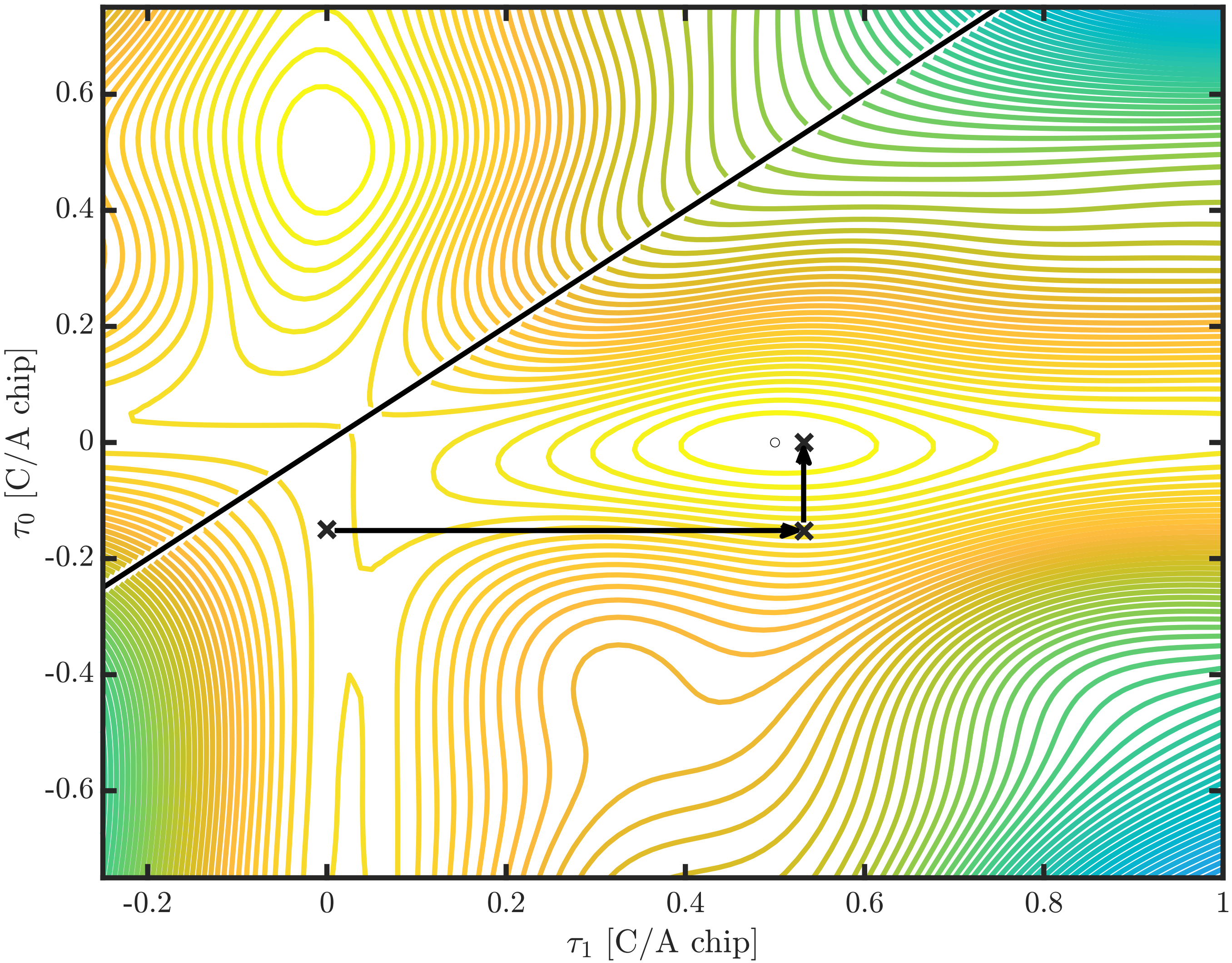

Back-up: Alternate Projection estimator

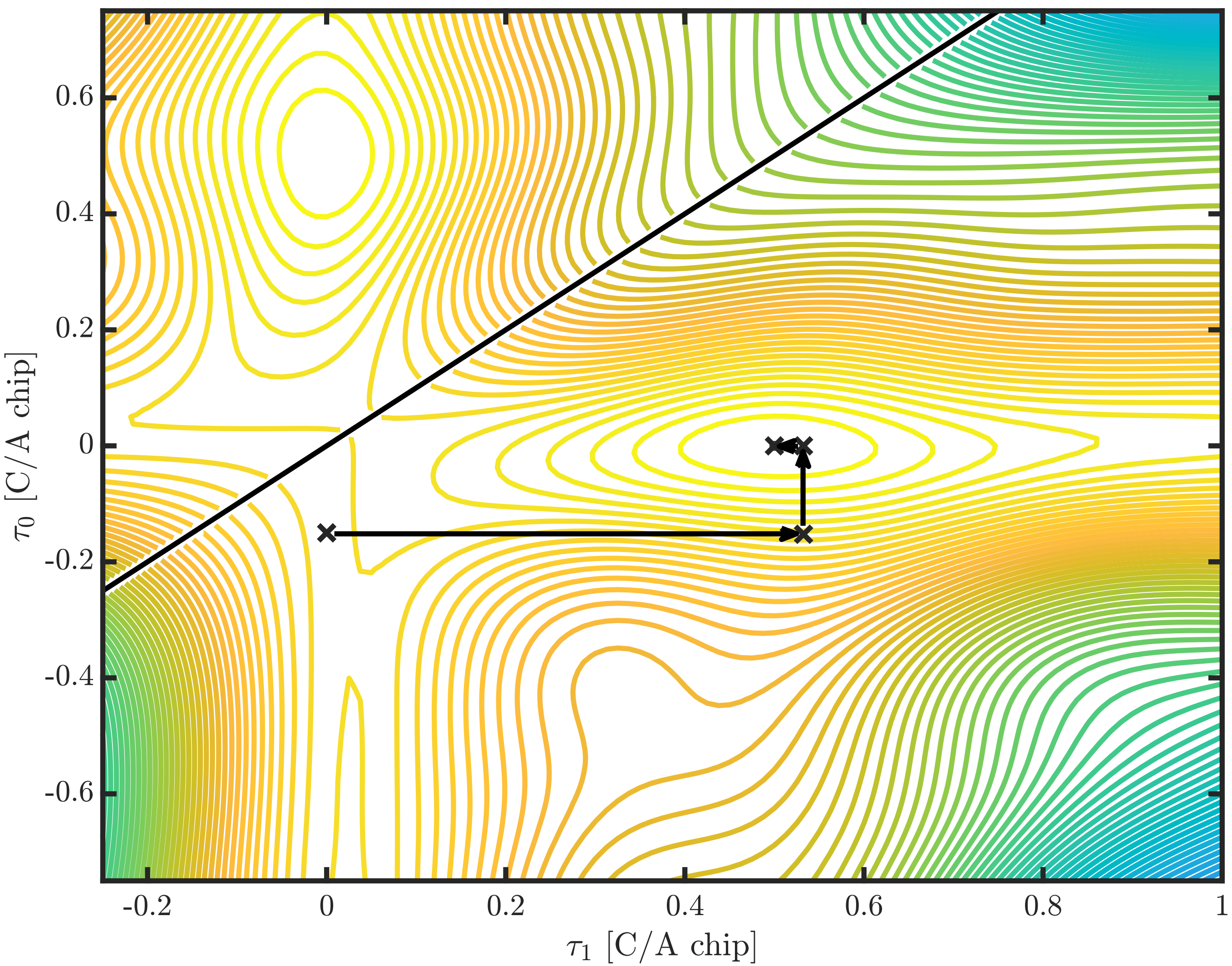

Back-up: Alternate Projection estimator

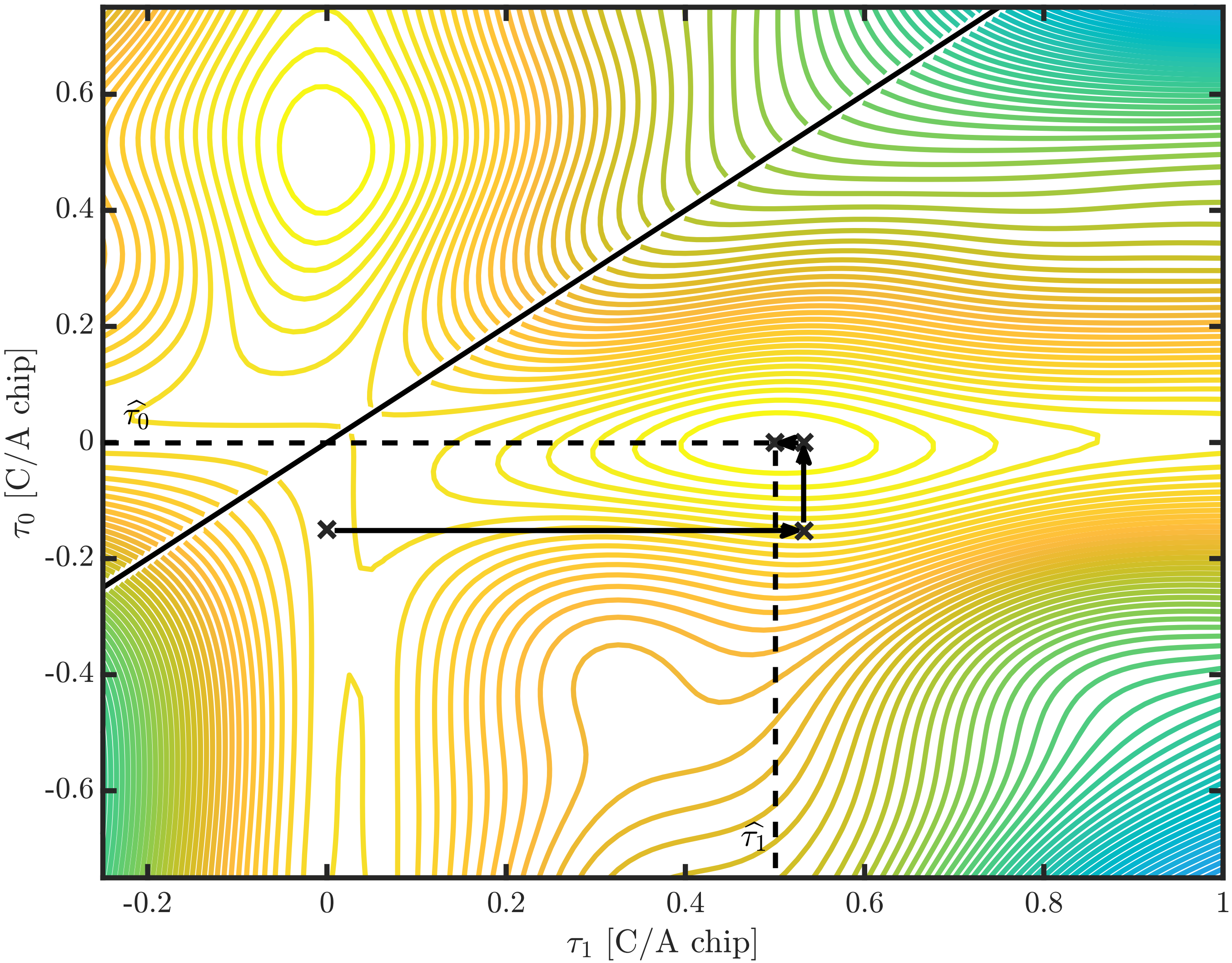

Back-up: Gruissan experiment 2S processing limits

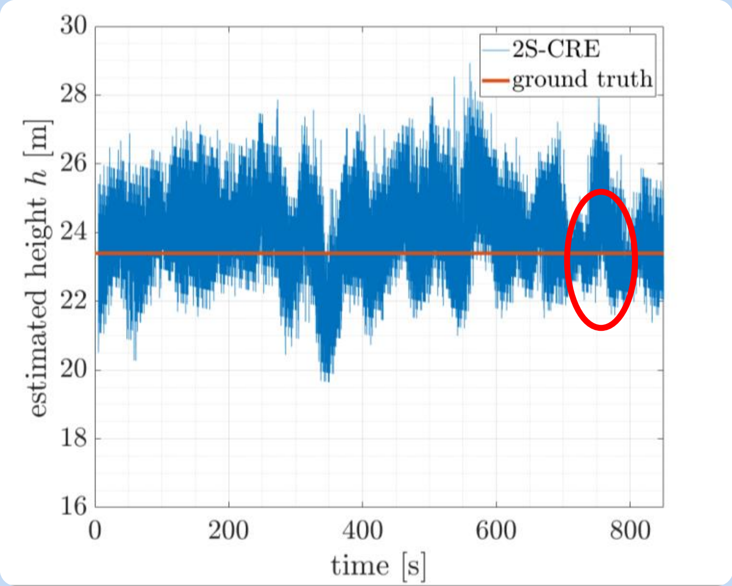

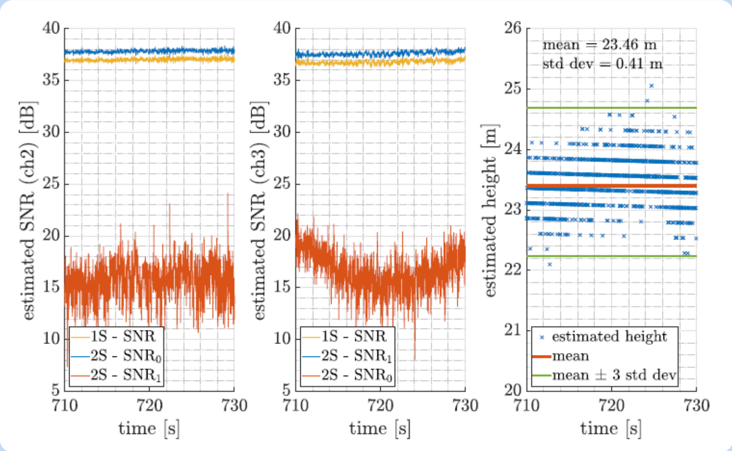

- Gruissan experiment on GPS L5Q signal:
  - CRB prediction: $\sqrt{CRB_h} = 0.27$m.
  - Height std dev: $\sigma_h = 0.41$m, 2dB off.
- Possible explanations:
  - Implementation: quantization error.
  - CLEAN-RELAX is biased for the considered path separation (22m): signal crosstalk.
  - Local replica used (RF filters).
  - Unidentified events during recording.
  - Specular reflection assumption:

Rayleigh Criterion: $\Delta h > \frac{\lambda}{8 \sin(e)} \approx 5\text{cm}.$

Back-up: Approximate MLE

- Close-to-ground hypotheses: i) $b_0 = b_1 = b$, ii) $\Delta\tau = \tau_1 - \tau_0$ very small compare to the width of the cross-correlation triangle.
- Dual source maximum likelihood estimation:

$$\left(\widehat{\tau_0}, \widehat{\Delta\tau}, \widehat{b}\right) = \min_{\tau_0, \Delta\tau, b} \{L(\tau_0, \Delta\tau, b)\} \text{ and } \widehat{\boldsymbol{\alpha}} = \left(\mathbf{A}^{\mathrm{H}}\mathbf{A}\right)^{-1}\mathbf{A}^{\mathrm{H}}\mathbf{x}.$$

- Third order Taylor approximation: $L(\tau_0, \Delta\tau, b) = \|\mathbf{P_A x}\|^2 \approx \sum_n^3 L_n(\tau_0, \Delta\tau, b)$.

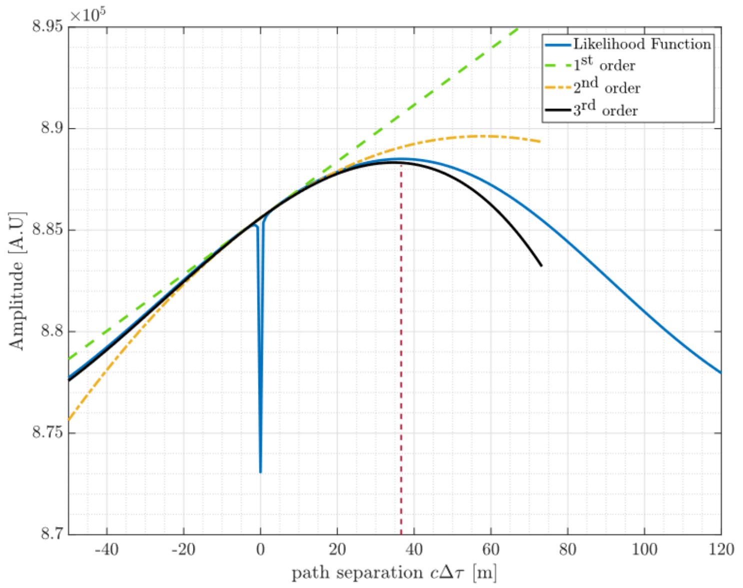

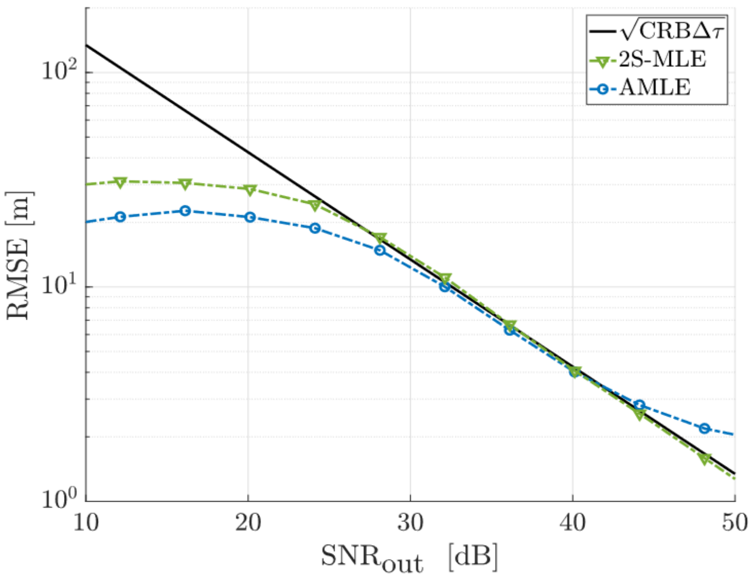

Back-up: Rayleigh criterion and reflection coherence

Rayleigh Criterion (rough)

$$\Delta h > \frac{\lambda}{8\sin(e)}$$

Path separation
$2\Delta h \sin(e)$

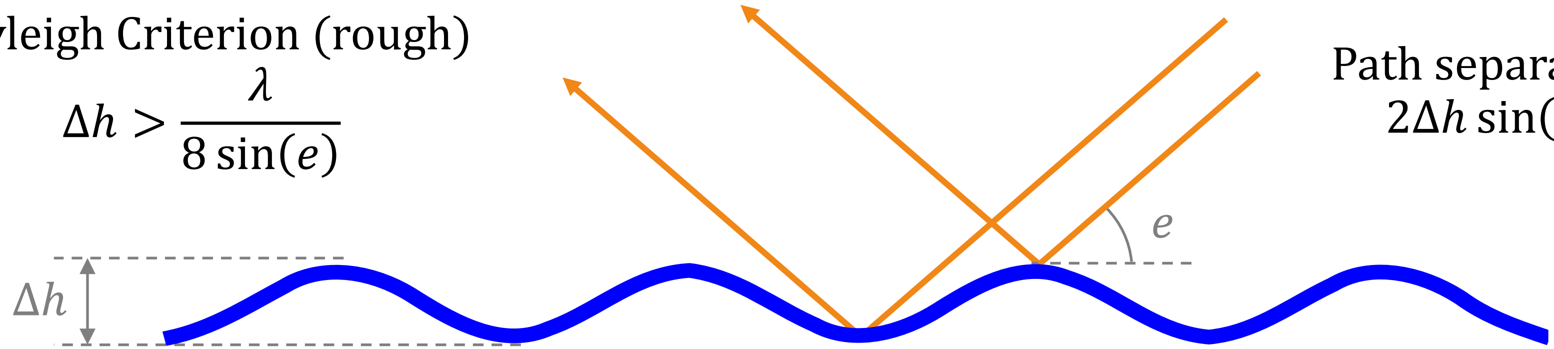

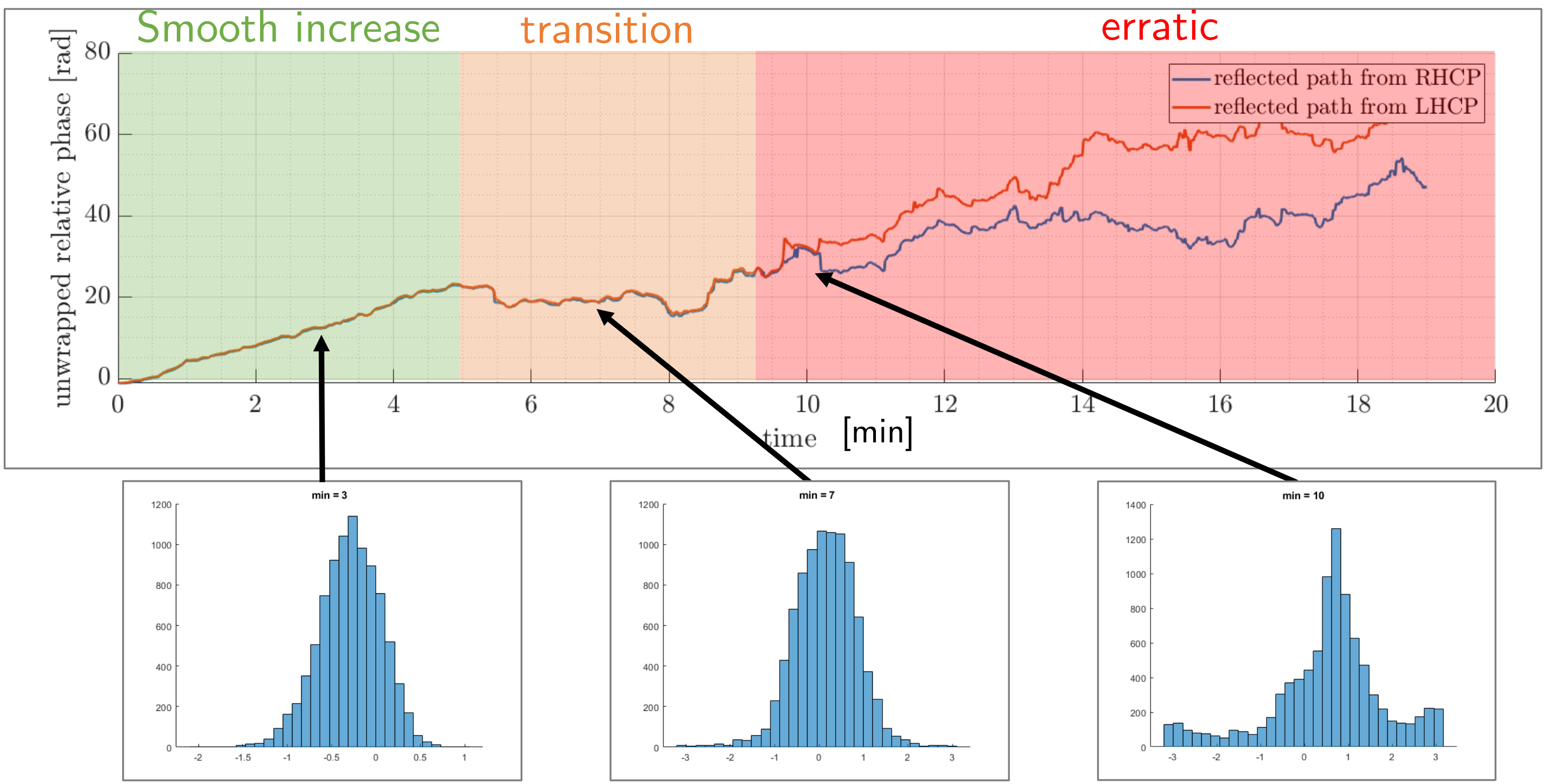

- Monte Carlo simulation (2000 runs).
- PD: probability of detecting the correct number of sources.
- P + next procedure:

SNR [dB]	PD	RMSE$_\tau$ [m]	$\sqrt{\text{CRB}_\tau}$ [m]
20	0.08	9.86	15.55
23	0.46	9.71	11.01
26	0.93	8.34	7.79

- Overshoot-and-decimate procedure:

SNR [dB]	PD	RMSE$_\tau$ [m]	$\sqrt{\text{CRB}_\tau}$ [m]
20	0.29	17.32	15.55
23	0.57	12.77	11.01
26	0.76	9.04	7.79